

**Multivariable Control of a Temperature Process with a  
Continuously Stirred Tank**

**M.Sc. Thesis  
in  
Electrical and Electronics Engineering  
University of Gaziantep**

**Supervisor  
Assist. Prof. Dr. Tolgay KARA**

**by  
Hazhar RASUL**

**August 2016**



© 2016 [Hazhar RASUL]

REPUBLIC OF TURKEY  
UNIVERSITY OF GAZIANTEP  
GRADUATE SCHOOL OF NATURAL & APPLIED SCIENCES  
ELECTRICAL & ELECTRONICS ENGINEERING

Name of the thesis: Multivariable Control of a Temperature Process with a  
Continuously Stirred Tank

Name of the student: Hazhar RASUL

Exam date: 05.August.2016

Approval of the Graduate School of Natural and Applied Sciences

  
Prof. Dr. Metin BEDİR  
Director

I certify that this thesis satisfies all the requirements as a thesis for the degree of Master  
of Science.

  
Prof. Dr. Ergun ERÇELEBİ  
Head of Department

This is to certify that we have read this thesis and that in our consensus opinion it is  
fully adequate, in scope and quality, as a thesis for the degree of Master of Science.



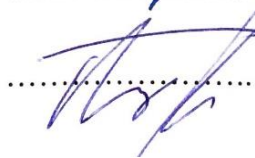
  
Assist. Prof. Dr. Tolgay KARA  
Supervisor

Examining Committee Members:

Prof. Dr. Celal KORAŞLI

Prof. Dr. Ergun ERÇELEBİ

Assist. Prof. Dr. Tolgay KARA

Signature  
  
  


**I hereby declare that all information in this document has been obtained and presented in accordance with academic rules and ethical conduct. I also declare that, as required by these rules and conduct, I have fully cited and referenced all material and results that are not original to this work.**

Hazhar RASUL

**ABSTRACT**  
**MULTIVARIABLE CONTROL OF A TEMPERATURE PROCESS WITH A  
CONTINUOUSLY STIRRED TANK**

RASUL, Hazhar

MSc. in Electrical and Electronics Engineering

Supervisor: Assist. Prof. Dr. Tolgay KARA

August 2016, 100 pages

Control of a continuously stirred tank (CST) is a benchmark process control problem, which can be utilized to describe and suggest control solutions to many industrial and domestic temperature processes. The current research idea is using a CST as a blender for cold and hot water through two control valves escorted with a pump to achieve a desired temperature and flow rate at the outlet of a domestic shower system. The process control system is in multivariable (MV) structure with three control inputs and two outputs. The control goal is to track the set points and maintain stable, smooth and minimum-overshoot responses despite perturbations of each inlet including temperature and flow variations.

In current research, the system dynamic mathematical model is developed. The MV system is linearized to make the elimination of loop interaction easier. In closed loop, two sub-processes of temperature and flow rate are controlled using fuzzy logic self-tuning proportional integral derivative (PID) control and fuzzy logic control (FLC) with a proportional gain, respectively.

Performance of proposed control mechanism and decoupler is tested via a number of simulations. Performance of proposed MV control system is tested with respect to reference and disturbance variations. Proposed MV control system tracks the reference point and gives good system stability and performance in rejecting disturbances.

**Key Words:** Multivariable Control, Linearization, Decoupling, Proportional Integral Derivative (PID) control, Fuzzy Logic Control, Fuzzy Logic Self-Tuning PID.

**ÖZET**  
**SÜREKLİ KARIŞTIRILAN TANK İÇEREN SICAKLIK SÜRECİNİN ÇOK**  
**DEĞİŞKENLİ DENETİMİ**

RASUL, Hazhar

Yüksek Lisans Tezi, Elektrik-Elektronik Mühendisliği Bölümü

Tez Yöneticisi: Yrd. Doç. Dr. Tolgay KARA

Ağustos 2016, 100 sayfa

Sürekli karıştırılan tank (SKT) denetimi, birçok endüstriyel ve evsel süreci açıklamak ve denetim çözümleri önermek için faydalanılabilecek temel bir süreç denetim problemidir. Mevcut araştırma fikri, evsel bir duş sisteminin çıkışında arzu edilen sıcaklık ve debiye ulaşmak amacıyla iki denetim vanası ve bir pompa aracılığıyla SKT'yi bir soğuk sıcak su karıştırıcısı olarak kullanmaktır. Süreç denetim sistemi, üç denetim girişi ve iki çıkışla çok değişkenli yapıdadır. Denetim hedefi, girişlerdeki hem sıcaklık hem de debi değişimlerinde sarsımlara rağmen set değerlerini takip etmek ve kararlı, yumuşak ve en düşük aşma değerine sahip yanıtları elde etmektir.

Mevcut çalışmada, sistem dinamik matematiksel modeli geliştirilmiştir. Çok değişkenli sistem, döngü etkileşiminin giderilmesini daha kolay yapabilmek için sistem doğrusallaştırılmıştır. Kapalı döngüde, sıcaklık ve debi süreçleri sırasıyla bulanık mantık özayarlama oransal tümevsel türevsel (PID) denetim ve oransal kazançlı bulanık mantık denetimi ile denetlenmiştir.

Önerilen denetim mekanizması ve etkileşim gidericinin başarımı benzetimlerle test edilmiştir. Önerilen çok değişkenli denetim sistemi, referans değeri ve bozucu değişimlerine karşı test edilmiştir. Önerilen çok değişkenli denetim sistemi referans değerini takip ederken iyi bozucu savurması ve kararlılık özellikleri göstermiştir.

**Anahtar Kelimeler:** Çok Değişkenli Denetim, Doğrusallaştırma, Etkileşim Giderme, Oransal Tümevsel Türevsel (PID) denetim, Bulanık Mantık Denetimi, Bulanık Mantık Özayarlama PID.



To My Parents

## ACKNOWLEDGEMENTS

First and foremost I offer my sincerest gratitude to my supervisor, Assist. Prof. Dr. Tolgay KARA who has supported me throughout my thesis with his patience and knowledge. I attribute the level of my Master's degree to his encouragement and effort. One simply could not wish for a better or friendlier supervisor.

Second I would like to deep in my heart thank my parents for all the moral support and the amazing chances they've given me over the years.

Finally, thanks for every single person who said a good word through my life.



## TABLE OF CONTENTS

ABSTRACT .....	v
ÖZET.....	vi
ACKNOWLEDGEMENTS .....	viii
LIST OF FIGURES .....	xi
LIST OF TABLES .....	xv
LIST OF SYMBOLS/ABBREVIATIONS .....	xvi
CHAPTER I .....	1
INTRODUCTION.....	1
1.1. Motivation .....	1
1.2. Literature Review .....	2
1.3. Goals and Contribution of Thesis .....	4
1.4. Organization of Thesis .....	5
CHAPTER II.....	6
MATHEMATICAL DYNAMIC MODEL OF CONSIDERED SYSTEM.....	6
2.1. Introduction .....	6
2.2. Developing Mathematical Models .....	7
2.2.1. Temperature Control Mathematical Model.....	7
2.2.2. Pump Speed Mathematical Model [18].....	8
2.2.3. Control Valve Mathematical Model.....	12
2.3. Combining the System Dynamic Equations .....	14
2.4. Linearization of the Nonlinear Model.....	15
2.4.1. Linearization Technique .....	17
2.4.2. Interpretation of Linearization.....	18
2.5. Laplace Domain Transformation.....	25
2.5.1. Transformation Technique .....	25
2.5.2. System State-Space Transformation to Laplace .....	26
CHAPTER III.....	28
MULTIVARIABLE CONTROL DESIGN .....	28
3.1. Introduction .....	28
3.2. Decoupler Design .....	29

3.2.1. Loop Interaction and Decoupling Method .....	29
3.2.2. Decoupler Design from Block Diagrams .....	30
3.2.3. Static and Dynamic Decoupling .....	32
3.3. Proposed MV Temperature-Flow Rate Controller .....	32
3.3.1. Fuzzy Self-tuning PID Control for Temperature Control .....	33
3.3.2. Fuzzy Logic Control for Flow Rate Control .....	36
CHAPTER IV .....	38
SIMULATION TESTS AND RESULTS .....	38
4.1 Linearization Results .....	38
4.2. Decoupler Performance .....	44
4.2.1. Static vs. Dynamic Decoupler on Linearized System .....	46
4.2.2. Static vs. Dynamic Decoupler on Nonlinear System .....	50
4.3. Closed Loop Feedback Control Design performances .....	54
4.3.1. Fuzzy Control Toolbox.....	54
4.3.2. Controllers Performances through Control Inputs .....	58
4.3.2.1. Statically Decoupled Linearized System Performances .....	58
4.3.2.2. Statically Decoupled Nonlinear System Performances .....	64
4.3.2.3. Dynamically Decoupled Linearized System Performances .....	69
4.3.2.4. Dynamically Decoupled Nonlinear System Performances .....	74
4.3.3. Controllers Performances through Disturbance Rejection.....	79
4.3.4. Mean Square Error MSE .....	89
4.4. Discussion.....	90
CHAPTER V .....	93
CONCLUSIONS .....	93
5.1. Concluding Remarks .....	93
5.2. Future Work and Recommendations .....	94
REFERENCES .....	95
APPENDICES .....	98
A.1. DC Motor Specifications .....	98
A.2. Pump Impeller Specifications.....	99
A.3. Estimated J Pump Moment of Inertia .....	100

## LIST OF FIGURES

Figure 1.1. The proposed multivariable continuously stirred tank system piping and instrumentation diagram.....	2
Figure 2.1. Separately excited armature controlled DC motor diagram. ....	11
Figure 2.2. Proposed thesis open loop system black box block diagram including inputs, outputs and disturbances. ....	19
Figure 2.3. Pump speed vs. flow variations within constant valve positions, approximated to a linearly change through curve fitting. ....	24
Figure 3.1. Open loop proposed thesis system block diagram.....	30
Figure 3.2. Open loop plant with proposed decoupler design.....	31
Figure 3.3. General structure block diagram of fuzzy self-tuning PID controller .....	33
Figure 3.4. Fuzzy logic flow control loop block diagram. ....	36
Figure 4.1. Linearized mathematical based open loop system model in computer simulation.....	39
Figure 4.2. Nonlinear mathematical based open loop system model in computer simulation.....	40
Figure 4.3. Linearized vs. nonlinear CST plant comparison.....	41
Figure 4.4. Linearized vs. nonlinear tank temperature behavior for a step input to the first valve position. ....	41
Figure 4.5. Linearized vs. nonlinear tank temperature behavior for a step input to the second valve position.....	42
Figure 4.6. Linearized vs. nonlinear tank temperature behavior for a step reduction input to the motor applied voltage. ....	42
Figure 4.7. Linearized vs. nonlinear out stream flow rate behavior for a step input to the first valve position. ....	43
Figure 4.8. Linearized vs. nonlinear out stream flow rate behavior for a step input to the second valve position.....	43
Figure 4.9. Linearized vs. nonlinear stream flow rate for a step input to the motor applied voltage. ....	44
Figure 4.10. Designed static decoupler computer simulated block.....	45
Figure 4.11. Designed dynamic decoupler computer simulated block.....	45
Figure 4.12. Static and dynamic decoupled vs. non-decoupled linearized system comparison blocks.....	46
Figure 4.13. Temperature output variable behavior of the linearized system to a step input 0.2 in the first valve position. ....	47

Figure 4.14. Temperature output variable behavior of the linearized system to a step input 0.2 in the second valve position. ....	47
Figure 4.15. Temperature output variable behavior of the linearized system to a step input 0.2 in the motor applied voltage selector. ....	48
Figure 4.16. Flow rate output variable behavior of the linearized system to a step input 0.2 in the first valve position. ....	48
Figure 4.17. Flow rate output variable behavior of the linearized system to a step input 0.2 in the second valve position. ....	49
Figure 4.18. Flow rate output variable behavior of the linearized system to a step input 0.2 in the motor applied voltage selector. ....	49
Figure 4.19. Static and dynamic decoupled vs. non-decoupled nonlinear system comparison blocks. ....	50
Figure 4.20. Temperature output variable behavior of the nonlinear system to a step input 0.2 in the first valve position. ....	51
Figure 4.21. Temperature output variable behavior of the nonlinear system to a step input 0.2 in the second valve position. ....	51
Figure 4.22. Temperature output variable behavior of the nonlinear system to a step reduction input 0.2 in the motor applied voltage selector. ....	52
Figure 4.23. Flow rate output variable behavior of the nonlinear system to a step input 0.2 in the first valve position. ....	52
Figure 4.24. Flow rate output variable behavior of the nonlinear system to a step input 0.2 in the second valve position. ....	53
Figure 4.25. Flow rate output variable behavior of the nonlinear system to a step input 0.2 in the motor applied voltage selector. ....	53
Figure 4.26. Input variable of FLC, error membership function for the self-tuning PID temperature control loop. ....	55
Figure 4.27. Input variable FLC change of error membership function for the self-tuning PID temperature control loop. ....	55
Figure 4.28. Input variable FLC error membership function for the flow rate control loop. ....	55
Figure 4.29. Input variable FLC change of error membership function for the flow rate control loop. ....	56
Figure 4.30. Output variable of FLC, proportional gain $k_p$ membership function for the self-tuning PID temperature control loop. ....	56
Figure 4.31. Output variable of FLC, integral $k_i$ membership function for the self-tuning PID temperature control loop. ....	56
Figure 4.32. Output variable of FLC, derivative $k_d$ membership function for the self-tuning PID temperature control loop. ....	57
Figure 4.33. Output variable of FLC, valve position membership function for flow rate control loop. ....	57

Figure 4.34. Output variable of FLC, motor applied voltage membership function for flow rate control loop. ....	57
Figure 4.35. The output variable surfaces of both FLC controllers according to error and change of error for each control loop. ....	58
Figure 4.36. Statically decoupled linearized closed loop controlled MV system. ....	59
Figure 4.37. Response of statically decoupled linearized system to a step change to the temperature set point. ....	60
Figure 4.38. Response of statically decoupled linearized system to a step change to the flow rate set point. ....	61
Figure 4.39. Response of statically decoupled linearized system injected with a square wave input to the temperature set point. ....	62
Figure 4.40. Response of statically decoupled linearized system injected with a square wave input to the temperature set point. ....	63
Figure 4.41. Statically decoupled nonlinear closed loop controlled MV system. ....	64
Figure 4.42. Response of statically decoupled nonlinear system to a step change to the temperature set point. ....	65
Figure 4.43. Response of statically decoupled nonlinear system to a step change to the flow rate set point. ....	66
Figure 4.44. Response of statically decoupled nonlinear system injected with a square wave input to the temperature set point. ....	67
Figure 4.45. Response of statically decoupled nonlinear system injected with a square wave input to the temperature set point. ....	68
Figure 4.46. Dynamically decoupled linearized closed loop controlled MV system. ....	69
Figure 4.47. Response of dynamically decoupled linearized system to a step change to the temperature set point. ....	70
Figure 4.48. Response of dynamically decoupled linearized system to a step change to the flow rate set point. ....	71
Figure 4.49. Response of dynamically decoupled linearized system injected with a square wave input to the temperature set point. ....	72
Figure 4.50. Response of dynamically decoupled linearized system injected with a square wave input to the temperature set point. ....	73
Figure 4.51. Dynamically decoupled nonlinear closed loop controlled MV system. ....	74
Figure 4.52. Response of dynamically decoupled nonlinear system to a step change to the temperature set point. ....	75
Figure 4.53. Response of dynamically decoupled nonlinear system to a step change to the flow rate set point. ....	76
Figure 4.54. Response of dynamically decoupled nonlinear system injected with a square wave input to the temperature set point. ....	77

Figure 4.55. Response of dynamically decoupled nonlinear system injected with a square wave input to the temperature set point. ....	78
Figure 4.56. System controlled temperature variable behavior through each intake flow temperature disturbed with a step change. ....	80
Figure 4.57. System controlled temperature variable behavior through each intake flow temperature disturbed with a sine wave. ....	81
Figure 4.58. System controlled temperature variable behavior through each intake flow temperature disturbed with a random signal. ....	82
Figure 4.59. System controlled temperature variable behavior through each intake flow pressure disturbed with a step change. ....	83
Figure 4.60. System controlled temperature variable behavior through each intake flow pressure disturbed with a sine wave. ....	84
Figure 4.61. System controlled temperature variable behavior through each intake flow pressure disturbed with a random signal. ....	85
Figure 4.62. System controlled flow rate variable behavior through each intake flow pressure disturbed with a step change. ....	86
Figure 4.63. System controlled flow rate variable behavior through each intake flow pressure disturbed with a sine wave. ....	87
Figure 4.64. System controlled flow rate variable behavior through each intake flow pressure disturbed with a random signal. ....	88
Figure A.1. 100ZYT Series Electric DC Motor 100ZYT36- 200- 1700.....	98
Figure A.2. SHURFLO REVOLUTION™ 4008 SERIES PUMP.....	99
Figure A.3. SHURFLO pump manufacture characteristic curve .....	99

## LIST OF TABLES

Table 3.1. $k_p$ Fuzzy control rule. ....	35
Table 3.2. $k_i$ Fuzzy control rule .....	35
Table 3.3. $k_d$ Fuzzy control rule .....	35
Table 3.4. $m_2(x)$ and $m_3(x)$ Fuzzy control rule. ....	37
Table 4.1. Numerical MSE for temperature output variable of purposed Fuzzy Self-tuning PID controller against conventional PID controller to mentioned disturbance subjections. ....	89
Table 4.2. Numerical MSE for temperature output variable of purposed Fuzzy Self-tuning PID controller against conventional PID controller to mentioned disturbance subjections. ....	89
Table 4.3. Numerical MSE for flow rate output variable of purposed Fuzzy Logic controller against conventional PID controller to mentioned disturbance subjections. ....	90
Table A.1. 100ZYT Series Electric DC Motor Specification.....	98
Table A.2. SHURFLO pump manufacture characteristic.....	99

## LIST OF SYMBOLS/ABBREVIATIONS

MV	Multivariable
CST	Continuous Stirred Tank
PID	Proportional Integral Derivative
FLC	Fuzzy Logic Control
MIMO	Multi-Input Multi-Output
SISO	Single-Input Single-Output
TTT	Temperature Transducer Transfer-function
FTT	Flow Transducer Transfer-function
DC	Direct Current
MSE	Mean Square Error
NL	Negative Large
NI	Negative Intermediate
NM	Negative Medium
NS	Negative Small
Z	Zero
PS	Positive Small
PM	Positive Medium
PI	Positive Intermediate
PL	Positive Large



## CHAPTER I

### INTRODUCTION

Since decades, continuously stirred tank (CST) is an important subject, which is used in many chemical processes such as reactors which is a mixing vessel used for blending between two or more components and reacting to produce one or more products.

In recent years, great strides have been made in making homes automated. Since these homes provide secure and relaxation life, in addition they save time and money which is economically improved. Through on going this idea, an automated shower for providing a certain comfortable water temperature and soft flow rate at the instant, which the water is releasing the showerhead is one of the CST applications, for specific available conditions like: cold and hot water supply temperature and pressure typically varies during circling of the seasons or lag in the heating rate in the boiler and level variation of water in the storage tanks.

#### 1.1. Motivation

Temperature and flow rate control for the CST has many advantages in industrial and chemical process applications, such as reactors, mixers and others especially in refineries and biochemistry labs beside the normal life home applications.

As part of our daily routine, the shower has evolved from the place which can make you feel fresh to a place of therapy and relaxation. Hence most of the people enjoy a proper nice shower, a shower that its flow rate almost powerful enough to give a good massage and release ache from tired muscles, with a comfort hot temperature. And since the worst option for a shower is one that's gravity fed with an inadequate head of water, since the head of water provides the water pressure through the stored cold water containers (traditionally in the loft) above the shower, which feeds the shower with cold water directly, and also forces hot water from a storage cylinder (The hot water is heated by an immersion heater or 'regular' or 'heat-only' boiler), as considered in current thesis.

Hence control of mentioned temperature and flow rate through the CST is the purposed challenge. These control issues have been subject to many researches to develop various control algorithms to deal with stability, set point tracking and disturbance rejection. It is thus clear that there is a need to develop control techniques applicable to both temperature and flow rate control systems. To investigate these control problems, a CST with two control valves and a pump at the outlet is considered as shown in Figure 1.1.

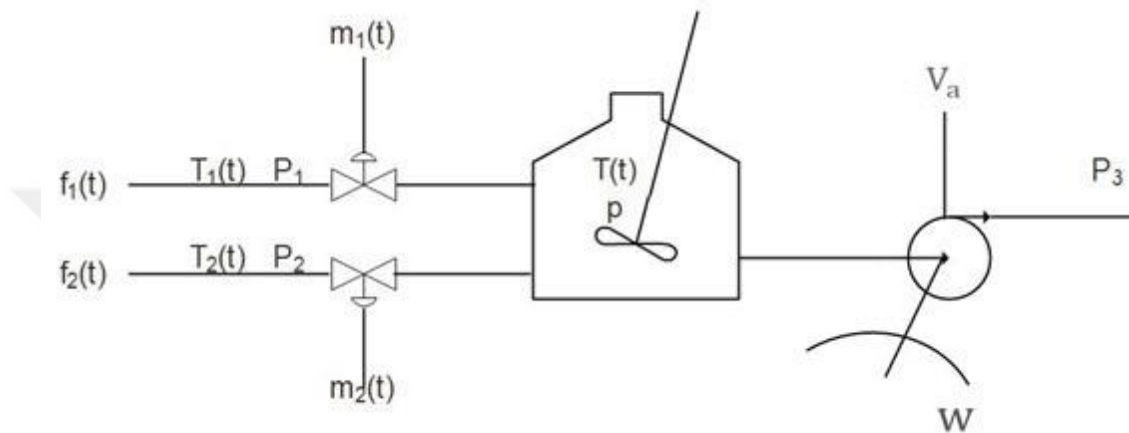


Figure 1.1. The proposed multivariable continuously stirred tank system piping and instrumentation diagram.

## 1.2. Literature Review

Many researchers have studied and proposed controller methods for multiple-input, multiple-output (MIMO) temperature and mass flow rate control on a tank in different processes including both temperature and mass flow rate control. Those temperature and mass flow rate control designs have been done through heater and valve position actuators respectively in real physical systems and simulations, which are linear and nonlinear methods depending on the physical plant dynamics. Often in MV control processes various control objectives interact with each other. Blending tanks are processes in which usually loop interactions happen while it is necessary to control both the flow and composition of the outlet stream. Accomplishing this objective may get easy through manipulating the flow of the inlets.

There are many studies proceeded to emphasize this objective through decoupling the interacted loops statically (relative gains) and dynamically. Since most processes are considered as nonlinear MV systems with mutual interactions, the good control performance cannot be obtained by simple controllers. Makoto, Toru and Yoshimi [1]

used a designed decoupler which has been generated by the sum of a static decoupler and a neural-net based decoupler. Then, the former has been used so as to approximately decouple the controlled object. Arjin ,Theerachai, Tianchai, Phongchai and Jutarut [2] used conventional decoupling method for diagonalization of a plant. Zheng and GAO [3] proposed a decoupler to reduce the interactions of two control loops.

On the other hand, for the temperature control objective many studies were done in individual processes different than proposed thesis work. Yuvraj and Yaduvir [4] have used classical PID controller for controlling temperature at the outlet stream of heat exchanger. Chia-Feng and Jung-Shing [5] implemented a hardware for controlling bath temperature based of a recurrent neural fuzzy controller. The design realized on an Field-Programmable Gate Array (FPGA) chip. Several sets of experiments were performed on a practical water bath temperature control, comparing with the generally adopted controllers. Mary et al [6] proposes a novel approach based on self-tuning FLC and genetic algorithm (GA) optimized fuzzy logic controller, for the design of a temperature control process. The process was simulated using the mathematical model of the real water bath plant. The controlled variable is the output temperature of water while the manipulated variable is the heat flowing inward the system. Also for same previous plant mechanism, Chen et al [7] compared the functional-link-based fuzzy neural network (FLFNN) controller to the PID controller, the manually designed fuzzy controller (FC), the functional link neural network (FLNN) and the Takagi-Sugeno-Kang-type fuzzy neural network (TSK-type FNN). Tavoosi [8] have proposed an adaptive Neuro- Fuzzy Inference Systems (ANFIS) used as controller for control of water temperature in the bath system. A Sugeno fuzzy model was chosen. There are five layers of network. The hybrid learning algorithm, a combination of least square and back propagation methods is used for training this network. Recursive least square method for adjusting linear output parameters is proposed. This controller has five membership functions using Gaussian type membership function. There are twenty five rules used for this system. Also the design of PID self-tuning controller was presented by Therese and Nair [9]. The controller consists of conventional PID controller and FLC, which is capable of tracking the set point through self-tuning. The proposed method is applied in a MV process which was a heater-mixer set up. The heater-mixer setup consists of two non-interacting stirred tanks. Leena and Vishal [10]

carried out the comparison between the fuzzy logic and adaptive neuro-fuzzy controller. They made use these two control systems to regulate the water temperature of a bath system. Treesalayapun, Ualrongjil and Kanlapanil [11] presented a novel fuzzy neural network called Fuzzy Graphic Rule Network (FGRN), which is a simple structure used to control the water bath temperature.

Absolutely for flow control objective also many studies have been done in various processes like boilers, water distribution and fluid flow in air conditioning systems etc. Jahmeerbacus [12] proposed a fuzzy logic based flow rate regulation scheme for a pumping system driven by an induction motor. The output signal from fuzzy controller is used to generate the torque producing component of the stator current. The performance of the controller is tested with variable flow rate command, and with large step changes in the pumping system curve parameters. Khan, Choudhry and Zeeshan [13] proposed a GA based Adaptive Fuzzy Logic Controller (AFLC) design for the MV control by manipulating valve positions to adjust the water and steam flow rates. A method for the adaptation of FLC by modifying Fuzzy Rule Matrix (FRM) based on GA has been proposed. The proposed adaptive controller outperforms the existing fuzzy controller in terms of steady state error, rise time and settling time. Xiaoyan and Wanneng [14] used two kinds of methods to regulate the flow rate. The controlling unit of the system is a neuron-based adaptive controller whose property is compared with that of traditional auto control system - PID control system. Jiri and Petr [15] controlled the water tank level via input volumetric flow rate through the proportional solenoid valve. The adaptive approach with the recursive identification was employed for controlling the system. The controller could be tuned by the choice of the pole position in the pole-placement method.

### **1.3. Goals and Contribution of Thesis**

Temperature and flow rate control problem for the CST as shown in Figure 1.1 is considered in this thesis. In particular, the control actuators here are two valves and a pump where they have to work simultaneously which is in contrast with the vast majority of literature on the temperature or flow rate control for the CST. As long as in the current thesis the tank temperature can be maintain to a desired set point by varying the water inlet flow rates where enter the tank, at same instant keeping the output flow rate at a desired set point, although through use a pump, high pressure

water streaming can be maintain and it also works as a reserve during pressure reduction caused by low level water in the storage tanks. Also the small volume blender tank is used to reduce high rate inlet fluctuations because of above described dynamics, which is may lead the user expose to scalding or frigid water during numerous temperature fluctuations.

Furthermore, as we will see in following chapters, linearization of the system about some nominal point can give same response of the nonlinear real system, which is facilitated in the design of decoupling and conventional closed loop control methods. As long as there are limited ranges for the control inputs, those conventional control methods are not capable to provide the same response for every different set point step changes beside the disturbance rejecting performance. Achieving and maintaining comforted temperature and smoothed flow rate of water must be emphasized in accordance with disturbances, hence, the advanced Fuzzy logic self-tuning PID and FLC with a proportional gain respectively is proposed.

#### **1.4. Organization of Thesis**

The previous sections give short definition of CST and an overview about control objectives which occur in these systems. Then in the previous studies some control solutions for other specific projects with similar conditions are given. The mathematical model development for the system is applied including linearization the developed nonlinear system, brief background of linearization technique, Laplace transformation criteria and other specifications are discussed further in Chapter II.

Chapter III presents control problems of the thesis specified CST system. A short background of MV systems, loop interactions, and proposed decoupling method escorted with control methodologies and strategies are also given.

After the decouplers and controllers are designed, simulations of CST system based on the above designed stages is given in Chapter IV and performances of CST system are tested through the simulated system. In Chapter V results and conclusions are discussed.

## CHAPTER II

### MATHEMATICAL DYNAMIC MODEL OF CONSIDERED SYSTEM

#### 2.1. Introduction

Developing the mathematical model for the process control systems is the first step in controller design. Mathematical models are sets of equations that describe a process. Through transfer functions and block diagrams the mathematical models are developed [16]. in which transfer functions are in linear systems. Traditionally, processes can be controlled using linear system analysis and design tools. This approach was employed despite the fact that most chemical processes are modelled by non-linear equations. The main reason for the extensive use of linear dynamic systems theory is that closed-form analytical solutions exist for linear systems which can be used easily to prove universal stability and controller performance. Also, non-linear systems are adequately approximated by linear systems near some operating conditions [17].

Considering current system as described in Figure 1.1, the thermodynamic and fluid equations may be used to find the equations of motion of mechanisms. In this section the dynamic modeling equations to find the tank temperature and flow rate are developed under these assumptions:

- The volume of liquids (sum of hot and cold water) are constant with constant density and heat capacity.
- Perfect mixing is assumed in the tank.
- The tank inlet flow rates and inlet temperatures may change.
- The rate of heat transfer from the tank to the ambient is governed by equation  $Q = UA(T_o - T_a)$ , where  $U$  is the overall heat transfer coefficient and  $A$  is the area for heat transfer.

The mathematical dynamical models that are developed starting from a balance on a conserved quantity: mass or energy. The balance can be written as:

$$\begin{aligned} & \left( \text{flow of mass/energy} \right)_{\text{into control volume}} - \left( \text{flow of mass/energy} \right)_{\text{out of control volume}} \\ & = \left( \text{Rate of change of mass/energy} \right)_{\text{accumulated in the control volume}} \end{aligned} \quad (2.1)$$

## 2.2. Developing Mathematical Models

### 2.2.1. Temperature Control Mathematical Model

We are interested in developing the mathematical model that describes how the outlet temperature,  $T_o$ , responds to the changes of inlet temperatures,  $T_1$  and  $T_2$ , taking the contents of the tank as the control volume, an unsteady state energy balance gives us the desired relation between the inlets and outlet temperatures.

Applying (2.1) in term of an equation:

$$\frac{d[V\rho u(t)]}{dt} = f_1(t) \rho h_1(t) + f_2(t) \rho h_2(t) - f_o(t) \rho h_o(t) - Q(t) \quad (2.2)$$

where:

$u(t)$  = internal energy of liquid in tank, J/kg.

$f_1(t), f_2(t), f_o(t)$  = volumetric flow rate,  $m^3/s$ .

$\rho$  = liquid density,  $kg/m^3$ .

$V$  = volume of liquid in tank,  $m^3$ .

$h_1(t), h_2(t), h_o(t)$  = inlet and outlet liquid enthalpies, J/kg.

In this process chemical reactions do not exist. Also in terms of temperatures, using as reference state for  $u(t)$  and  $h(t)$  the pure component in the liquid state at 0 degree and the pressure of the system, the forgoing equation can be written as:

$$\frac{d[V\rho u(t)]}{dt} = f_1(t) \rho K_p T_1 + f_2(t) \rho K_p T_2 - f_o(t) \rho K_p T_o - Q(t) \quad (2.3)$$

where:

$K_p$  = liquid heat capacity at constant pressure, J/kg-°C.

$K_v$  = liquid heat capacity at constant volume, J/kg-°C.

$Q(t)$  = rate of heat transfer to the surrounding, J/s.

Because the densities and the heat capacities are assumed constant and equal over the operating temperature range, inserting:

$$u(t) = K_v T_o \quad (2.4)$$

The last equation can be written as:

$$V\rho K_v \frac{d[T_o]}{dt} = f_1(t)\rho K_p T_1 + f_2(t)\rho K_p T_2 - f_o(t)\rho K_p T_o - Q(t) \quad (2.5)$$

According to the material balance with constant density and volume:

$$\frac{dV}{dt} = 0 \quad (2.6)$$

Then:

$$f_1(t) + f_2(t) = f_o(t) \quad (2.7)$$

From (2.5) and (2.7):

$$V\rho K_v \frac{d[T_o]}{dt} = f_1(t)\rho K_p T_1 + f_2(t)\rho K_p T_2 - f_1(t)\rho K_p T_o - f_1(t)\rho K_p T_o - Q(t) \quad (2.8)$$

$$V\rho K_v \frac{d[T_o]}{dt} = f_1(t)\rho K_p [T_1 - T_o] + f_2(t)\rho K_p [T_2 - T_o] - Q(t)$$

$$\frac{d[T_o]}{dt} = \frac{f_1(t)\rho K_p}{V\rho K_v} [T_1 - T_o] + \frac{f_2(t)\rho K_p}{V\rho K_v} [T_2 - T_o] - \frac{Q(t)}{V\rho K_v} \quad (2.9)$$

Also

$$Q(t) = UA[T_o - T_a] \quad (2.10)$$

where:

U= heat transfer rate to the surroundings, J/s.

A= heat transfer area, m<sup>2</sup>.

T<sub>a</sub>= temperature of surroundings, C°, an input variable.

Substituting (2.10) in (2.9):

$$\frac{d[T_o]}{dt} = \frac{f_1(t)\rho K_p}{V\rho K_v} [T_1 - T_o] + \frac{f_2(t)\rho K_p}{V\rho K_v} [T_2 - T_o] - \frac{UA[T_o - T_a]}{V\rho K_v} \quad (2.11)$$

### 2.2.2. Pump Speed Mathematical Model [18]

As prescribed in previous sections this thesis focuses on a system that consists of centrifugal pump powered by a variable speed DC electric motor and pumping out from a constant volume water-tank. The tank receives liquid through two intakes having flow rates  $f_1(t)$  and  $f_2(t)$  through two control valves.



Mathematical model is developed by analyzing the dynamics of the plant and it is based on fundamental laws of physics and fluid mechanics. Determining the mathematical model of the plant includes determining mathematical models of centrifugal pump and tank.

The counterpart of Newton's law of force says that the angular acceleration is proportional to the torque on the axis. Hence, the equation of motion for the motor-pump set can be written as:

$$J \frac{dw}{dt} = \tau_a - \tau_p = \tau_{MT} - (\tau_p + \tau_\zeta) \quad (2.12)$$

where:

$J$  = moment of inertia (kg.m<sup>2</sup>)

$\tau_a = \tau_{MT}$  = active output torque of the DC motor (N.m)

$\tau_p$  = passive/resistive torque of the pump (N.m)

$\tau_\zeta$  = is the viscous torque (N.m)

The pump torque includes two terms, passive torque  $M_p$  and viscous torque  $M_\zeta$  which is defined as when an object moves through a fluid, the viscosity of the fluid acts on the moving object with a force that resists the motion of the object. Commonly, viscous torque is modeled by either Newton's or Stokes' models. Both models agree that the drag force acts in the direction opposite to the velocity vector for the object in motion [19].

The pump viscous torque and passive torque are given by:

$$\tau_\zeta = k_\zeta w \quad (2.13)$$

$$\tau_p = \frac{\rho g f_o(t) H}{\eta w} \quad (2.14)$$

where:

$k_\zeta$  = viscous torque constant (N.m/rad/s).

$w$  = pump speed (rpm or rad/s)

$g$  = gravity (m/s<sup>2</sup>)

From (2.14) it can be concluded that the basic parameters of centrifugal pump are: pump flow rate  $f_o(t)$ , pump head  $H$  and angular velocity  $w$ . Pump flow rate can be expressed by peripheral cross section of the impeller channels and meridian component of velocity. Thus, for different modes of operation the flow is proportional to the angular velocity, as it is:

$$\frac{H'}{H} = \frac{w'^2}{w^2} \quad (2.15)$$

It should be noted that the last equation is obtained assuming that the pump efficiency coefficient is constant. Basically it is slightly changed in different modes, which to some extent reflects to the parameters. Equation (2.15) is valid for any two modes, so if it is written for arbitrary and nominal mode and replaced into (2.14) it is obtained:

$$\tau_p = \frac{\rho g H_N}{\eta w_N^2} f_o(t) w = k_r f_o(t) w \quad (2.16)$$

Pump suppliers set the pump characteristics ( $f_o(t)$ - $H$  and  $f_o(t)$ - $\eta$  curves) for a nominal speed  $n$ . Due to the complexity of centrifugal pump dynamics, the assumption that  $f_o(t)$ - $H$  curve with sufficient accuracy describes the behavior of the pump in transitional regimes is accepted into analysis of their work, i.e. static characteristic of the pump is used. The characteristic curve of a centrifugal pump can be described by the equation:

$$H = Aw^2 + Bwf_o(t) + Cf_o^2(t) \quad (2.17)$$

where  $A$ ,  $B$  and  $C$  are characteristic constants for each pump, that is a parabola family with parameter  $w$ , i.e. this expression determines the family of static characteristics of centrifugal pump. From (2.17), expressing  $f_o(t)$  and  $w$  through their nominal values, the pump head will be:

$$\begin{aligned} H &= \left( A + B \frac{f_{oN}(t)}{w_N} + C \frac{f_{oN}(t)^2}{w_N^2} \right) w^2 \\ &= k_w w^2 \end{aligned} \quad (2.18)$$

where:

$k_w$  is constant assuming a limitation for the pump speed and flow.

The head of a pump in terms of the pressure difference across the pump can be expressed as [20]:

$$H = \frac{P_3 - P}{\rho g} + \frac{S^2}{2g} \quad (2.19)$$

where:

$P_3, P$  = static pressures after and before the pump, respectively, kPa

$S$  = dynamic pressure, kPa

From (2.18) and (2.19) we can derive

$$\frac{P_3 - P}{\rho g} + \frac{S^2}{2g} = k_w w^2$$

$$P = P_3 + \frac{\rho S^2}{2} - \rho g k_w w^2 \quad (2.20)$$

As long as today's technology needs to be easier and faster responses, which means using few number of components for controlling an equipment. DC motor is one of such equipments, whose speed is directionally proportional to the supply voltage. The DC motor uses electricity and a magnetic field to produce torque.

In modeling the armature controlled DC motor for this study, simple electrical circuit of armature controlled DC motor diagram as shown in Figure 2.1 was employed [21, 22].

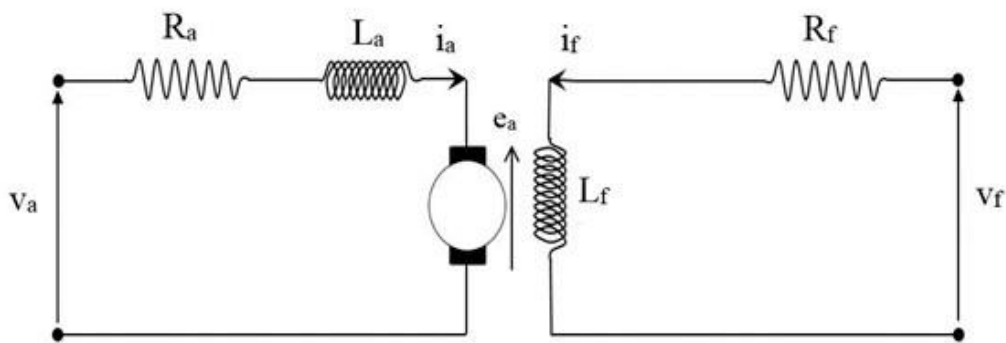


Figure 2.1. Separately excited armature controlled DC motor diagram.

Instantaneous armature current is:

$$V_a = i_a R_a + e_a + L_a \frac{di_a}{dt} \quad (2.21)$$

where:

$L_a$  and  $R_a$  are the armature inductance and resistance, respectively.

The motor back emf, which is also known as speed voltage, is expressed as:

$$e_a = k_n \omega_a \quad (2.22)$$

where:

$k_n$  = motor voltage constant (in V/A-rad/s).

In assumptions that the field excitation circuit is constant and under steady state operation the time derivative is zero, assuming the motor is not saturated:

$$V_a = i_a R_a + e_a \quad (2.23)$$

The torque developed by the motor is:

$$\tau_{MT} = i_a k_T \gg i_a = \frac{\tau_{MT}}{k_T} \quad (2.24)$$

where:

$k_T$  = torque constant in V/A-rad/sec.

$M_{MT}$  can be derived by substituting (2.22) and (2.20) into (2.21):

$$\tau_{MT} = \frac{k_T V_a}{R_a} - \frac{k_T k_n}{R_a} \omega \quad (2.25)$$

The speed of DC motor can simply be set by applying the correct voltage [23].

In assumption that simple term  $m_3(x)$  is a motor setting point voltage, (2.25) will be:

$$\tau_{MT} = \frac{k_T V_a m_3(x)}{R_a} - \frac{k_T k_n}{R_a} \omega \quad (2.26)$$

### 2.2.3. Control Valve Mathematical Model

In process control systems valve is a control device, it can be used to regulate the flow of materials within a process. Nowadays several different kinds of valves (butterfly, ball, globe etc.) exist, depending on the application and chemical process in consideration they can be selected. The sizing of valves depends on the fluids processing unit (heat exchanger, tank, pump etc.) which is in series with the valve [23].

Also the control valve is simply an orifice with a variable area of flow. If  $C_v$  is defined as valve coefficient, the basic principles regulating flow through an orifice provide the following formula for the liquid flow rate through the valve [16].

$$f(t) = C_v m(x) \sqrt{\frac{\Delta P_v}{s.g}} \quad (2.27)$$

where:

$f(t)$ =liquid flow rate

$\Delta P_v$  =pressure drop across the valve

s.g =specific gravity of liquid

$m(x)$ =flow characteristic.

$C_v$  =valve coefficient.

The above equation is a general equation which is used to describe flow through a valve. This is the equation to start with when you want to model a valve and it can be modified for different situations. The key is  $m(x)$ , inherent flow characteristic in modeling the flow through a valve, and depends on the kind of valve you are using [23].

Here in this thesis the linear ( $m(x) = x$  for linear valve control) is assumed which means flow is directly proportional to the valve lift. Also according to the pump speed interaction to the valves flow, it gives a nonlinearity to the system. For developing the mathematical models of both valves within pump speed the following steps are done:

The  $\Delta P_v$  are between  $P_i$  and  $P$ , so we can derive equations like:

$$\begin{aligned} f_i(t) &= C_s m_i(x) \sqrt{\Delta P_v} \quad \text{and } i = 1, 2 \\ &= C_s m_i(x) \sqrt{P_i - P} \end{aligned} \quad (2.28)$$

where:

$$C_s = \frac{C_v}{\sqrt{1/s.g}}$$

By substituting (2.20) in (2.28)

$$f_1(t) = C_s m_1(x) \sqrt{P_1 - P_3 + \frac{\rho(S_1^2 - S_3^2)}{2} + \rho g k_w w^2} \quad (2.29)$$

Also this equation applies for the second valve

$$f_2(t) = C_s m_2(x) \sqrt{P_2 - P_3 + \frac{\rho(S_2^2 - S_3^2)}{2} + \rho g k_w w^2} \quad (2.30)$$

where:

$P_1, P_2, P_3$  and  $P$  are static pressures in front of the two valves, outtake of pump and inside the tank followed by  $S_1, S_2$  and  $S_3$  the dynamic pressures respectively.

### 2.3. Combining the System Dynamic Equations

By substituting (2.29) and (2.30) in (2.7)

$$f_o(t) = C_s m_1(x) \sqrt{P_1 - P_3 + \frac{\rho(S_1^2 - S_3^2)}{2} + \rho g k_w w^2} + C_s m_2(x) \sqrt{P_2 - P_3 + \frac{\rho(S_2^2 - S_3^2)}{2} + \rho g k_w w^2} \quad (2.31)$$

By substituting (2.31) into (2.16)

$$\tau_p = C_s k_r w (m_1(x) \sqrt{G_1} + m_2(x) \sqrt{G_2}) \quad (2.32)$$

where:

$$G_1 = P_1 - P_3 + \frac{\rho(S_1^2 - S_3^2)}{2} + \rho g k_w w^2$$

$$G_2 = P_2 - P_3 + \frac{\rho(S_2^2 - S_3^2)}{2} + \rho g k_w w^2$$

Substituting (2.13), (2.26) and (2.32) into (2.12) gives

$$\frac{dw}{dt} = \frac{k_T V_a m_3(x)}{J R_a} - \frac{k_T k_n}{J R_a} w - \left( \frac{C_s k_r w}{J} (m_1(x) \sqrt{G_1} + m_2(x) \sqrt{G_2}) \right) + \frac{k_\zeta}{J} w \quad (2.33)$$

Also substituting (2.29) and (2.30) into (2.11) gives

$$\begin{aligned} \frac{dT_o}{dt} = & \frac{C_s m_1(x) \sqrt{G_1} \rho K_p}{V \rho K_v} [T_1 - T_o] \\ & + \frac{C_s m_2(x) \sqrt{G_2} \rho K_p}{V \rho K_v} [T_2 - T_o] - \frac{UA [T_o - T_a]}{V \rho K_v} \end{aligned} \quad (2.34)$$

After neglecting the work done by the mixing impeller and other mentioned assumptions, two equations are derived which are the system output variables. Equations (2.34) and (2.31) are the system tank state temperature and output flow rate variables respectively. Equation (2.33) is the speed change of the pump which means partly related to the output flow rate, since flow rate is also related to the valve positions.

#### 2.4. Linearization of the Nonlinear Model

Many dynamic chemical processes are modeled by set of nonlinear, first-order differential equations that generally arise from material and energy balances around the system [24]. As described above in this thesis two nonlinear, first order differential equations exist which they state tank temperature variation, which is directly related to the temperature controlled variable and pump speed variation, which gives controlled flow rate variable under constant valve position assumption.

Process models are often linearized to perform stability analysis. Linear models are easier to understand and are necessary for most control system design methods [24].

State-space models use a system of first order ordinary differential equations in order to describe the dynamic behavior of the state variables. The model is comprised of an equation for each of the state variables that describes how this variable changes in time as a function of the other state variables and the external inputs [25].





### 2.4.1. Linearization Technique

Before we generalize our results, we will illustrate linearization for a single variable problem, considering a system with one state variable and one input variable. A general single variable nonlinear model is:

$$\dot{x} = \frac{dx}{dt} = f(x, u) \quad (2.39)$$

The function of a single variable,  $f(x, u)$ , can be approximated by a truncated Taylor series approximation around the steady-state operating point  $(x_s, u_s)$ :

$$\begin{aligned} \dot{x} = f(x_s, u_s) &= \left. \frac{\partial f}{\partial x} \right|_{x_s u_s} (x - x_s) + \left. \frac{\partial f}{\partial u} \right|_{x_s u_s} (u - u_s) \\ &+ \frac{1}{2} \left. \frac{\partial^2 f}{\partial x^2} \right|_{x_s u_s} (x - x_s)^2 + \left. \frac{\partial^2 f}{\partial x \partial u} \right|_{x_s u_s} (x - x_s)(u - u_s) \\ &+ \frac{1}{2} \left. \frac{\partial^2 f}{\partial u^2} \right|_{x_s u_s} (u - u_s)^2 \dots \text{higher order terms} \end{aligned} \quad (2.40)$$

Truncating after the linear terms, we have:

$$\dot{x} \approx f(x_s, u_s) \left. \frac{\partial f}{\partial x} \right|_{x_s u_s} (x - x_s) + \left. \frac{\partial f}{\partial u} \right|_{x_s u_s} (u - u_s) \quad (2.41)$$

Realizing that  $f(x_s, u_s) = 0$  and  $dx/dt = d(x - x_s)/dt$

$$\frac{d(x - x_s)}{dt} \approx \left. \frac{\partial f}{\partial x} \right|_{x_s u_s} (x - x_s) + \left. \frac{\partial f}{\partial u} \right|_{x_s u_s} (u - u_s) \quad (2.42)$$

Using deviation variables,  $\dot{x} = x - x_s$  and  $\dot{u} = u - u_s$ ,

$$\frac{d\dot{x}}{dt} \approx \left. \frac{\partial f}{\partial x} \right|_{x_s u_s} \dot{x} + \left. \frac{\partial f}{\partial u} \right|_{x_s u_s} \dot{u} \quad (2.43)$$

which can be written:

$$\frac{d\dot{x}}{dt} = A\dot{x} + B\dot{u} \quad (2.44)$$

where:

$$a = \left. \frac{\partial f}{\partial x} \right|_{x_s u_s} \quad \text{and} \quad b = \left. \frac{\partial f}{\partial u} \right|_{x_s u_s}$$

If there is a single output that is a function of the states and inputs, then:

$$y = g(x, u) \quad (2.45)$$

Again, performing a Taylor series expansion and truncating the quadratic and higher terms:

$$g(x, u) \approx g(x_s, u_s) + \left. \frac{\partial g}{\partial x} \right|_{x_s, u_s} (x - x_s) + \left. \frac{\partial g}{\partial u} \right|_{x_s, u_s} (u - u_s) \quad (2.46)$$

Since  $g(x_s, u_s)$  is simply the steady-state value of the output ( $y_s$ ), we can write:

$$y \approx g(x_s, u_s) + \left. \frac{\partial g}{\partial x} \right|_{x_s, u_s} (x - x_s) + \left. \frac{\partial g}{\partial u} \right|_{x_s, u_s} (u - u_s) \quad (2.47)$$

or

$$y - y_s = C(x - x_s) + D(u - u_s) \quad (2.48)$$

where:

$$c = \left. \frac{\partial g}{\partial x} \right|_{x_s, u_s} \quad \text{and} \quad d = \left. \frac{\partial g}{\partial u} \right|_{x_s, u_s}$$

using deviation notation:

$$\dot{y} = C\dot{x} + D\dot{u} \quad (2.49)$$

The above description shows how to linearize single-state variable systems. In the thesis above technique is generalized for any number of states which is MIMO system.

Generally, the (·) notation is dropped and it is understood that the model is in deviation variable form:

$$\dot{x} = Ax + Bu \quad (2.37)$$

$$y = Cx + Du \quad (2.38)$$

#### 2.4.2. Interpretation of Linearization

In Section 2.3 the method of linearization of models into state-space form is illustrated. The objective of this section is to illustrate what is meant by linearization of a function. Now considering out thesis system the stirred tank with two control valves in series with a pump at the outtake as shown in Figure 2.2.

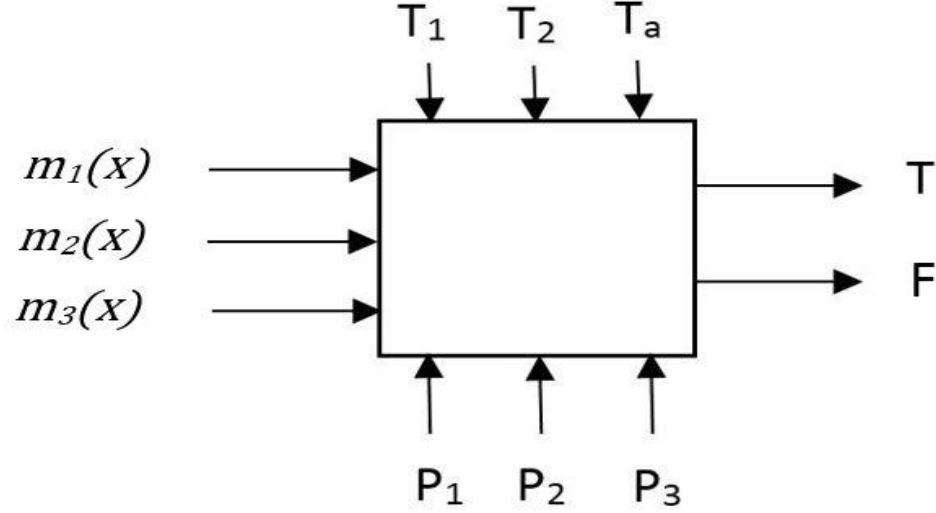


Figure 2.2. Proposed thesis open loop system black box block diagram including inputs, outputs and disturbances.

Linearization will be applied considering that  $m_1(x)$ ,  $m_2(x)$  and  $m_3(x)$  are the system controller inputs.  $T$  and  $F$  are temperature and flow output controlled variables, within taking  $(T_1, T_2, T_a, P_1, P_2, P_3)$  as system major and minor disturbances.

Equations (2.33) and (2.34) are obtained thesis dynamic models and valid for any mode of operation of the plant, and therefore, they can be applied to the nominal mode, in which case they get the form [18]:

$$\begin{aligned} \frac{C_s m_1(x) \sqrt{G_1} \rho K_p}{V \rho K_v} [T_1 - T_o] \\ + \frac{C_s m_2(x) \sqrt{G_2} \rho K_p}{V \rho K_v} [T_2 - T_o] - \frac{UA [T_o - T_a]}{V \rho K_v} = 0 \end{aligned} \quad (2.50)$$

$$\begin{aligned} \frac{k_T V_a m_3(x)}{J R_a} - \frac{k_T k_n}{J R_a} w - \left( \frac{C_s k_r w}{J} (m_1(x) \sqrt{G_1} + m_2(x) \sqrt{G_2}) \right) \\ + \frac{k_\zeta}{J} w = 0 \end{aligned} \quad (2.51)$$

In the general nonlinear model,  $X$  is a vector of  $n=2$  state variables ( $T_o$  and  $w$ ),  $U$  is a vector of  $m=3$  input variables  $m_1(x)$ ,  $m_2(x)$ , and  $m_3(x)$  and  $Y$  is a vector of  $r=2$  output variables ( $T_o$  and  $F$ ).  $Z$  is also a vector of 6 disturbance variables ( $T_1, T_2, T_a, P_1, P_2$  and  $P_3$ ).

$$\left. \begin{aligned} \dot{x}_1 &= \frac{dT_o}{dt} = f_1(T_o, w, m_1(x), m_2(x), m_3(x), T_1, T_2, T_a, P_1, P_2, P_3) \\ \dot{x}_2 &= \frac{dw}{dt} = f_2(T_o, w, m_1(x), m_2(x), m_3(x), T_1, T_2, T_a, P_1, P_2, P_3) \end{aligned} \right\} \quad (2.52)$$

$$\left. \begin{aligned} y_1 &= g_1(T_o, w, m_1(x), m_2(x), m_3(x), T_1, T_2, T_a, P_1, P_2, P_3) \\ y_2 &= g_2(T_o, w, m_1(x), m_2(x), m_3(x), T_1, T_2, T_a, P_1, P_2, P_3) \end{aligned} \right\} \quad (2.53)$$

Normalized values are based on steady-state operating values. The equations that describe the behavior of the system can be presented in state space form by selecting the appropriate state variables. In addition, whenever it is possible, it is necessary to conduct linearization in order to get a simplified mathematical description of the system. In the case study, assuming that the relative deviations of individual variables are small enough, the linearization of the functions  $f_1$  and  $f_2$  can be performed. The choice of state variables is made as follows:

$$x_1 = T_o$$

$$x_2 = w$$

$$X = [x_1 \ x_2]^T$$

$$U = [u_1 \ u_2 \ u_3]^T$$

$$Z = [z_1 \ z_2 \ z_3 \ z_4 \ z_5 \ z_6]^T$$

where:

$X$  is a state vector and  $Z$  is the vector of disturbances mentioned above.

As a result of the linearization procedure of the functions  $f_1$  and  $f_2$ , the following constants are obtained:

$$\begin{aligned} a_{11} &= \frac{\partial f_1}{\partial x_1} = \frac{\partial f_1}{\partial (T - T_{os})} = \frac{\partial f_1}{\partial T} \\ &= - \frac{C_s m_1(t) \sqrt{G_1} \rho K_p}{V \rho K_v} - \frac{C_s m_2(t) \sqrt{G_2} \rho K_p}{V \rho K_v} - \frac{UA}{V \rho K_v} \Big|_{\text{Nominals}} \end{aligned} \quad (2.54)$$

where:

Nominals are steady state values

$$= T_{os}, w_s, m_{1N}(x), m_{2N}(x), m_{3N}(x), T_{1N}, T_{2N}, T_{aN}, P_{1N}, P_{2N}, P_{3N}$$

$$\begin{aligned}
a_{12} &= \frac{\partial f_1}{\partial x_2} = \frac{\partial f_1}{\partial (w - w_s)} = \frac{\partial f_1}{\partial w} \\
&= [T_1 - T_0] \frac{C_s m_1(t) \rho g k_w w \rho K_p}{V \rho K_v \sqrt{G_1}} \\
&\quad + [T_2 - T_0] \frac{C_s m_2(t) \rho g k_w w \rho K_p}{V \rho K_v \sqrt{G_2}} \Big|_{\text{Nominals}}
\end{aligned} \tag{2.55}$$

$$a_{21} = \frac{\partial f_2}{\partial x_1} = \frac{\partial f_2}{\partial (T - T_{os})} = 0 \tag{2.56}$$

$$\begin{aligned}
a_{22} &= \frac{\partial f_2}{\partial x_{21}} = \frac{\partial f_2}{\partial (w - w_s)} = \frac{\partial f_2}{\partial w} \\
&= - \frac{k_T}{J R_a} k_n - \frac{C_s k_r}{J} \left\{ (m_1(t) (\sqrt{G_1} + \frac{\rho g k_w w^2}{\sqrt{G_1}})) \right. \\
&\quad \left. + (m_2(t) (\sqrt{G_2} + \frac{\rho g k_w w^2}{\sqrt{G_2}})) \right\} + \frac{k_z}{J} \Big|_{\text{Nominals}}
\end{aligned} \tag{2.57}$$

$$b_{11} = \frac{\partial f_1}{\partial u_1} = \frac{\partial f_1}{\partial (m_1 - m_{1N})} = \frac{\partial f_1}{\partial m_1} = \frac{C_s \sqrt{G_1} \rho K_p}{V \rho K_v} [T_1 - T_0] \Big|_{\text{Nominals}} \tag{2.58}$$

$$b_{12} = \frac{\partial f_1}{\partial u_2} = \frac{\partial f_1}{\partial (m_2 - m_{2N})} = \frac{\partial f_1}{\partial m_2} = \frac{C_s \sqrt{G_2} \rho K_p}{V \rho K_v} [T_2 - T_0] \Big|_{\text{Nominals}} \tag{2.59}$$

$$b_{13} = \frac{\partial f_1}{\partial u_3} = \frac{\partial f_1}{\partial (m_3 - m_{3N})} = \frac{\partial f_1}{\partial m_3} = 0 \tag{2.60}$$

$$b_{21} = \frac{\partial f_2}{\partial u_1} = \frac{\partial f_2}{\partial (m_1 - m_{1N})} = \frac{\partial f_2}{\partial m_1} = - \frac{C_s k_r}{J} w \sqrt{G_1} \Big|_{\text{Nominals}} \tag{2.61}$$

$$b_{22} = \frac{\partial f_2}{\partial u_2} = \frac{\partial f_2}{\partial (m_2 - m_{2N})} = \frac{\partial f_2}{\partial m_2} = - \frac{C_s k_r}{J} w \sqrt{G_2} \Big|_{\text{Nominals}} \tag{2.62}$$

$$b_{23} = \frac{\partial f_2}{\partial u_3} = \frac{\partial f_2}{\partial (m_3 - m_{3N})} = \frac{\partial f_2}{\partial m_3} = \frac{k_T V_a}{J R_a} \Big|_{\text{Nominals}} \tag{2.63}$$

Also by the same form as calculated linearized input controller vector, the disturbance vector F is found.

$$v_{11} = \frac{\partial f_1}{\partial z_1} = \frac{\partial f_1}{\partial (T_1 - T_{1s})} = \frac{\partial f_1}{\partial T_1} = \frac{C_s m_1(t) \sqrt{G_1} \rho K_p}{V \rho K_v} \Big|_{\text{Nominals}} \tag{2.64}$$

$$v_{12} = \frac{\partial f_1}{\partial z_2} = \frac{\partial f_1}{\partial(T_2 - T_{2s})} = \frac{\partial f_1}{\partial T_2} = \frac{C_s m_2(t) \sqrt{G_2} \rho K_p}{V \rho K_v} \Big|_{\text{Nominals}} \quad (2.65)$$

$$v_{13} = \frac{\partial f_1}{\partial z_3} = \frac{\partial f_1}{\partial(T_a - T_{as})} = \frac{\partial f_1}{\partial T_a} = \frac{UA}{V \rho K_v} \Big|_{\text{Nominals}} \quad (2.66)$$

$$v_{14} = \frac{\partial f_1}{\partial z_4} = \frac{\partial f_1}{\partial(P_1 - P_{1s})} = \frac{\partial f_1}{\partial P_1} = + \frac{C_s m_1(t) \rho K_p}{2 \sqrt{G_1}} [T_1 - T_0] \Big|_{\text{Nominals}} \quad (2.67)$$

$$v_{15} = \frac{\partial f_1}{\partial z_5} = \frac{\partial f_1}{\partial(P_2 - P_{2s})} = \frac{\partial f_1}{\partial P_2} = + \frac{C_s m_2(t) \rho K_p}{2 \sqrt{G_2}} [T_2 - T_0] \Big|_{\text{Nominals}} \quad (2.68)$$

$$\begin{aligned} v_{16} &= \frac{\partial f_1}{\partial z_6} = \frac{\partial f_1}{\partial(P_3 - P_{3s})} = \frac{\partial f_1}{\partial P_3} \\ &= - \frac{C_s m_1(t) \rho K_p}{2 V \rho K_v \sqrt{G_1}} [T_1 - T_0] \\ &\quad - \frac{C_s m_2(t) \rho K_p}{2 V \rho K_v \sqrt{G_2}} [T_2 - T_0] \Big|_{\text{Nominals}} \end{aligned} \quad (2.69)$$

$$v_{21} = \frac{\partial f_2}{\partial z_1} = \frac{\partial f_2}{\partial(T_1 - T_{1s})} = \frac{\partial f_2}{\partial T_1} = 0 \quad (2.70)$$

$$v_{22} = \frac{\partial f_2}{\partial z_2} = \frac{\partial f_2}{\partial(T_2 - T_{2s})} = \frac{\partial f_2}{\partial T_2} = 0 \quad (2.71)$$

$$v_{23} = \frac{\partial f_2}{\partial z_3} = \frac{\partial f_2}{\partial(T_a - T_{as})} = \frac{\partial f_2}{\partial T_a} = 0 \quad (2.72)$$

$$v_{24} = \frac{\partial f_2}{\partial z_4} = \frac{\partial f_2}{\partial(P_1 - P_{1s})} = \frac{\partial f_1}{\partial P_1} = - \frac{C_s m_1(t) w k_r}{2 J \sqrt{G_1}} \Big|_{\text{Nominals}} \quad (2.73)$$

$$v_{25} = \frac{\partial f_2}{\partial z_5} = \frac{\partial f_2}{\partial(P_2 - P_{2s})} = \frac{\partial f_2}{\partial P_2} = - \frac{C_s m_2(t) w k_r}{2 J \sqrt{G_2}} \Big|_{\text{Nominals}} \quad (2.74)$$

$$\begin{aligned} v_{26} &= \frac{\partial f_2}{\partial z_6} = \frac{\partial f_2}{\partial(P_3 - P_{3s})} = \frac{\partial f_2}{\partial P_3} \\ &= \frac{C_s k_r}{2 J} w \left( \frac{m_1(t)}{\sqrt{G_1}} + \frac{m_2(t)}{\sqrt{G_2}} \right) \Big|_{\text{Nominals}} \end{aligned} \quad (2.75)$$

The state variables method is used here to describe more easily the dynamics of the system. The compact representation of the mathematical model using matrices is the advantage of this method which in this form allows computer simulation of system dynamics and designing controller in relatively easy way. Thus, by choosing the

appropriate state variables and linearization carried out, the linear mathematical model of the plant in the state space form has been obtained [18].

$$\dot{X} = AX + BU + VZ$$

$$\begin{bmatrix} \dot{x}_1 \\ \dot{x}_2 \end{bmatrix} = \begin{bmatrix} a_{11} & a_{12} \\ a_{21} & a_{22} \end{bmatrix} \begin{bmatrix} x_1 \\ x_2 \end{bmatrix} + \begin{bmatrix} b_{11} & b_{12} & b_{13} \\ b_{21} & b_{22} & b_{23} \end{bmatrix} \begin{bmatrix} u_1 \\ u_2 \\ u_3 \end{bmatrix} + \begin{bmatrix} v_{11} & v_{12} & v_{13} & v_{14} & v_{15} & v_{16} \\ v_{21} & v_{22} & v_{23} & v_{24} & v_{25} & v_{26} \end{bmatrix} \begin{bmatrix} z_1 \\ z_2 \\ z_3 \\ z_4 \\ z_5 \\ z_6 \end{bmatrix}$$

$$\begin{bmatrix} \frac{dT}{dt} \\ \frac{dw}{dt} \end{bmatrix} = \begin{bmatrix} \frac{\partial f_1}{\partial T} & \frac{\partial f_1}{\partial w} \\ \frac{\partial f_2}{\partial T} & \frac{\partial f_2}{\partial w} \end{bmatrix} \begin{bmatrix} T \\ w \end{bmatrix} + \begin{bmatrix} \frac{\partial f_1}{\partial m_1} & \frac{\partial f_1}{\partial m_2} & \frac{\partial f_1}{\partial V_a} \\ \frac{\partial f_2}{\partial m_1} & \frac{\partial f_2}{\partial m_2} & \frac{\partial f_2}{\partial V_a} \end{bmatrix} \begin{bmatrix} m_1(x) \\ m_2(x) \\ m_3(x) \end{bmatrix} + \begin{bmatrix} \frac{\partial f_1}{\partial T_1} & \frac{\partial f_1}{\partial T_2} & \frac{\partial f_1}{\partial T_a} & \frac{\partial f_1}{\partial P_1} & \frac{\partial f_1}{\partial P_2} & \frac{\partial f_1}{\partial P_3} \\ \frac{\partial f_2}{\partial T_1} & \frac{\partial f_2}{\partial T_2} & \frac{\partial f_2}{\partial T_a} & \frac{\partial f_2}{\partial P_1} & \frac{\partial f_2}{\partial P_2} & \frac{\partial f_2}{\partial P_3} \end{bmatrix} \begin{bmatrix} T_1 \\ T_2 \\ T_a \\ P_1 \\ P_2 \\ P_3 \end{bmatrix}$$

$$Y = CX + DU$$

$$\begin{bmatrix} y_1 \\ y_2 \end{bmatrix} = \begin{bmatrix} c_{11} & c_{12} \\ c_{21} & c_{22} \end{bmatrix} \begin{bmatrix} x_1 \\ x_2 \end{bmatrix} + \begin{bmatrix} d_{11} & d_{12} & d_{13} \\ d_{21} & d_{22} & d_{23} \end{bmatrix} \begin{bmatrix} u_1 \\ u_2 \\ u_3 \end{bmatrix}$$

Since one state is measured,  $c_{11}$  and  $c_{12}$  are equal to one and zero, respectively. The output temperature is the same as state variable temperature while it is deviated variable from the steady state value.  $c_{21}$  is also equal to zero as long as there is no chemical interaction process and limited temperature level.  $c_{22}$  equated to some value taken from (2.31) after curve fitted to linearized value. Figure 2.3 shows the flow change according to pump speed and the curve fitting. Also D matrix elements are zero except  $d_{21}$  and  $d_{22}$  because valve positions are directly related to the output flow rate, and they are equal,  $d_{21} = d_{22}$ . The numerical value calculated through (2.29) and (2.30) and assuming 3 seconds time response to each valve is assumed.

$$\begin{aligned} & \begin{bmatrix} T_o \\ F \end{bmatrix} \\ &= \begin{bmatrix} 1 & 0 \\ 0 & 0.00596 \end{bmatrix} \begin{bmatrix} T_o \\ w \end{bmatrix} \\ &+ \begin{bmatrix} 0 & 0 & 0 \\ 11.5 \times 1(t-3) & 11.5 \times 1(t-3) & 0 \end{bmatrix} \begin{bmatrix} m_1(x) \\ m_2(x) \\ m_3(x) \end{bmatrix} \end{aligned}$$

where:  $1(t)$  is the unit step function.

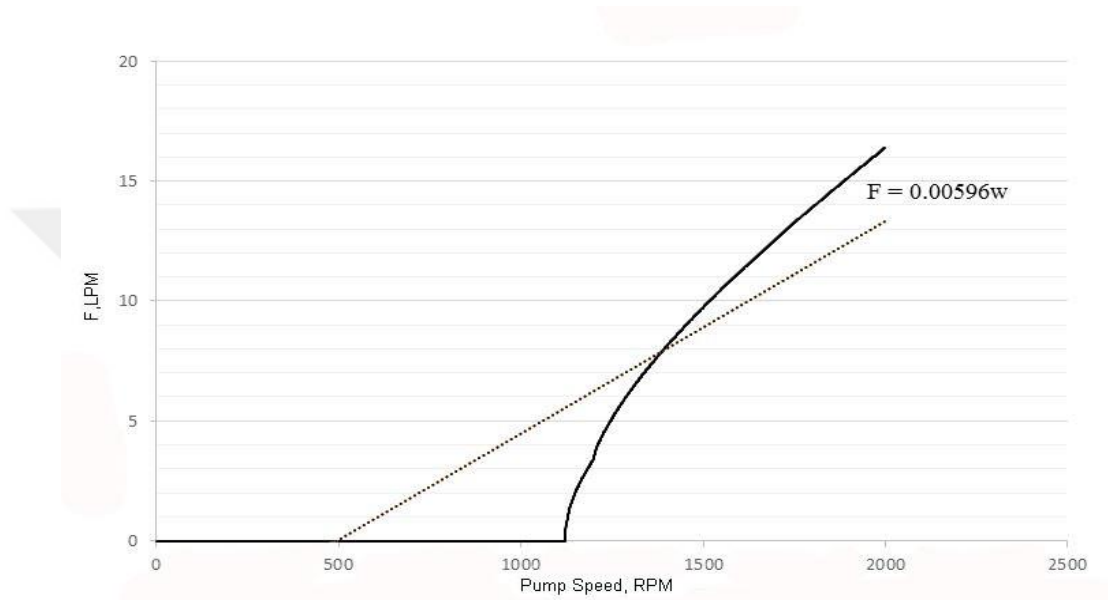


Figure 2.3. Pump speed vs. flow variations within constant valve positions, approximated to a linearly change through curve fitting.

Considering the Tables 2.1 and 2.2, the steady state values and parameters are given respectively to perform linearization:

Table 2.1. Steady state values of proposed system which are taken from real environment (Appendix 1).

variable	s.s value	variable	s.s value	variable	s.s value
$T_{1s}$	9.44 $C^{\circ}$	$P_{2s}$	115.8 kPa	$m_2(x)$	0.8
$T_{2s}$	48.8 $C^{\circ}$	$P_{3s}$	250 kPa	$m_3(x)$	1
$T_{os}$	42 $C^{\circ}$	w	1700 rpm	$V_a$	36 Volt
$P_{1s}$	96.52 kPa	$m_1(x)$	0.2		



Table 2.2. Assumed and real environment system parameters (Appendices 2, 3).

Parameter	values	Parameter	values	Parameter	values
$\rho$	1000kg/m <sup>3</sup>	J	0.05512kg.m <sup>2</sup>	$k_n$	0.0182
V	0.018 m <sup>3</sup>	g	9.81 m/s <sup>2</sup>	$K_p$	4.181
$R_a$	0.6758 $\Omega$	$k_T$	0.1527N/mA	$k_r$	0.926
$C_s$	0.67	$k_w$	0.000010935		

Notice that the values of UA and  $k_z$  have not been specified. These values can be obtained by solving the two dynamic Equations (2.32) (2.33) at steady-state.

From  $\frac{dw}{dt} = 0$  at steady-state, solve (2.32) to obtain  $k_z = \mathbf{0.0004527 \text{ N. m/rad/s}}$

From  $\frac{dT_o}{dt} = 0$  at steady-state, solve (2.33) to obtain  $UA = \mathbf{0.0042 \frac{kJ}{s.C}}$

According to equations (2.54 – 2.75), the numerical values of matrix entries in equations (2.37, 2.38) are calculated and following state space model is obtained:

$$\begin{aligned}
 & \begin{bmatrix} \frac{dT}{dt} \\ \frac{dw}{dt} \end{bmatrix} \\
 &= \begin{bmatrix} -0.01174 & -0.000038 \\ 0 & -0.0932 \end{bmatrix} \begin{bmatrix} T_o \\ w \end{bmatrix} \\
 &+ \begin{bmatrix} -0.3628 & 0.08 & 0 \\ -5.728 & -6.08 & 147.57 \end{bmatrix} \begin{bmatrix} m_1(t) \\ m_2(t) \\ m_3(t) \end{bmatrix} \\
 &+ \begin{bmatrix} 0.0022 & 0.0094 & 0.000055 & -0.0015 & 0.00126 & 0.00025 \\ 0 & 0 & 0 & -0.025 & -0.0958 & 0.1212 \end{bmatrix} \begin{bmatrix} T_1 \\ T_2 \\ T_a \\ P_1 \\ P_2 \\ P_3 \end{bmatrix}
 \end{aligned}$$

## 2.5. Laplace Domain Transformation

### 2.5.1. Transformation Technique

The ability to obtain linear approximations of physical systems allows the analyst to consider the use of the Laplace transformation. The Laplace transform method substitutes relatively easily solved algebraic equations for the more difficult differential equations [26, 27].

Now we turn to the matter of determining the transfer functions  $G_{ij}(s)$  of a multi-input, multi-output (MIMO) system. Recalling (2.37) and (2.38)

where  $y$  is the vector of multiple output and  $u$  is the multiple input, The Laplace transforms of above equations can be obtained as:

$$sX_{ij}(s) = AX_{ij}(s) + BU_{ij}(s)$$

$$Y_{ij}(s) = CX_{ij}(s) + DU_{ij}(s)$$

where  $B$  here is a  $3 \times 2$  matrix, since  $u$  is multi-input. Note that we do not include initial conditions, since we seek the transfer functions. Rearranging equation, we obtain

$$(sI - A)X_{ij}(s) = BU_{ij}(s)$$

Since  $[sI - A]^{-1} = \varphi(s)$ ,

$$X_{ij}(s) = \varphi(s)BU_{ij}(s)$$

Substituting  $X_{ij}(s)$  into (2.38),

$$Y_{ij}(s) = (\varphi(s)B + D)U_{ij}(s)$$

Therefore, the transfer functions  $N_{ij}(s) = \frac{Y_{ij}(s)}{U_{ij}(s)}$  are

$$N_{ij}(s) = (\varphi(s)B + D) \quad (2.76)$$

### 2.5.2. System State-Space Transformation to Laplace

Recalling (2.76) and substituting  $A$ ,  $B$ ,  $C$  and  $D$  matrices, the transfer functions will be:

$$N_{ij}(s) = \begin{bmatrix} 1 & 0 \\ 0 & 0.00596 \end{bmatrix} \left( s \begin{bmatrix} 1 & 0 \\ 0 & 1 \end{bmatrix} - \begin{bmatrix} -0.01174 & -0.000038 \\ 0 & -0.0932 \end{bmatrix} \right)^{-1} \\ * \begin{bmatrix} -0.3628 & 0.08 & 0 \\ -5.728 & -6.08 & 147.57 \end{bmatrix} \\ + \begin{bmatrix} 0 & 0 & 0 \\ 11.5 \times 1(t-3) & 11.5 \times 1(t-3) & 0 \end{bmatrix}$$

$$N_{ij}(s) = \begin{bmatrix} N_{11}(s) & N_{12}(s) & N_{13}(s) \\ N_{21}(s) & N_{22}(s) & N_{23}(s) \end{bmatrix}$$

where:

$$N_{11}(s) = \frac{-0.3628s - 0.034}{s^2 + 0.1049s + 0.0011}$$

$$N_{21}(s) = \frac{0.08s + 0.00768}{s^2 + 0.1049s + 0.0011}$$

$$N_{31}(s) = \frac{-0.0056}{s^2 + 0.1049s + 0.0011}$$

$$N_{12}(s) = N_{22}(s) = \frac{3.46s^2 + 0.35s + 0.0037}{s^3 + 0.4349s^2 + 0.035717s + 0.000363}$$

$$N_{32}(s) = \frac{0.875s + 0.00875}{s^2 + 0.1049s + 0.0011}$$

The characteristic  $p_{1,2}(s)$  are polynomial  $s^2 + 0.1049s + 0.0011$  and  $s^3 + 0.4349s^2 + 0.035717s + 0.000363$ , with the poles are -0.0118, -0.0931 and (-0.011, -0.093 and -0.33) respectively.

Also the transfer functions relating the system disturbances through the outputs, using the same method are:

$$G_{ij}(s) = (\varphi(s)V + D)$$

$$G_{ij}(s) = \begin{bmatrix} G_{11}(s) & G_{12}(s) & G_{13}(s) & G_{14}(s) & G_{15}(s) & G_{16}(s) \\ G_{21}(s) & G_{22}(s) & G_{23}(s) & G_{24}(s) & G_{25}(s) & G_{26}(s) \end{bmatrix}$$

where:

$$G_{11}(s) = \frac{0.0023s + 0.0002}{s^2 + 0.1049s + 0.0011}$$

$$G_{12}(s) = \frac{0.0094s + 0.0009}{s^2 + 0.1049s + 0.0011}$$

$$G_{13}(s) = \frac{(0.558s + 0.052)e - 04}{s^2 + 0.1049s + 0.0011}$$

$$G_{14}(s) = \frac{-0.0015s - 0.0001}{s^2 + 0.1049s + 0.0011}$$

$$G_{15}(s) = \frac{0.0013s + 0.0001}{s^2 + 0.1049s + 0.0011}$$

$$G_{16}(s) = \frac{0.0002}{s^2 + 0.1049s + 0.0011}$$

$$G_{21}(s) = G_{22}(s) = G_{23}(s) = 0$$

$$G_{24}(s) = G_{25}(s) = \frac{-0.18 * 10^{-5}s^2 - 6 * 10^{-7}s - 4 * 10^{-12}}{s^3 + 0.4349s^2 + 0.035717s + 0.000363}$$

$$G_{26}(s) = \frac{3.5s + 8.47 * 10^{-5}}{s^2 + 0.1049s + 0.0011}$$

## CHAPTER III

### MULTIVARIABLE CONTROL DESIGN

#### 3.1. Introduction

In conventional control systems the interest is to cope the lacks of the controlled process and cancel or reduce the effect of external disturbances. The main scope in this chapter is to keep the process controlled variables around desired values, and transfer the plant from one operating point to another or tracking the reference set point signal. In a general way, regulation and reference tracking result in very distinct control approaches and techniques.

The process should be capable of behaving in the required way. The best control subsystem will just provide the most suitable inputs to the process to fulfill the goals [28].

Since interactions are natural in many processes, they also exist in the current thesis proposed plant. Control goals, mainly based on qualitative and economical requirements as well as operational constraints, the controlled process structure should be simplified and a desirable controlled plant performances for “control design” should be derived.

In previous chapter the system mathematical model is linearized and transformed to transfer functions in order to ease the mechanism of loop interaction elimination and decouple the plant to sub-processes as explained in Section 3.2. Since in the linear case, existing interactions can be considered as (additive) disturbances [28], the main advantage is that the process is rearranged in such a way that nearly each input only influences one output which is lead to design the controllers and tuned independently. In other words variables can be grouped into several sets corresponding to each subsystem.

## **3.2. Decoupler Design**

### **3.2.1. Loop Interaction and Decoupling Method**

The proposed MIMO system, in which the controlled variables are the tank temperature and the flow rate out stream is accompanied by valve positioning and motor speed adjusting manipulated variables. The process is controlled by three loops, the chosen mechanism here is manipulating first valve position to control the tank temperature and the other two loops which are second valve position and adjusting pump speed to control the flow rate. Within this mechanism adjusting in the first control loop also changes the flow rate controlled variable, while the second loop which is adjustment in the second valve changes the tank temperature. The interesting point here is the third controlled loop, beside the flow rate controlling through decreasing the pressure afterwards of the valves effects the tank temperature due to nonlinearity at instant valve positions for the same pump speed as illustrates in the following section.

Hence there exist loop interactions for current thesis proposed MIMO system. Loop interactions need to be reduced or eliminated and pair the controlled and manipulated variables to minimize the effect of interaction, because changes in one loop might cause destabilizing changes in another loop. To avoid loop interactions, MIMO systems can be decoupled which means the system loops separate to independent loops.

The simplest way to reduce or eliminate the loop interaction in control systems is by decoupling. It can be profitable, realistic possibility when applied carefully [16]. The design objectives which are reduction of interactions can be realized, by adding additional controllers called decouplers to conventional multiloop configuration [29].

One may design the system (statically or dynamically decoupled), depending on requirements imposed on a system [30]. Decouplers can be designed from block diagrams or from basic engineering principles. The basic difference is that decouplers form part of feedback control of loops. Because of this, they must be selected and designed with great care. Static decoupling is accomplished by leaving out the dynamic terms. The advantage is that only the steady-state gains of the transfer functions need to be used in designing a static decoupler [16].

### 3.2.2. Decoupler Design from Block Diagrams

The block diagram of current MIMO system which is a 3X2 interacting system is given in Figure 3.1. This block diagram shows graphically that the interaction between the loops is caused by the process “cross” blocks with transfer functions  $N_{12}(s)$ ,  $N_{21}(s)$  and  $N_{31}(s)$ .

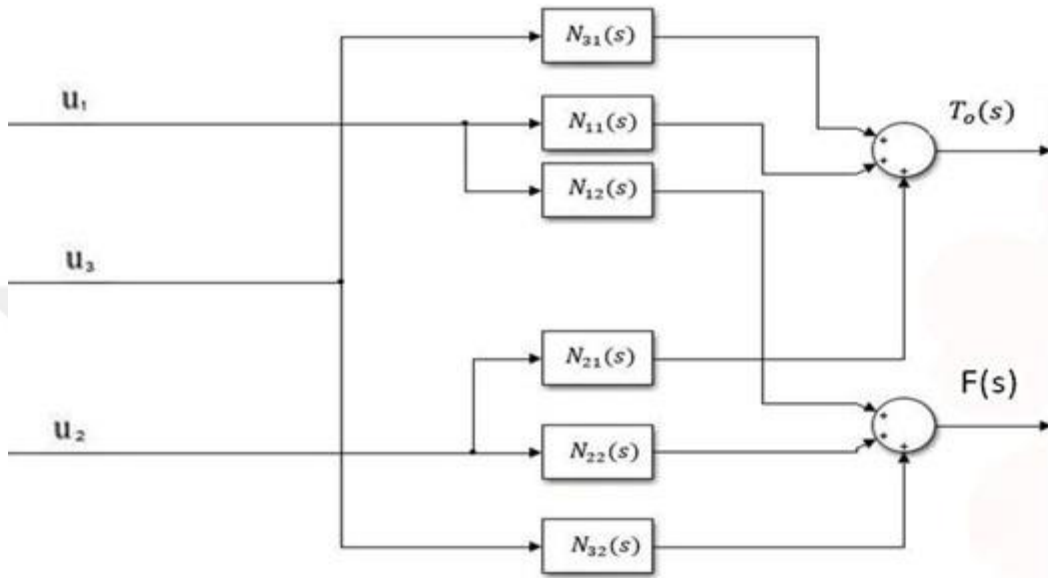


Figure 3.1. Open loop proposed thesis system block diagram.

To eliminate this interaction, keeping in mind the controlling mechanism procedure, three decoupler blocks with transfer functions  $D_{12}(s)$ ,  $D_{21}(s)$  and  $D_{31}(s)$  are installed, as in Figure 3.2. The purpose of the decouplers is to cancel the effect of the process cross blocks so that each controlled variable is not affected by changes in the manipulated variable of the other loop. In other words, decoupler  $D_{12}(s)$  cancels the effect of manipulated variables  $U_1(s)$  on controlled variable  $F(s)$ , and  $D_{21}(s)$  and  $D_{31}(s)$  cancel the effect of manipulated variable  $U_2(s)$  and  $U_3(s)$  respectively on controlled variable  $T_o(s)$ .

From block diagram algebra, these effects are:

$$\frac{F(s)}{U_1(s)} = D_{12}(s)N_{32}(s) + N_{12}(s) = 0 \quad (3.1)$$

$$\frac{T_o(s)}{U_2(s)} = D_{21}(s)N_{11}(s) + N_{21}(s) = 0 \quad (3.2)$$

$$\frac{T_o(s)}{U_3(s)} = D_{31}(s)N_{11}(s) + N_{31}(s) = 0 \quad (3.3)$$

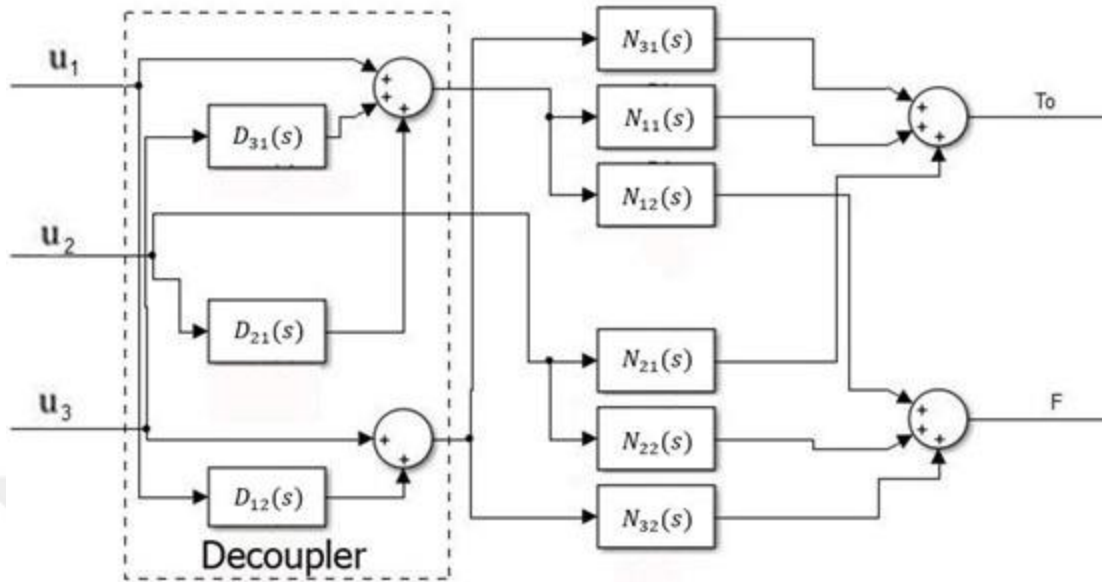


Figure 3.2. Open loop plant with proposed decoupler design.

The design formulas for the decouplers are obtained and solved from the decoupler transfer functions from (3.1 - 3.3)

$$D_{12}(s) = \frac{-N_{12}(s)}{N_{32}(s)} \quad (3.4)$$

$$D_{21}(s) = \frac{-N_{21}(s)}{N_{11}(s)} \quad (3.5)$$

$$D_{31}(s) = \frac{-N_{31}(s)}{N_{11}(s)} \quad (3.6)$$

The decouplers form part of the loops as pointed out above, which can also be seen from the block diagram of Figure 3.2. The relationship between each controlled variable and its manipulated variable in the decoupled diagram is obtained by block diagram algebra [16]:

$$\frac{F(s)}{U_1(s)} = D_{12}(s)N_{32}(s) + N_{12}(s) \quad (3.7)$$

$$\frac{T_o(s)}{U_2(s)} = D_{21}(s)N_{11}(s) + N_{21}(s) \quad (3.8)$$

$$\frac{T_o(s)}{U_3(s)} = D_{31}(s)N_{11}(s) + N_{31}(s) \quad (3.9)$$

The two terms in each formula tell us what the block diagram of Figure 3.2 tells us graphically, that in the decoupled system each controlled variables are affected by its manipulated variable through two parallel paths. As with the interacting system, these two paths may help each other if their effects are additive (positive interaction), or fight each other if the effects are of the opposite sign (negative interaction) [16].

### 3.2.3. Static and Dynamic Decoupling

As pointed out earlier, decoupling can be accomplished statically and dynamically. Static decoupling is accomplished by leaving out the dynamic terms. The advantage is that only the steady-state gains of the transfer functions need to be used in designing a static decoupler.

The steady-state gains can be calculated simply by dropping the dynamical part of the transfer functions. Using the system designed transfer functions from the previous chapter, the dynamic and static decouplers are:

$$D_{21}(s) = \frac{-N_{21}(s)}{N_{11}(s)} = \frac{0.08s + 0.00768}{0.3628s + 0.034} = 0.228639$$

$$D_{12}(s) = \frac{-N_{12}(s)}{N_{32}(s)} = \frac{-0.99s^2 - 0.1s - 0.00106}{0.25s^2 + 0.085s + 0.000825} = -1.2848$$

$$D_{31}(s) = \frac{-N_{31}(s)}{N_{11}(s)} = \frac{0.0056}{0.3628s + 0.034} = -0.1667$$

### 3.3. Proposed MV Temperature-Flow Rate Controller

All real-world systems comprise multiple interacting variables. The phenomenon of considering a signal for specified control loop as a disturbance while it is an originating signal in another control loop, is known interaction or coupling as described Section 3.2, which happens in MIMO systems. The main difficulty in the MIMO case is working on matrix, rather than scalar transfer functions [31]. To get release the linearization is applied to achieve transfer functions and decoupled the system interactions in order to behave the MIMO system as a SISO system and simplify the control design. The latter section focuses on SISO system control design for each controlling loop separately



### 3.3.1. Fuzzy Self-tuning PID Control for Temperature Control

Fuzzy control relies on the stimulating knowledge and language decision-making rules, which enhance the adaptive capacity of the control system, and has strong robustness [32]. Temperature Control System has the characteristics of nonlinearity within a small delay and inertia in the current proposed plant. Conventional PID controller can not achieve precise control and reference tracking because its control parameters are fixed, Fuzzy control technology is introduced based on the traditional PID control, in order to gain better control effect, This method combines fuzzy control theory which have the feature of better dynamic performance with the advantages of the traditional PID control method which has a high stable precision and strong robustness [33].

As the structure the Fuzzy Self-tuning PID controller takes conventional PID as the foundation, which the main idea of Fuzzy Self-tuning PID control system is full use of the operation experience of the operator to get the PID parameters in real-time non-linear adjustment, hence it can ensure the whole system to gain a better control performance [33, 34]. The structure of fuzzy self-tuning PID controller is shown in Figure 3.3.

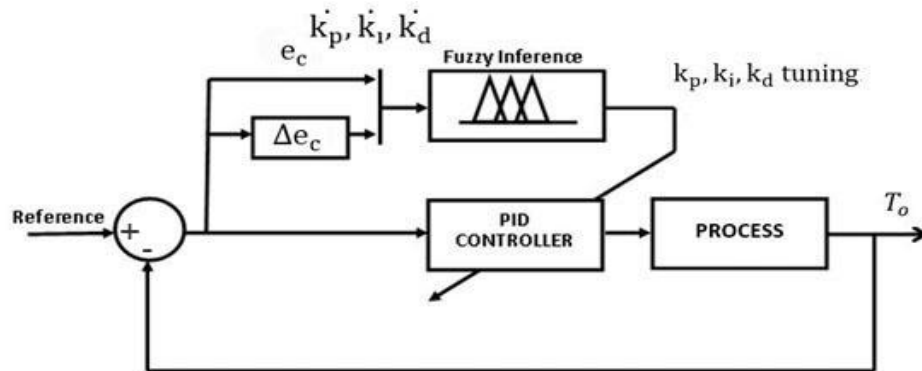


Figure 3.3. General structure block diagram of fuzzy self-tuning PID controller

For the fuzzy domain of the input and output variables, the inputs are temperature error and the change of error, denoted as;  $e, \Delta e_c$  its outputs are  $k_p, k_i, k_d$ . With the fuzzy control, combined with actual project experience, adaptive correction of the PID parameters can expressed be as the following [33].

$$k_p = \dot{k}_p + \{ e, \Delta e_c \} = \dot{k}_p + \Delta k_p$$

$$k_i = \dot{k}_i + \{ e, \Delta e_c \} = \dot{k}_i + \Delta k_i$$

$$k_d = \dot{k}_d + \{ e, \Delta e_c \} = \dot{k}_d + \Delta k_d$$

where  $k_p, k_i$  and  $k_d$  are the PID parameters after modifying;  $\Delta k_p, \Delta k_i, \Delta k_d$  are the output of fuzzy controller,  $\dot{k}_p, \dot{k}_i, \dot{k}_d$  are the PID parameters before modifying.

The signals of the error and the error variation are input into the fuzzy controller, which transforms the signals into fuzzy quantity at first. It is assumed that the error of water temperature is within  $\pm 50$  C°; combining with the practical experience, at the condition of regular heating and cooling, the temperature change could not exceed 10 C°, error is varying within  $\pm 50$  C°. That is  $e \in [-50, 50]$ ,  $e_c \in [-50, 50]$ . The basic range of  $\Delta k_p = [0, 12]$ ,  $\Delta k_i = [0, 16]$  and  $\Delta k_d = [0, 0.35]$ .

In general, quantitative grade of fuzzy domain is limited. If more grades are chosen, control rules are flexible and painstaking, but the control process becomes complicated; conversely, control rule are simple, but the effects of the control system always cannot reach the expectation. In general case, fuzzy domain is divided into 7 values. The fuzzy quantizing domains of  $e, \Delta e_c$  are both  $\{-50, -40, -30, -20, -10, 0, 10, 20, 30, 40, 50\}$  and  $\Delta k_p$  is  $\{0, 2, 4, 6, 8, 10, 12\}$ ; and the domains of  $\Delta k_i, \Delta k_d$  are both  $\{0.02, 0.04, 0.06, 0.08, 0.1, 0.12, 0.14, 0.16\}$  and  $\{0.05, 0.1, 0.15, 0.2, 0.25, 0.3, 0.35\}$  respectively. The fuzzy linguistic values of the variables both are  $\{NB, NM, NS, ZO, PS, PM, PB\}$ , respectively  $\{\text{negative large, negative middle, negative small, zero, positive small, positive middle, positive large}\}$  [33].

Under forming and reasoning of fuzzy control, the essential part is a set of linguistic rules. Any number of rules can be created to define the actions of the fuzzy controller. The fuzzy control rule is based on related technical knowledge and practical experience in debugging, according to the different influences of the parameters on the response, the setting requirements is different under different inputs [35]. The application of conventional fuzzy conditions and fuzzy relations "If  $e$  is  $A$  and  $\Delta e_c$  is  $B$  then  $k_p$  is  $C$ ,  $k_i$  is  $D$ ,  $k_d$  is  $E$ " [34] can establish fuzzy rules, the finally determined fuzzy rules are shown in the following tables.

Table 3.1.  $k_p$  Fuzzy control rule.

$k_p \backslash \Delta e_c$ $e_c$	NB	NM	NS	ZO	PS	PM	PB
NB	PB	PB	PM	PM	PS	ZO	ZO
NM	PB	PB	PM	PS	PS	ZO	NS
NS	PM	PM	PM	PS	ZO	NS	NS
ZO	PM	PM	PS	ZO	NS	NM	NM
PS	PS	PS	ZO	NS	NS	NM	NM
PM	PS	ZO	NS	NM	NM	NM	NB
PB	ZO	ZO	NM	NM	NM	NB	NB

Table 3.2.  $k_i$  Fuzzy control rule

$k_i \backslash \Delta e_c$ $e_c$	NB	NM	NS	ZO	PS	PM	PB
NB	PS	NS	NB	NB	NB	NM	PS
NM	PS	NS	NB	NM	NM	NS	ZO
NS	ZO	NS	NM	NM	NS	NS	ZO
ZO	ZO	NS	NS	NS	NS	NS	ZO
PS	ZO	ZO	ZO	ZO	ZO	ZO	ZO
PM	PB	NS	PS	PS	PS	PS	PB
PB	PB	PM	PM	PM	PS	PS	PB

Table 3.3.  $k_d$  Fuzzy control rule

$k_d \backslash \Delta e_c$ $e_c$	NB	NM	NS	ZO	PS	PM	PB
NB	NB	NB	NM	NM	NS	ZO	ZO
NM	NB	NB	NM	NS	NS	ZO	ZO
NS	NB	NM	NS	NS	ZO	PS	PS
ZO	NM	NM	NS	ZO	PS	PM	PM
PS	NM	NS	ZO	PS	PS	PM	PB
PM	ZO	ZO	PS	PS	PM	PB	PB
PB	ZO	ZO	PS	PM	PM	PB	PB

### 3.3.2. Fuzzy Logic Control for Flow Rate Control

Beside temperature control in previous section, flow rate measurement and control escorted in plant processes which is one of the essential objectives. It was aimed to shed some light on the development of fuzzy logic controller to determine PID parameters, also to maintain the output flow rate constant through manipulating two control inputs fuzzy logic controller is considered.

In view of the nonlinearity, valve position, time delay, pump speed and other properties affecting the control accuracy and effectively adjust the water flow rate, we proposed a fuzzy control method to obtain strong robustness and more desirable results compared to the commonly used control methods as in literature [36, 37, 38].

In order to ensure the outlet water flow of the tank constant, the corresponding control system should be designed for adjusting the valve position and the applied voltage of the DC motor, promoting the control precision and its system block diagram is shown in Figure 3.4.

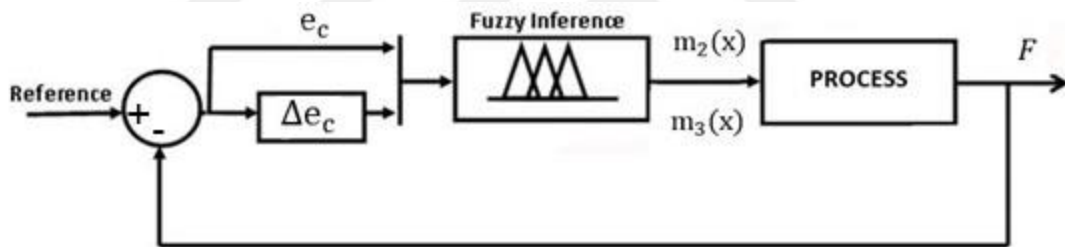


Figure 3.4. Fuzzy logic flow control loop block diagram.

Again for the flow rate control purpose, the fuzzy domain and its control input and output variables are given. The deviation  $e$  and the deviation change  $e_c$  are the inputs of the Fuzzy Controller, where the valve position  $m_2(x)$  and the applied driving voltage  $m_3(x)$  for adjusting DC motor speed are the outputs. Their fuzzy sets and value domains are as follows:

The fuzzy sets of  $e_c$ ,  $\Delta e_c$ ,  $m_2(x)$  and  $m_3(x)$  all are {NL, NI, NM, NS, Z, PS, PM, PI, PL}, the value domains of  $e_c$  and  $\Delta e_c$  are {-20 to 20} and {-17 to 17} respectively. Also the value domains of  $m_2(x)$  and  $m_3(x)$  are both {-1, -0.8, -0.6, -0.4, -0.2, 0, 0.2, 0.4, 0.6, 0.8, 1}.

The fuzzy control is established as in Table 3.4 based on the control purpose of reducing the deviation, the following table shows the fuzzy rules:

Table 3.4.  $m_2(x)$  and  $m_3(x)$  Fuzzy control rule.

$m_2(x) \Delta e_c$ $e_c / m_3(x)$	NL	NI	NM	NS	Z	PS	PM	PI	PL
NL	PL	PL	PL	PL	PL	PL	PL	PL	PL
NI	PM	PM	PS	PI	PI	PI	PS	PM	PM
NM	Z	PM	PM	PM	PM	PM	PM	PM	Z
NS	PS	Z	PS	PI	PS	PI	PS	Z	NS
Z	Z	Z	Z	Z	Z	Z	Z	Z	Z
PS	PS	Z	NS	NI	NS	NI	NS	Z	PS
PM	Z	NM	NM	NM	NM	NM	NM	NM	
PI	NM	NM	NS	NI	NI	NI	NS	NM	NM
PL	NL	NL	NL	NL	NL	NL	NL	NL	NL

## CHAPTER IV

### SIMULATION TESTS AND RESULTS

Following sections present proposed method performances starting with linear vs. nonlinear comparison up to the controller performances at different set point tracking and disturbance rejection performances, after theoretically, the CST system mathematical model analyzed and the control algorithm is designed. Since computer simulation is an interactive high-level platform for scientific calculation and technical computing environment for algorithm development, data visualization, data analysis and numerical analysis, made it possible to use for a wide range of applications, including calculus, algebra, up to control system design, testing and measuring systems [39]. A powerful software built-in toolbox is used to simulate CTS system, which supports linear and nonlinear systems, modelled in real time continuous simulation.

#### 4.1. Linearization Results

In this section we simulate the dynamic linearized open loop system model given in Equations (2.37) (2.38) compared with the real dynamic nonlinear open loop system given in Equations (2.31) (2.34), on the studied physical description which is given in Figure 1.1. First we can model the linearized open loop system by using its state-space form Figure 4.1 and Figure 4.2 illustrate the model of the linearized open loop CST plant and the real nonlinear open loop CST plant system, respectively.

Both systems are compared with the same step input change for each control inputs as shown in Figure 4.3, in order to validate the linearized model behavior given in Figure 4.1. Input valve positions and the motor applied voltage control inputs are subjected to the same change by increasing a step of 0.2. A step time of 1 s is chosen and the simulation time is 400 s for temperature loop and 80 s for flow rate loop. The temperature loop simulation time is kept long since physically, the temperature response time is sluggish.

The output responses of the linearized open loop dynamical model and nonlinear open loop model in accordance to each input subsection nearly are the same as shown in Figures (4.3 - 4.8).

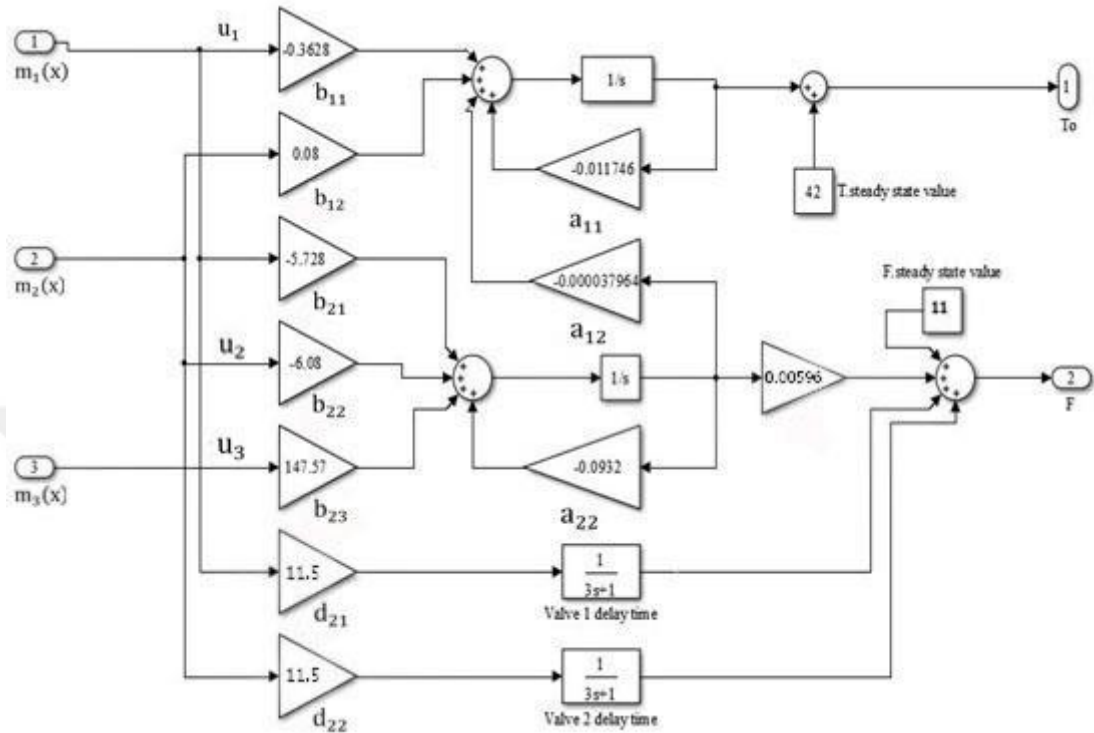


Figure 4.1. Linearized mathematical based open loop system model in computer simulation.

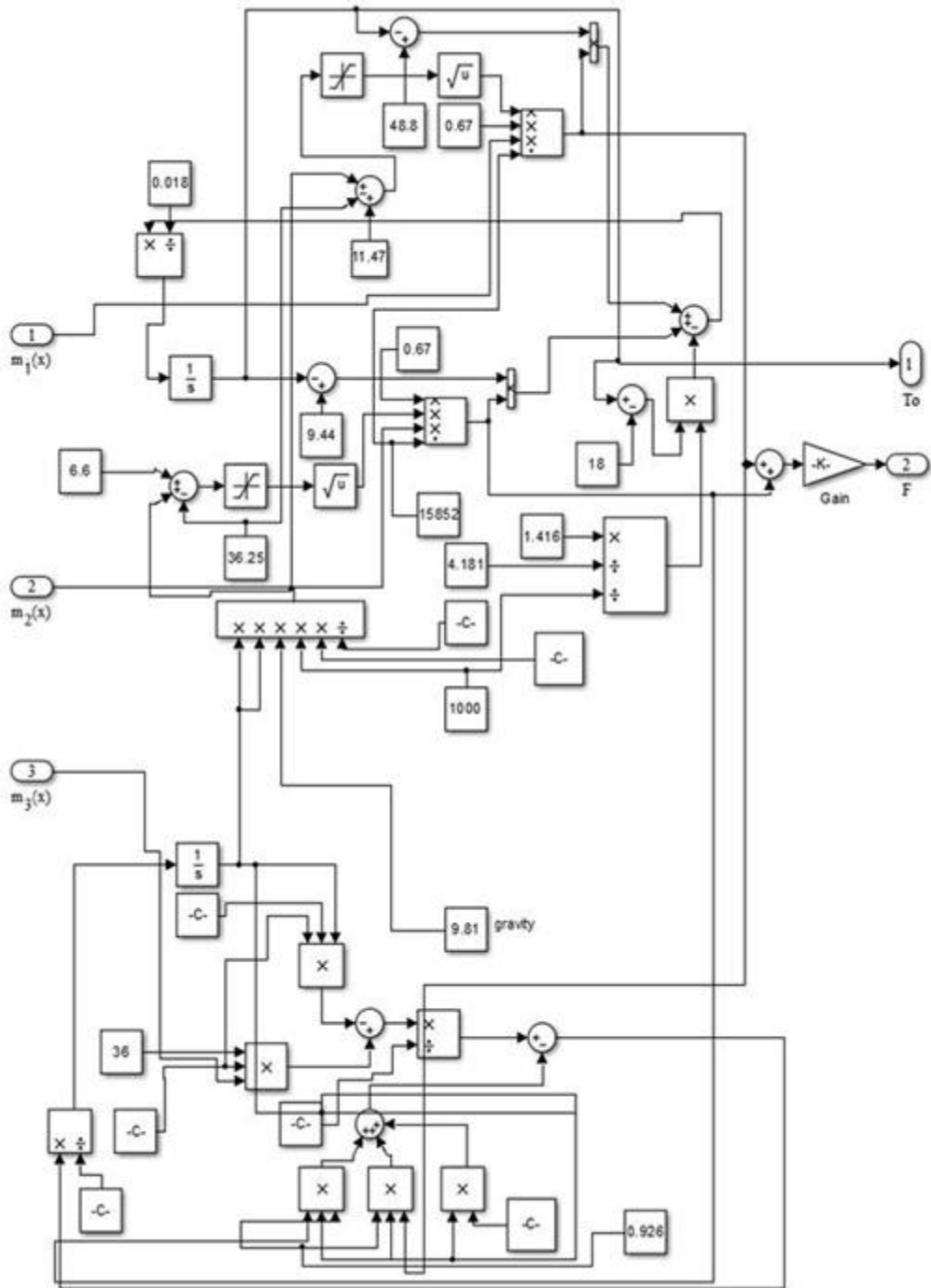


Figure 4.2. Nonlinear mathematical based open loop system model in computer simulation.



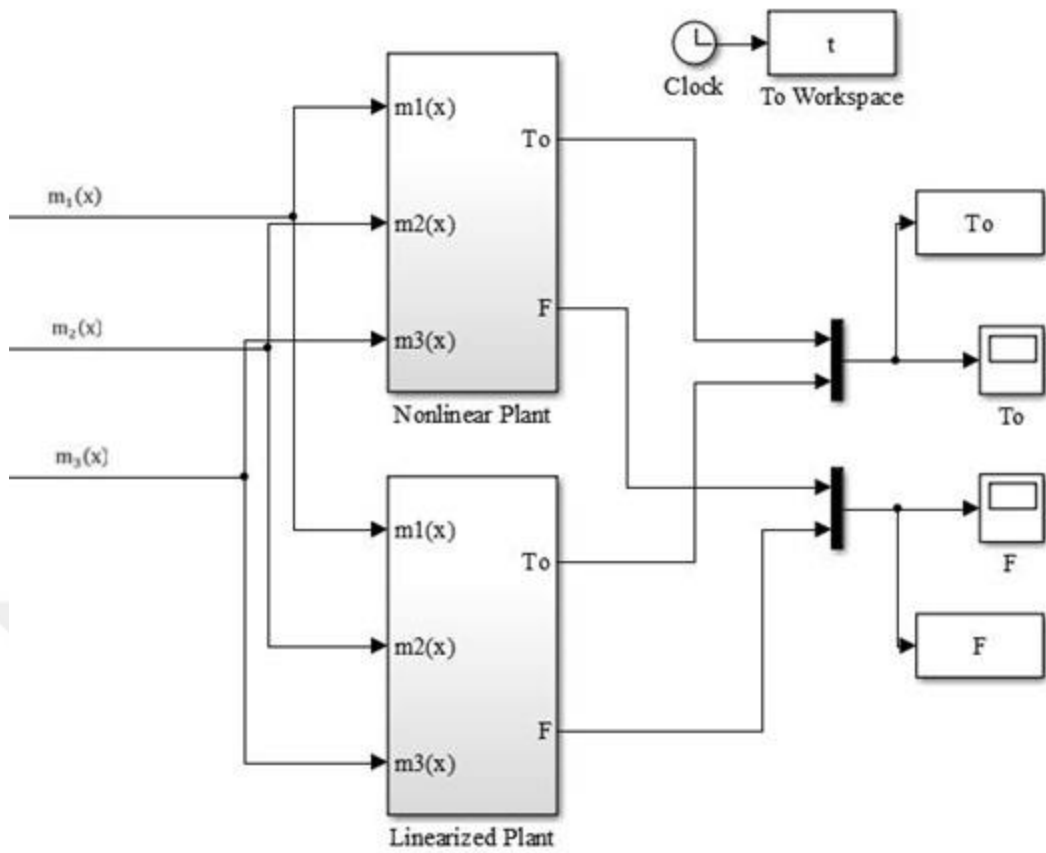


Figure 4.3. Linearized vs. nonlinear CST plant comparison.

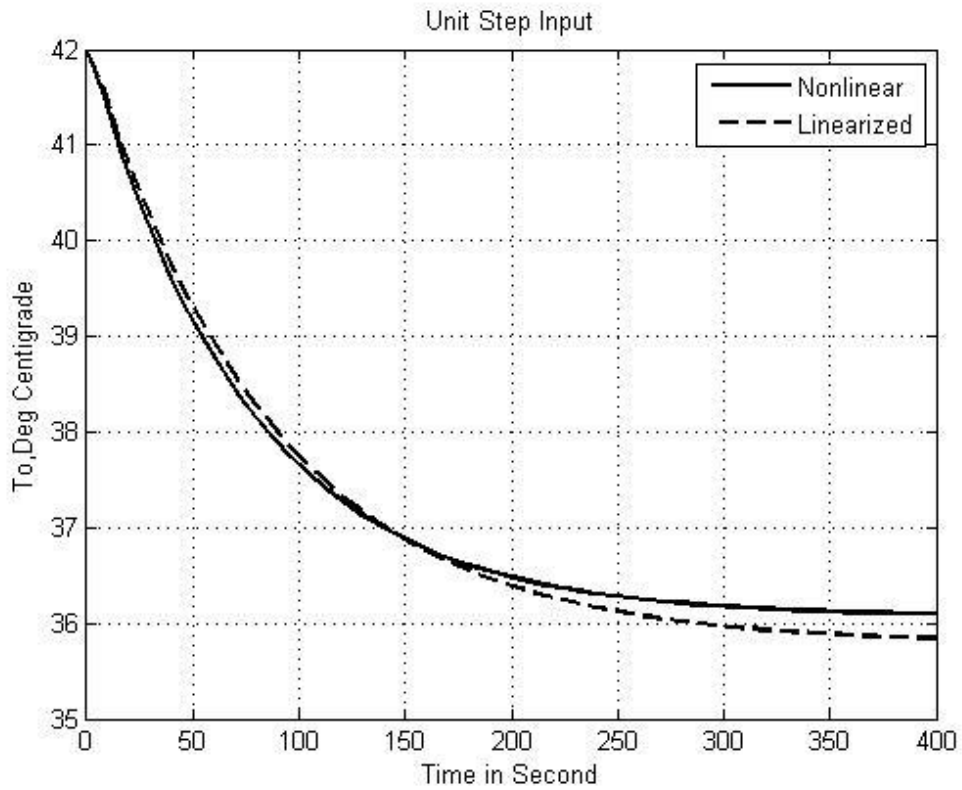


Figure 4.4. Linearized vs. nonlinear tank temperature behavior for a step input to the first valve position.

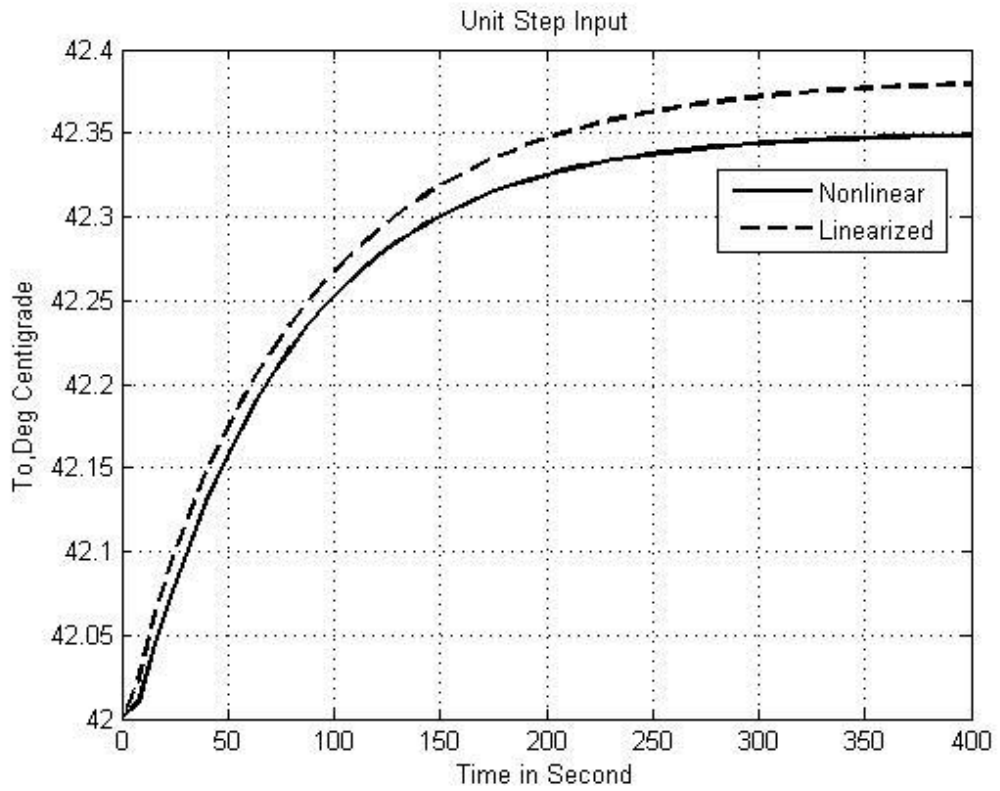


Figure 4.5. Linearized vs. nonlinear tank temperature behavior for a step input to the second valve position.

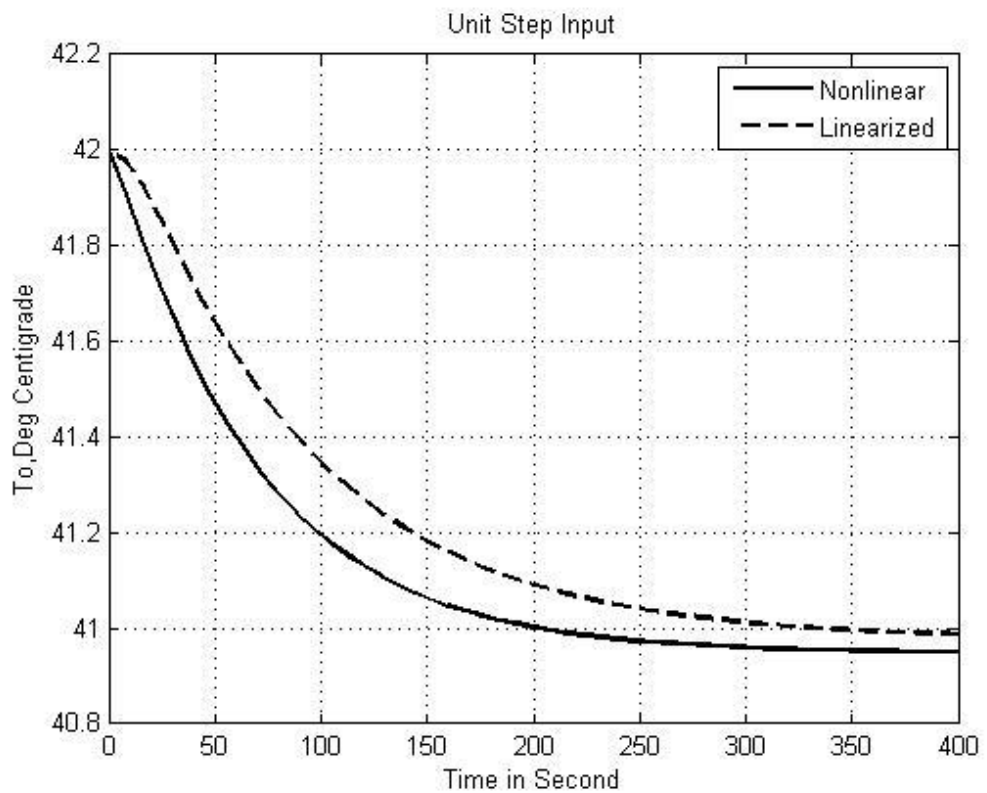


Figure 4.6. Linearized vs. nonlinear tank temperature behavior for a step reduction input to the motor applied voltage.

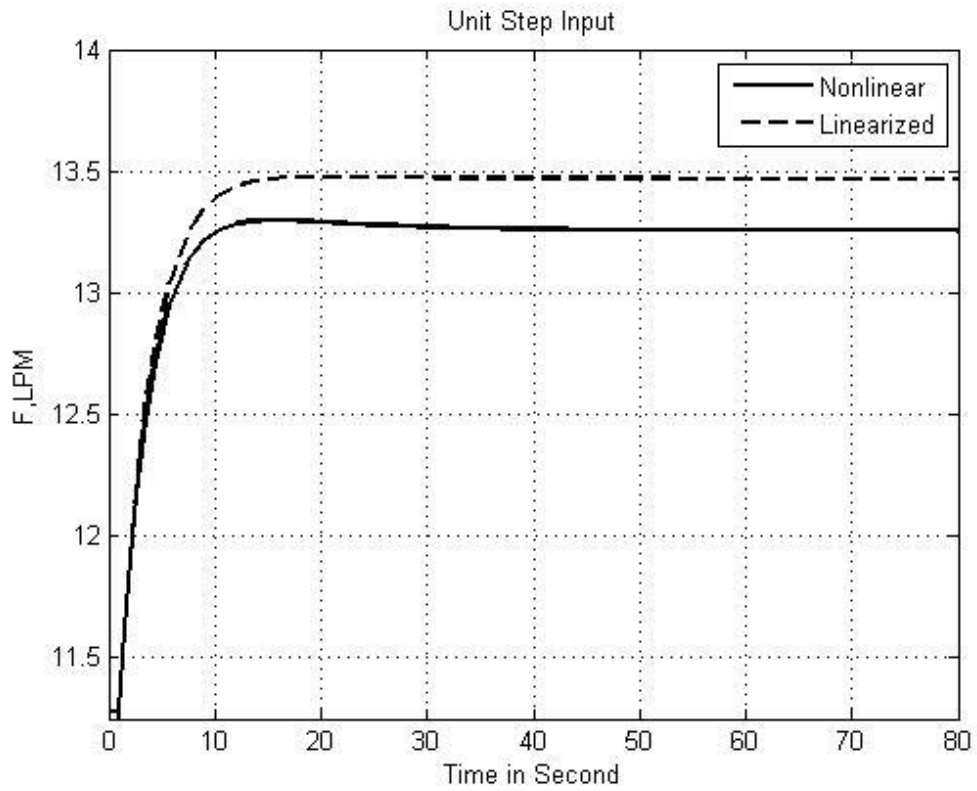


Figure 4.7. Linearized vs. nonlinear out stream flow rate behavior for a step input to the first valve position.

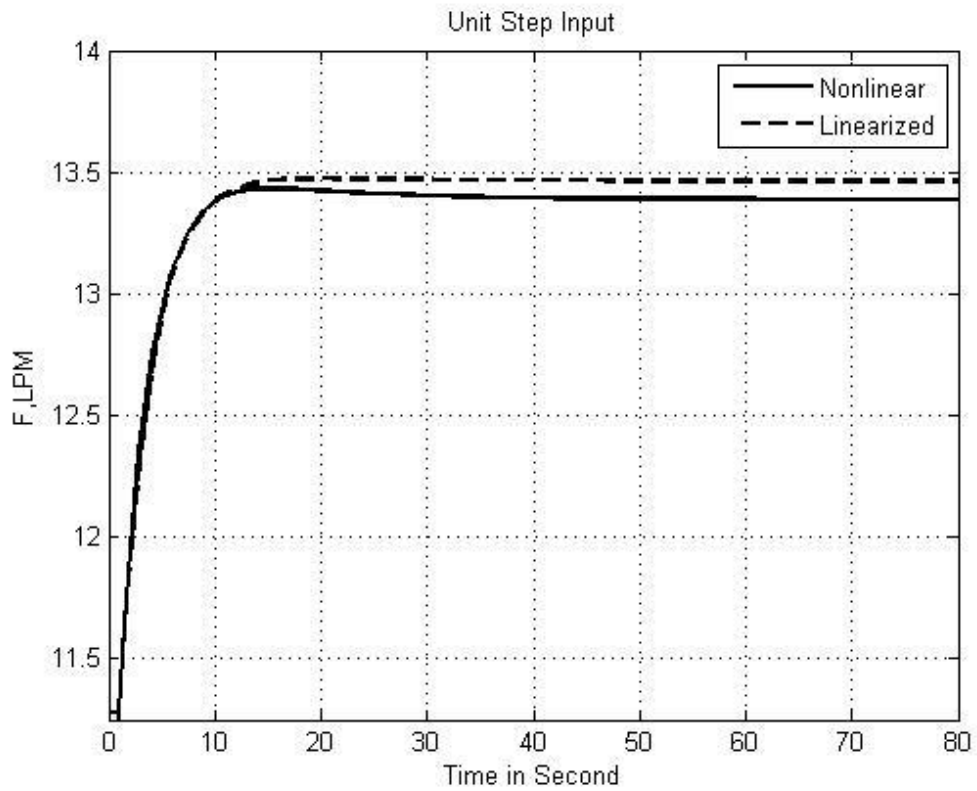


Figure 4.8. Linearized vs. nonlinear out stream flow rate behavior for a step input to the second valve position.

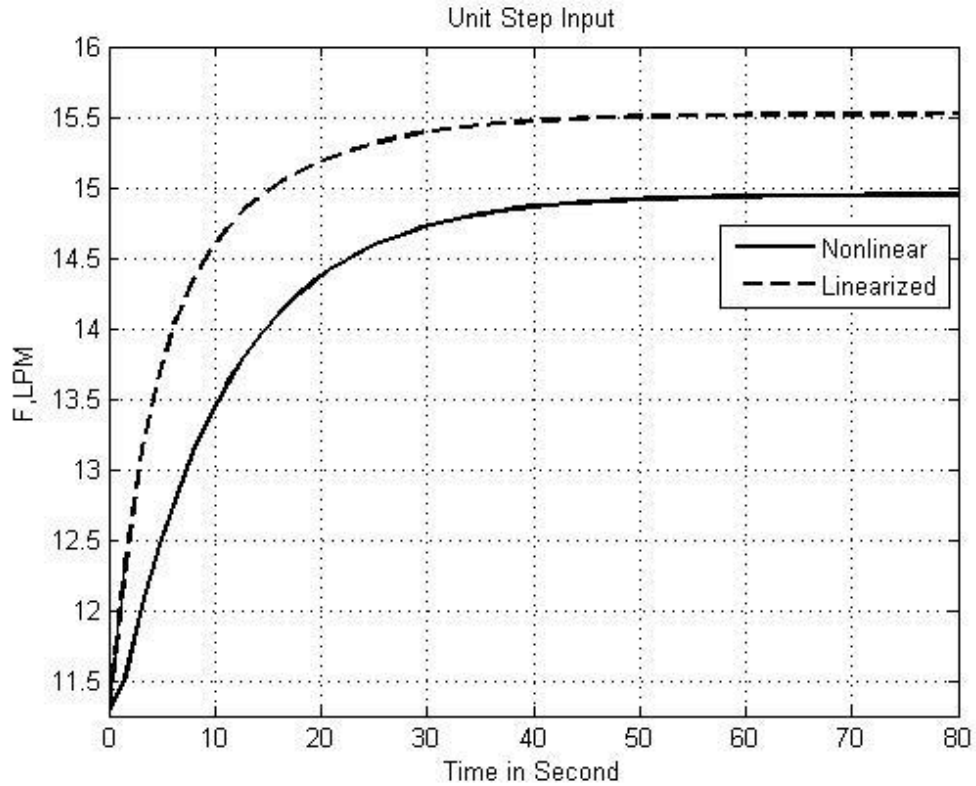


Figure 4.9. Linearized vs. nonlinear stream flow rate for a step input to the motor applied voltage.

#### 4.2. Decoupler Performance

Both the static and dynamic decouplers are designed within previous chapter. Equations (3.4 - 3.6) are decoupling blocks and both decouplers, static and dynamic computer simulated models are shown in Figures (4.10, 4.11).

Through this section the behavior of the linearized and nonlinear system are tested with considered and designed decouplers. For each, of the linearized and nonlinear system the results of both decouplers with non-decoupled system are compared through a step input 0.2 for all cases. The duration time again as section before is 400 s for temperature loop and 80 s for the flow rate loop due to the lack response in the temperature loop.

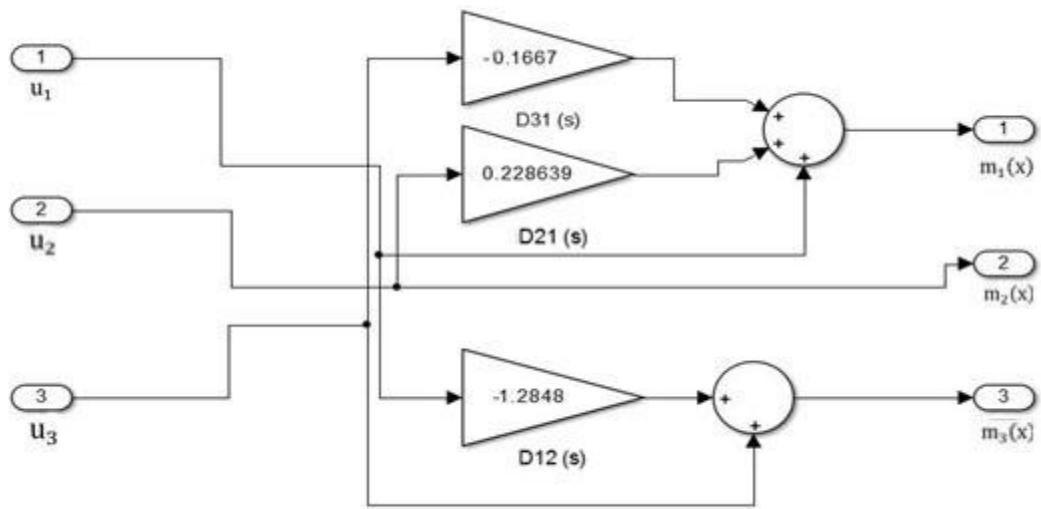


Figure 4.10. Designed static decoupler computer simulated block.

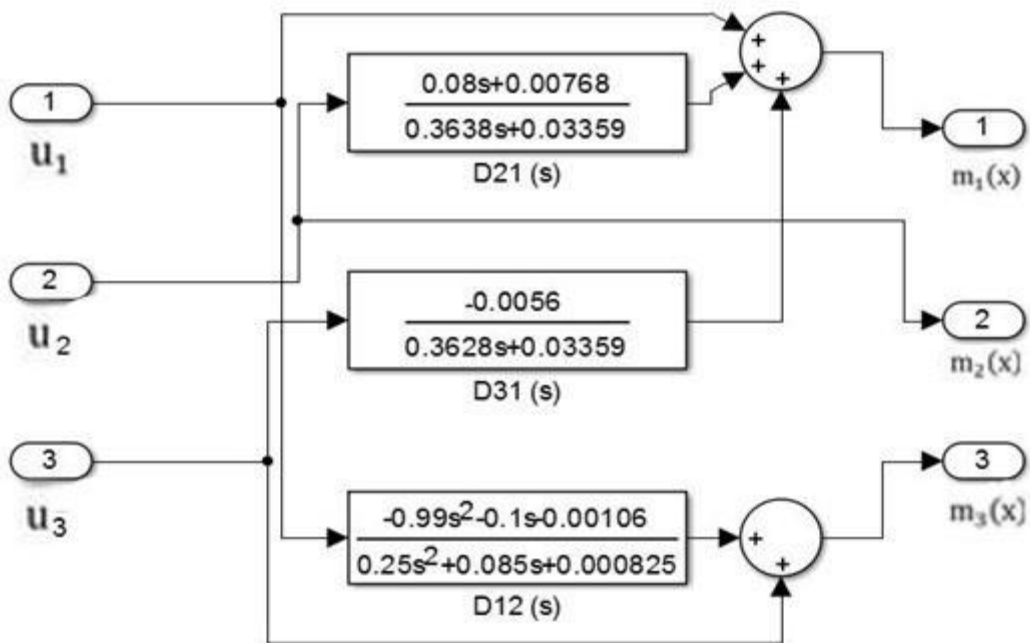


Figure 4.11. Designed dynamic decoupler computer simulated block.

In the following sub sections, the results of both decouplers are illustrated. It is clarified that the system interaction reduction or nearly cancellation is achieved for both the loops and it is obvious that the dynamic decoupling results are more convenient than the static decoupling in most of the case tests.

### 4.2.1. Static vs. Dynamic Decoupler on Linearized System

In this section we compared the response of both static and dynamic decouplers with the non-decoupled linearized system as in Figure 4.12. The output variable behavior, temperature and the flow rate changes are shown according to the step inputs for each of the inputs. The results are shown in Figures (4.13 - 4.18).

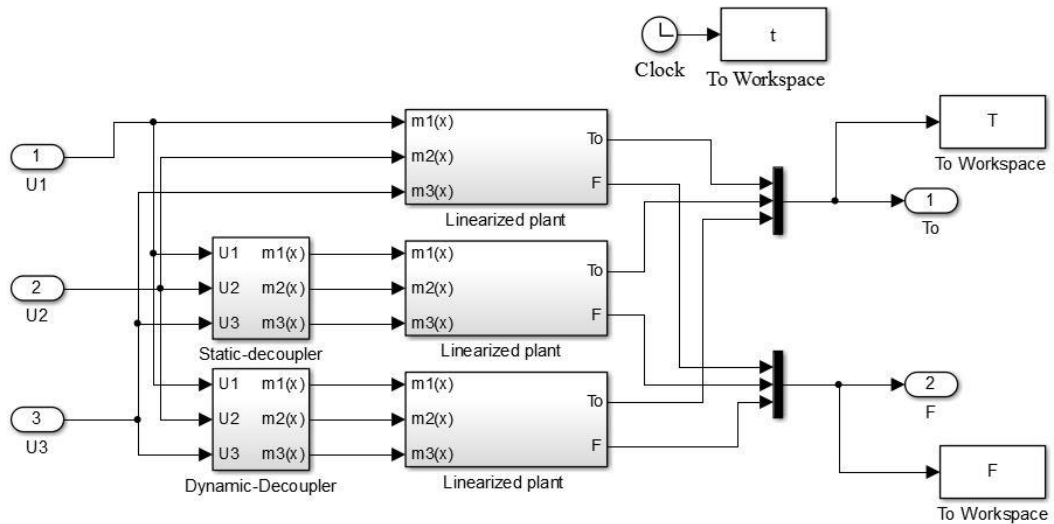


Figure 4.12. Static and dynamic decoupled vs. non-decoupled linearized system comparison blocks.

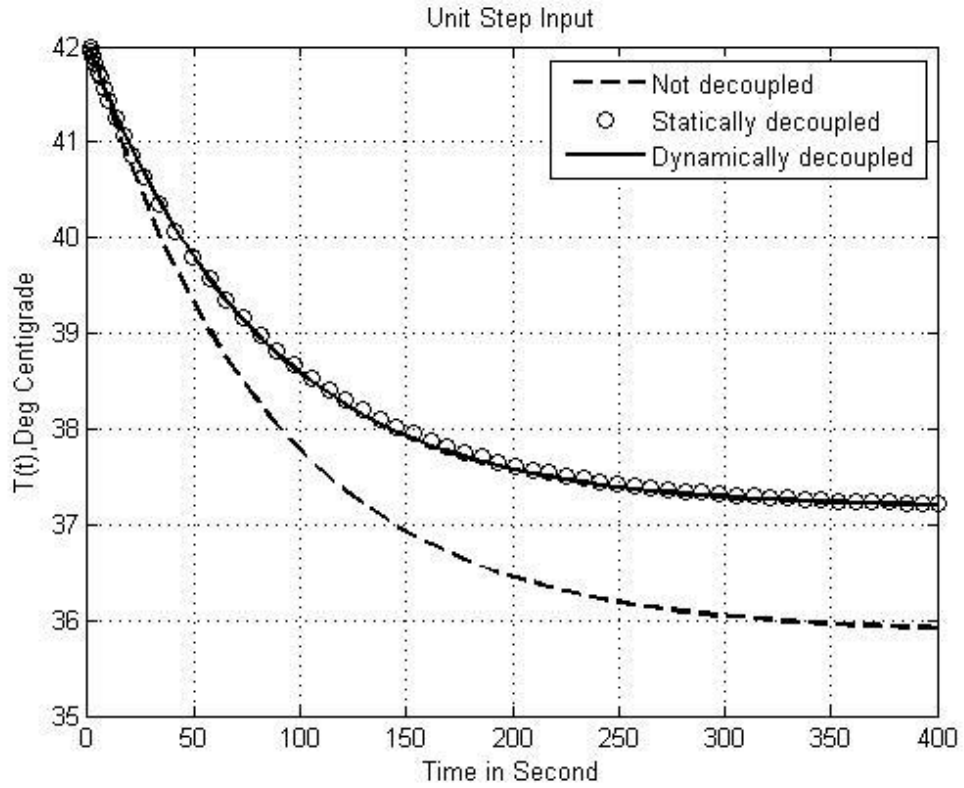


Figure 4.13. Temperature output variable behavior of the linearized system to a step input 0.2 in the first valve position.

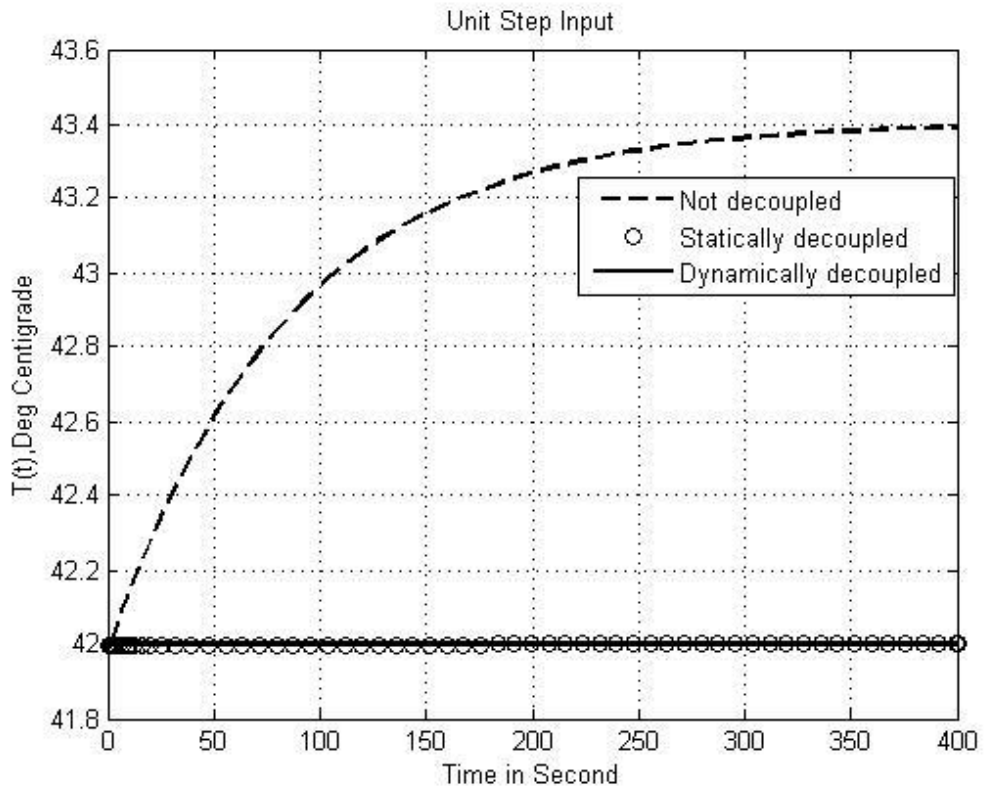


Figure 4.14. Temperature output variable behavior of the linearized system to a step input 0.2 in the second valve position.

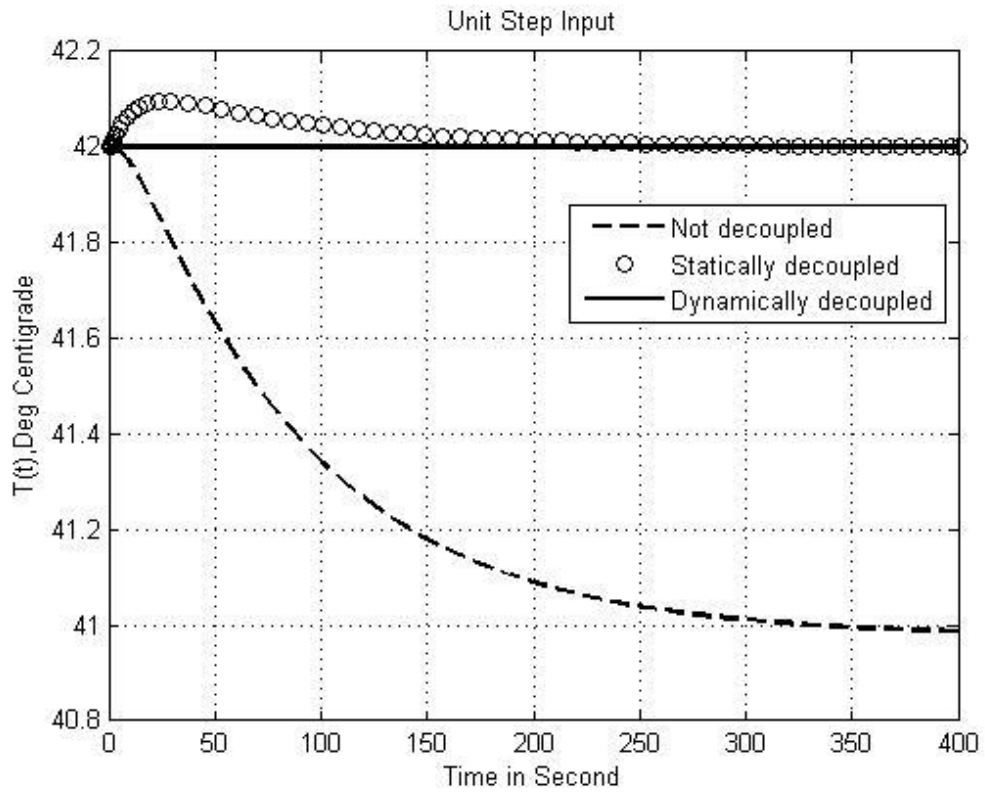


Figure 4.15. Temperature output variable behavior of the linearized system to a step input 0.2 in the motor applied voltage selector.

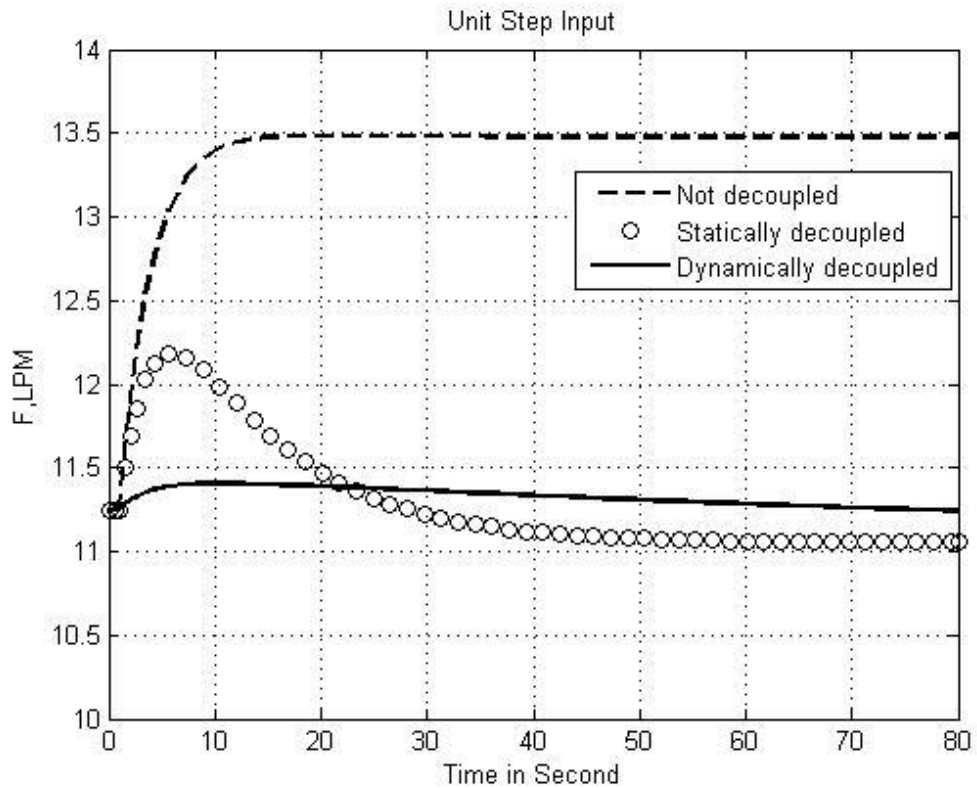


Figure 4.16. Flow rate output variable behavior of the linearized system to a step input 0.2 in the first valve position.



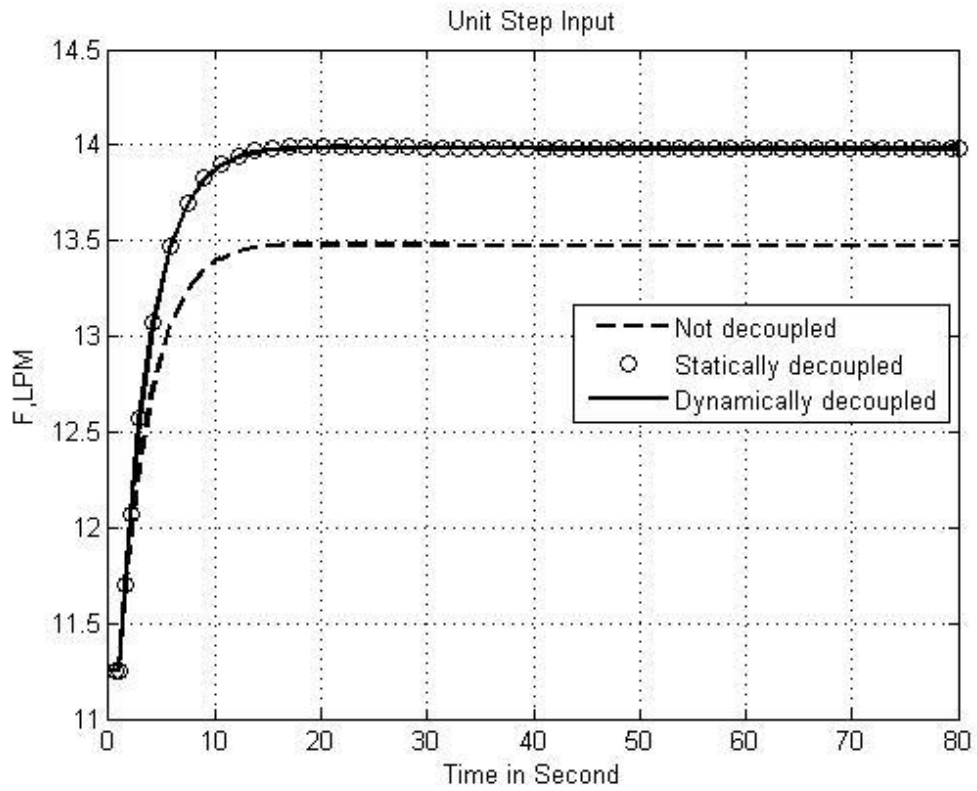


Figure 4.17. Flow rate output variable behavior of the linearized system to a step input 0.2 in the second valve position.

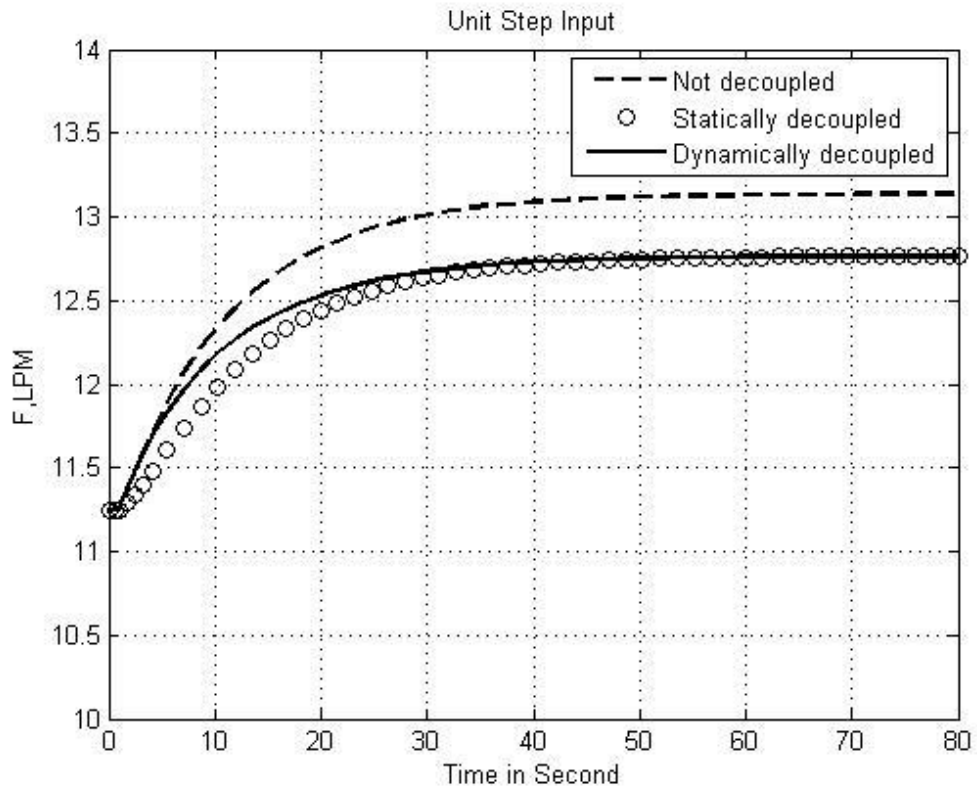


Figure 4.18. Flow rate output variable behavior of the linearized system to a step input 0.2 in the motor applied voltage selector.

### 4.2.2. Static vs. Dynamic Decoupler on Nonlinear System

After the performances of decouplers for the linearized system are shown in previous sub-section, by the same mechanism the pre-designed static and dynamic decouplers are tested within the real nonlinear system as its computer simulated model is shown in Figure 4.19. Also again the output variables, behavior of temperature and flow rate changes according to each step inputs are tested and shown in Figures (4.20 - 4.25).

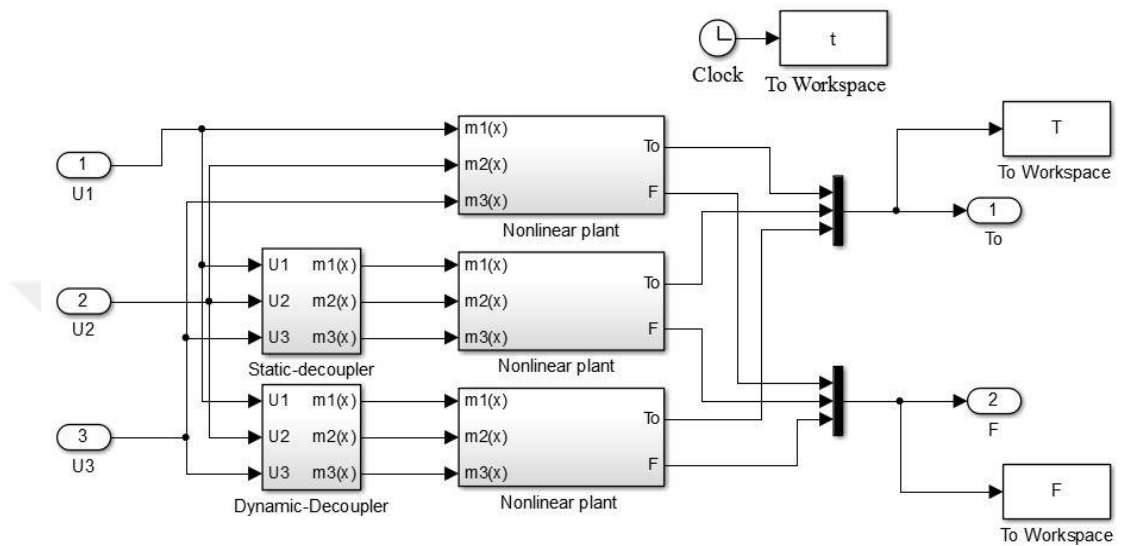


Figure 4.19. Static and dynamic decoupled vs. non-decoupled nonlinear system comparison blocks.

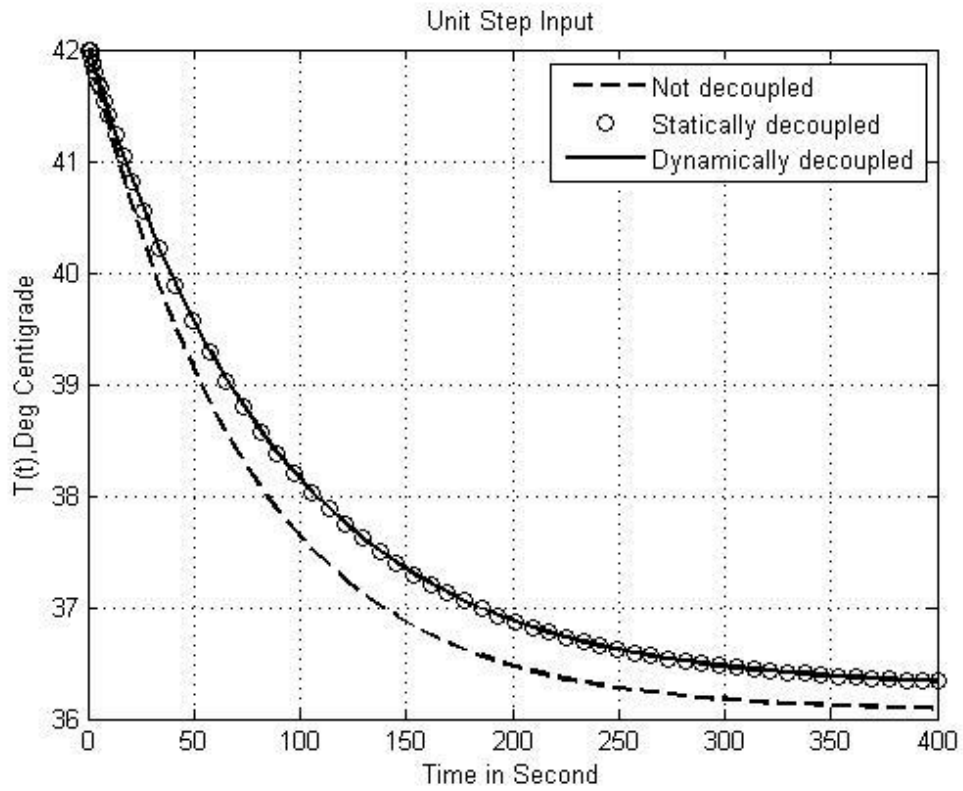


Figure 4.20. Temperature output variable behavior of the nonlinear system to a step input 0.2 in the first valve position.

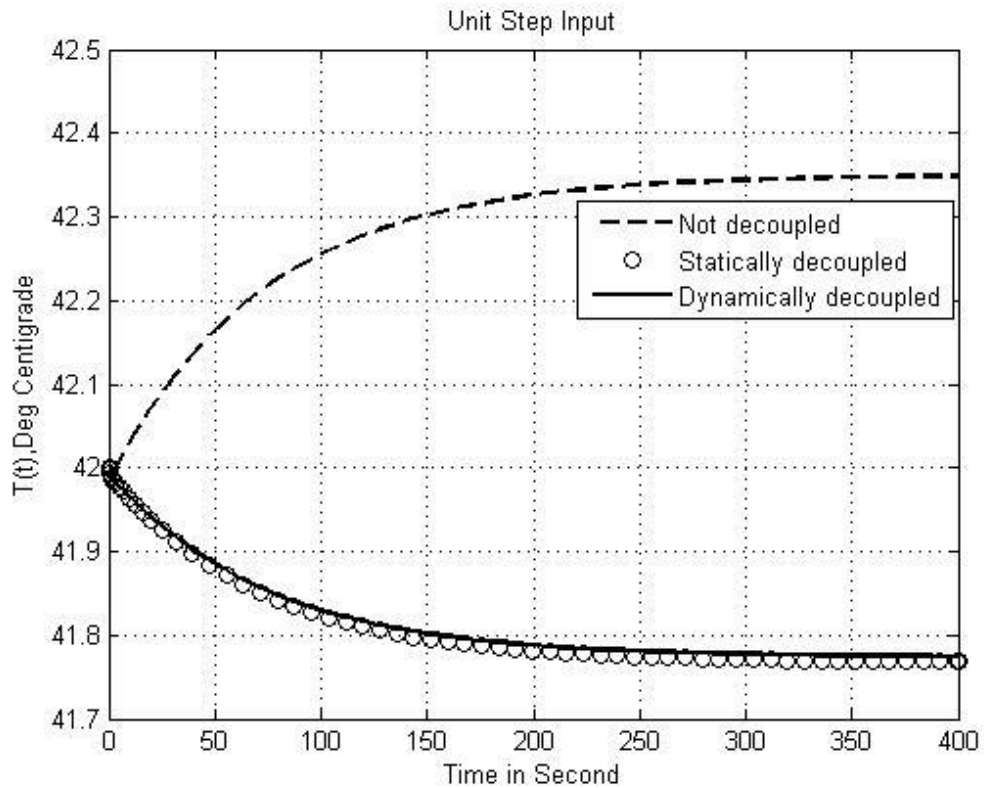


Figure 4.21. Temperature output variable behavior of the nonlinear system to a step input 0.2 in the second valve position.

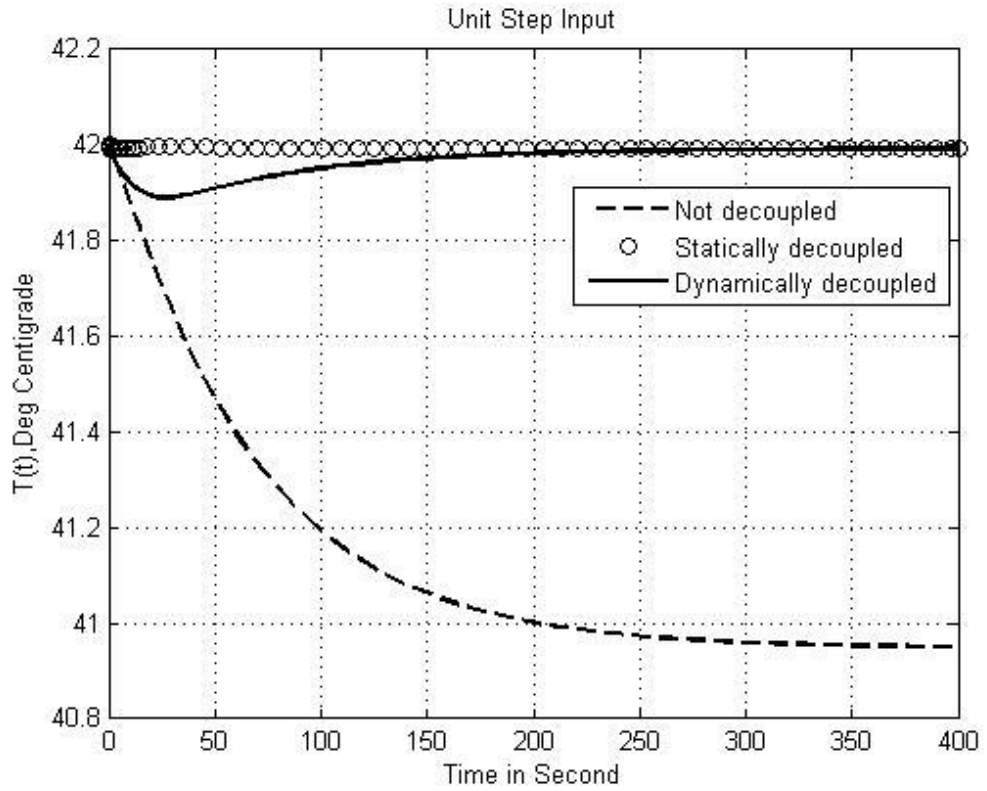


Figure 4.22. Temperature output variable behavior of the nonlinear system to a step reduction input 0.2 in the motor applied voltage selector.

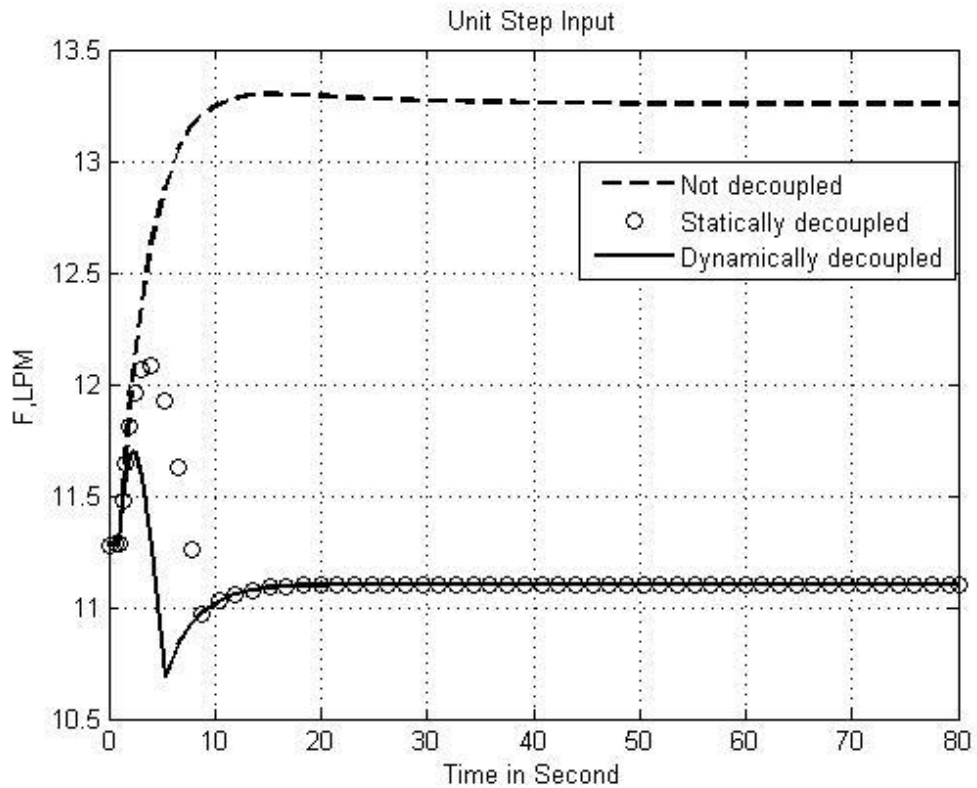


Figure 4.23. Flow rate output variable behavior of the nonlinear system to a step input 0.2 in the first valve position.

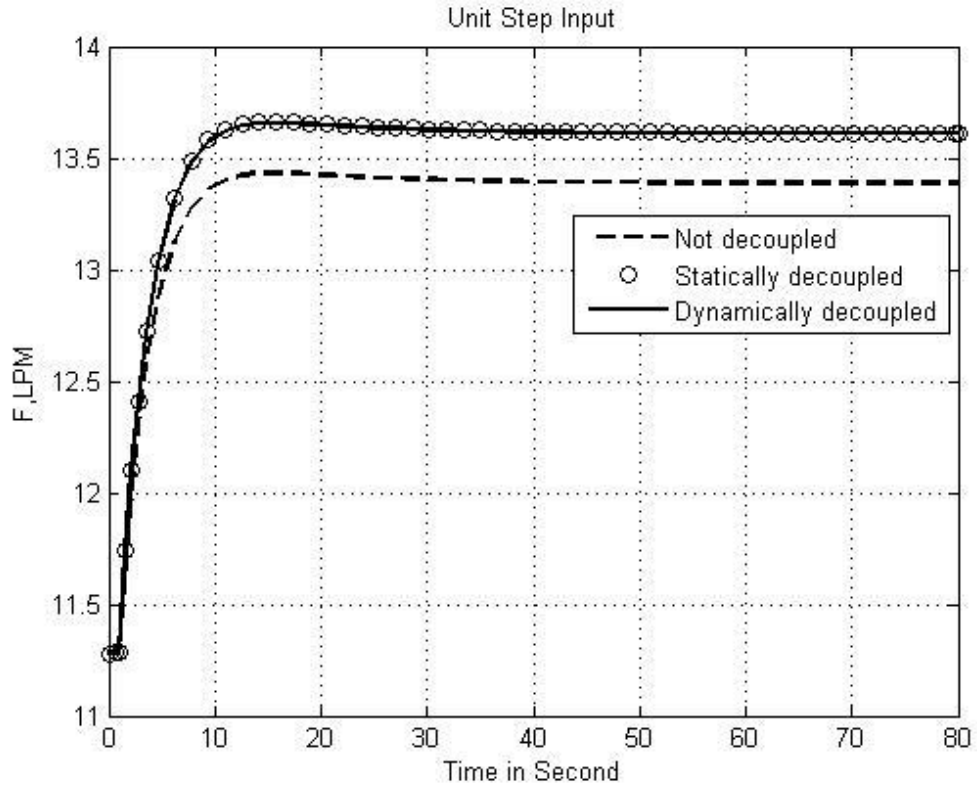


Figure 4.24. Flow rate output variable behavior of the nonlinear system to a step input 0.2 in the second valve position.

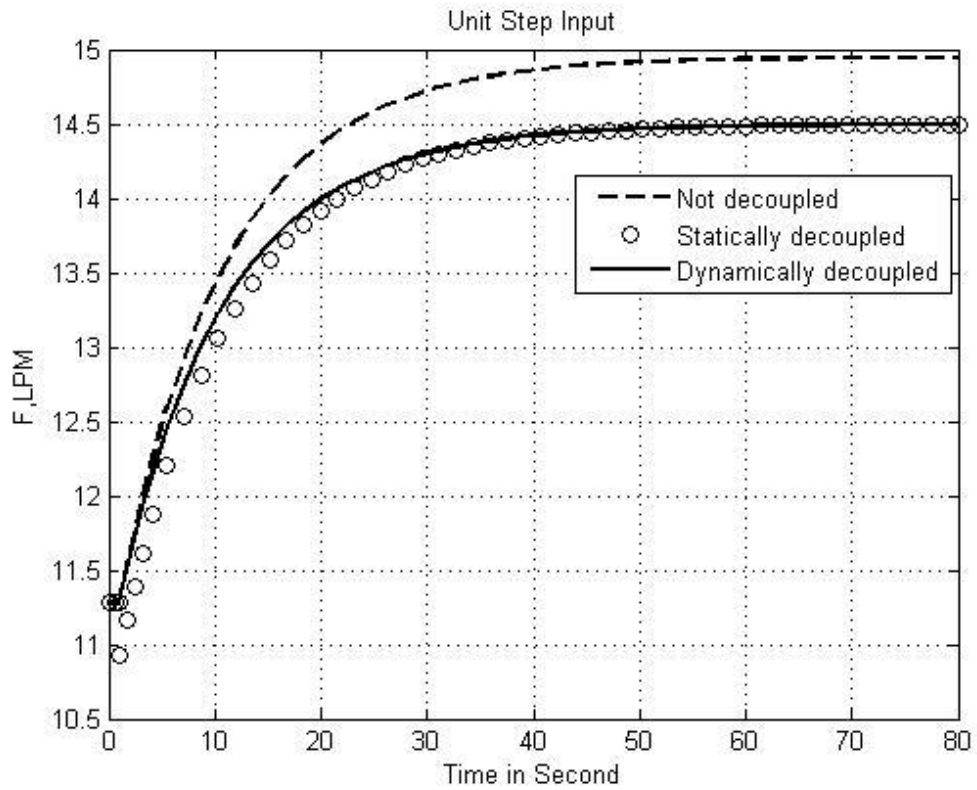


Figure 4.25. Flow rate output variable behavior of the nonlinear system to a step input 0.2 in the motor applied voltage selector.

### **4.3. Closed Loop Feedback Control Design performances**

The thesis uses controllers which are mainly FLC's, known as knowledge based controllers, that do not require a mathematical model of the process at any stage of the controller design and implementation. For the advantage of FLC without the need for mathematical modelling, it is different with other controllers. The rules of the fuzzy logic controller is particularly established on the knowledge of the system conduct and the experience [40]. The tables of rules for both control loops are described in previous chapter.

Design and simulations in the current thesis are not done under unity feedback assumption. For temperature loop control the Temperature Transducer Transfer function (TTT) and Flow rate Transducer Transfer function (FTT) for the flow control loop are used, which were taken from appropriate practical manufacture catalogues.

#### **4.3.1. Fuzzy Control Toolbox**

The 7X7 matrix rules for FLC for evaluating the parameters of PID controller is designed in order to achieve good response performance, stable, smooth and the least overshoot near the desired set point at specified time period, for temperature control loop as theoretically described in Chapter 3, also 9X9 matrix rule for FLC direct with a proportional gain is designed for the flow control loop to get above mentioned performances. The MAMDANI method is used in the inference engines. Gaussian membership function is applied for both controllers, as shown in Figures (4.26 - 4.34), and also the rule surfaces are shown in Figure 4.35. The results of the computer simulated model with efficient and good performance are presented in the following sections.

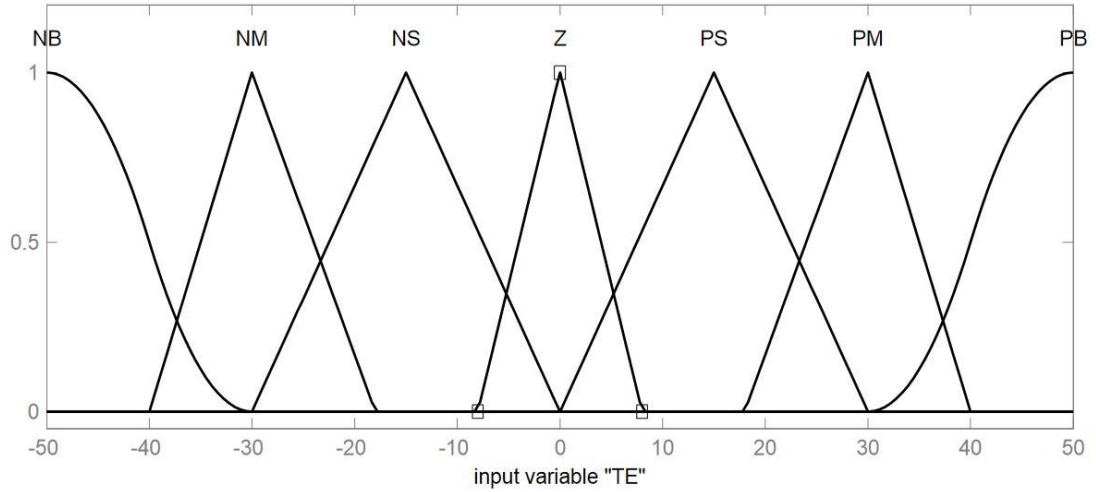


Figure 4.26. Input variable of FLC, error membership function for the self-tuning PID temperature control loop.

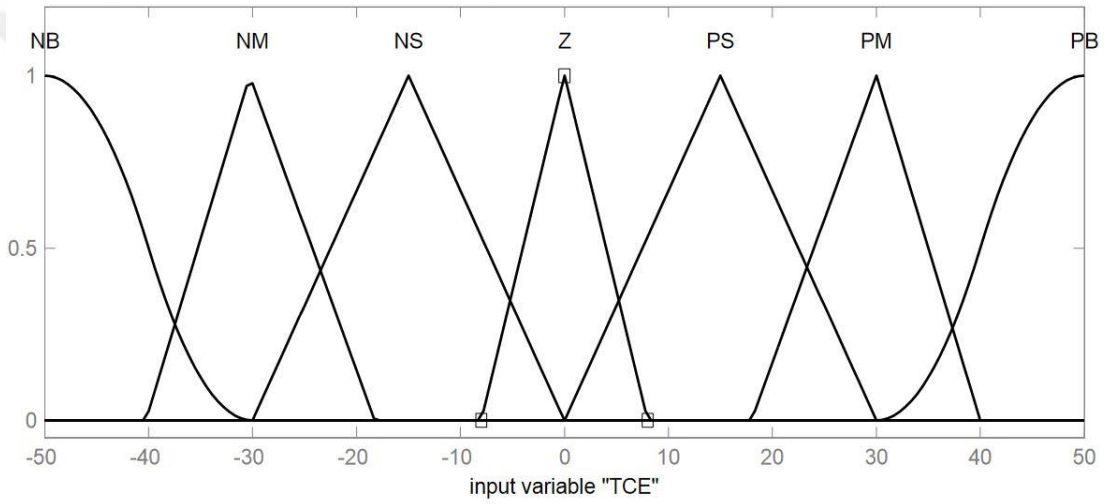


Figure 4.27. Input variable FLC change of error membership function for the self-tuning PID temperature control loop.

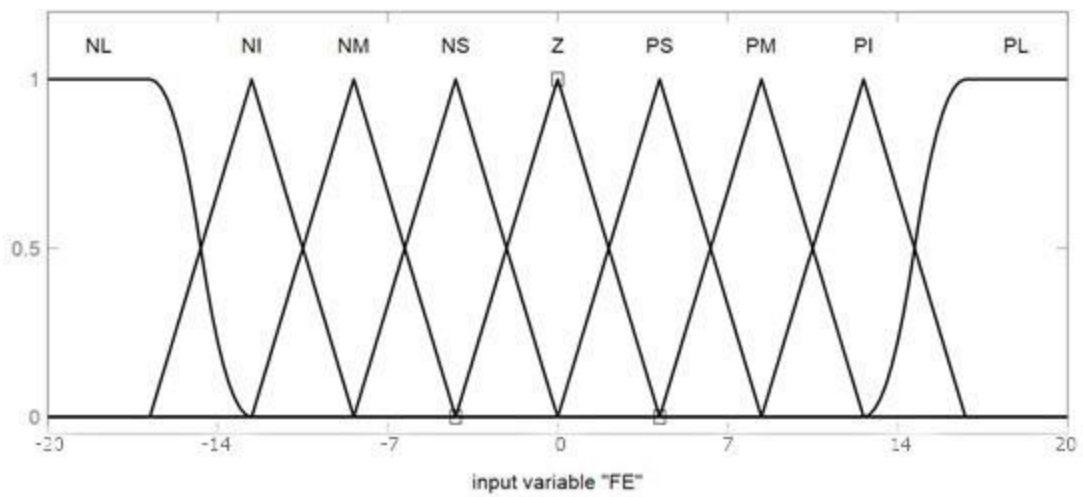


Figure 4.28. Input variable FLC error membership function for the flow rate control loop.

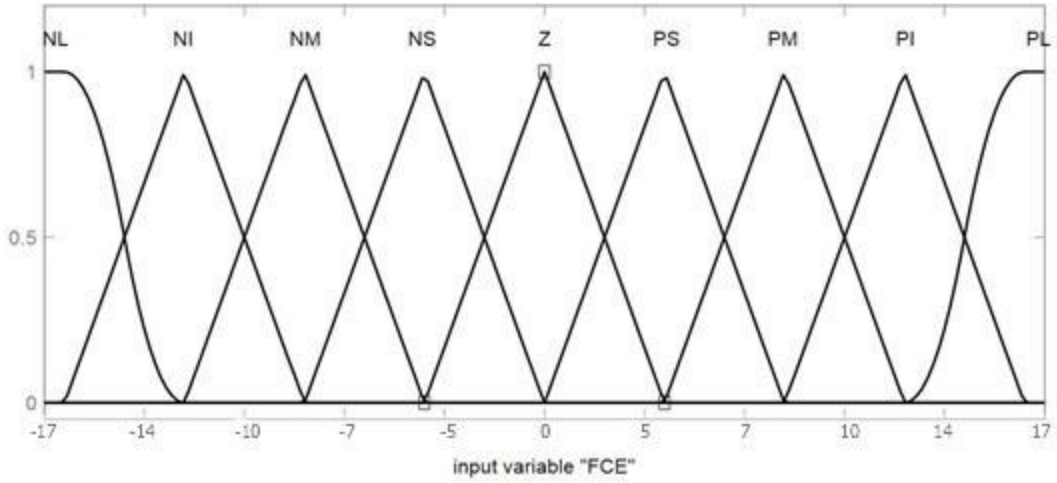


Figure 4.29. Input variable FLC change of error membership function for the flow rate control loop.

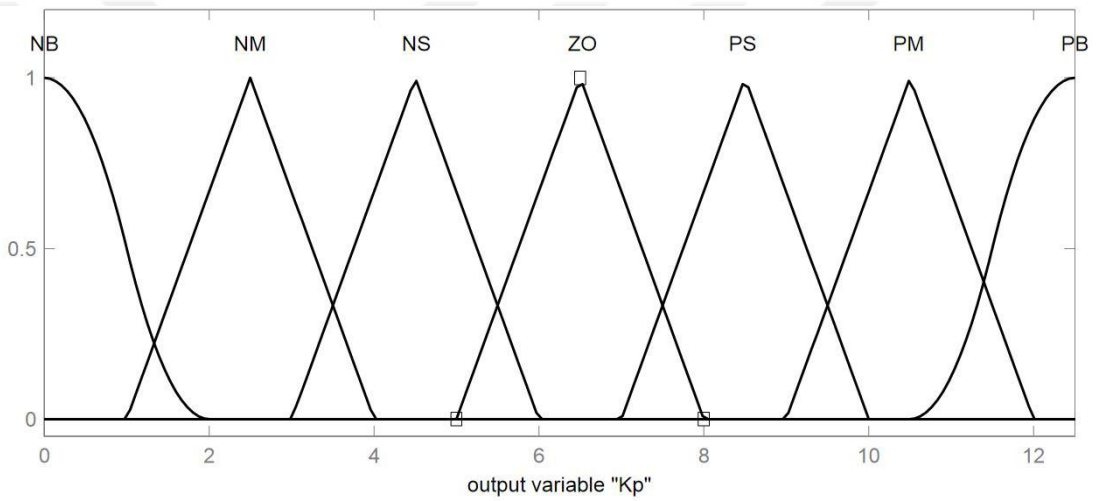


Figure 4.30. Output variable of FLC, proportional gain  $k_p$  membership function for the self-tuning PID temperature control loop.

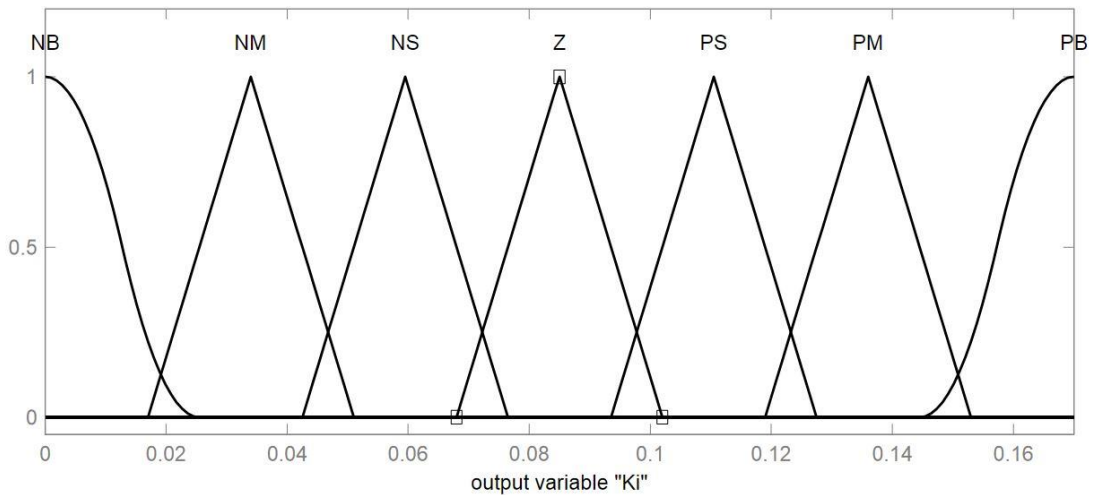


Figure 4.31. Output variable of FLC, integral  $k_i$  membership function for the self-tuning PID temperature control loop.



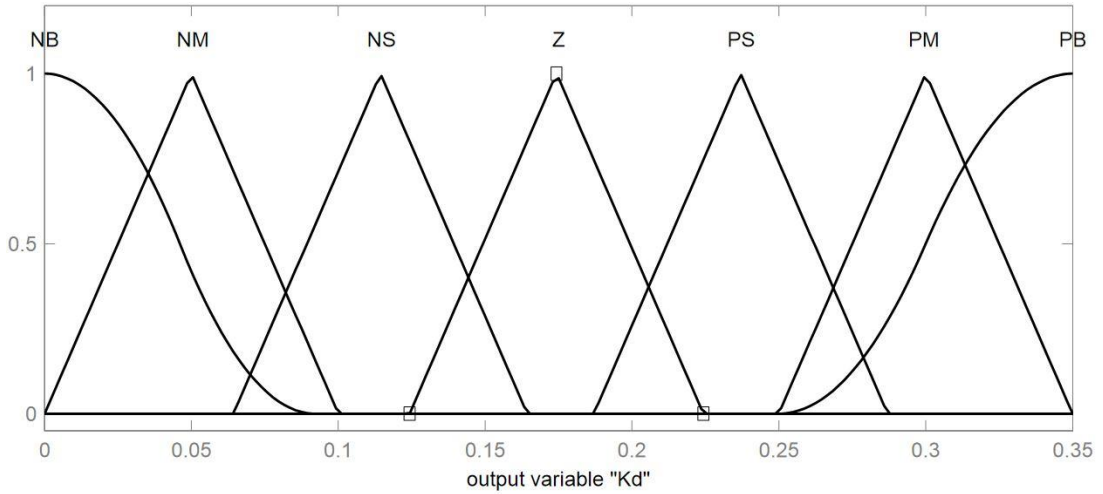


Figure 4.32. Output variable of FLC, derivative  $k_d$  membership function for the self-tuning PID temperature control loop.

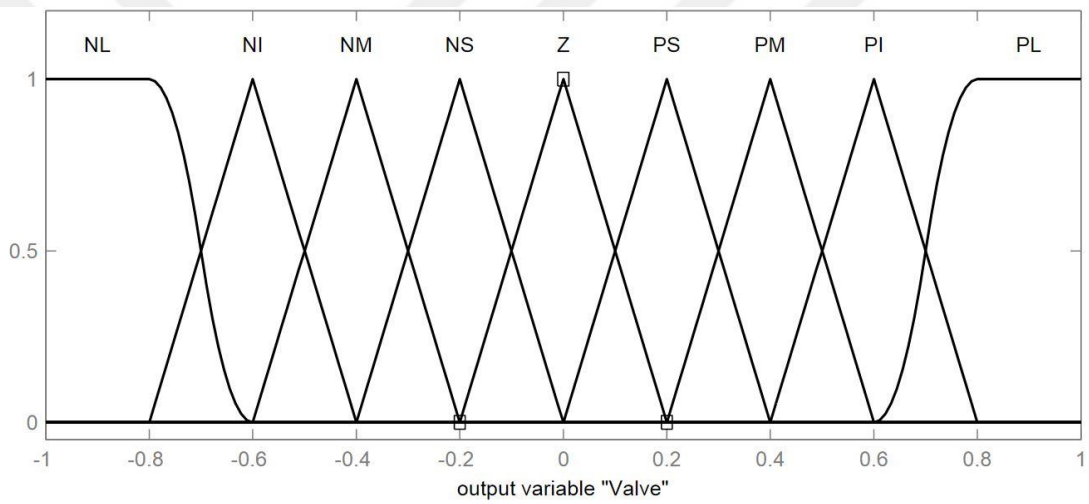


Figure 4.33. Output variable of FLC, valve position membership function for flow rate control loop.

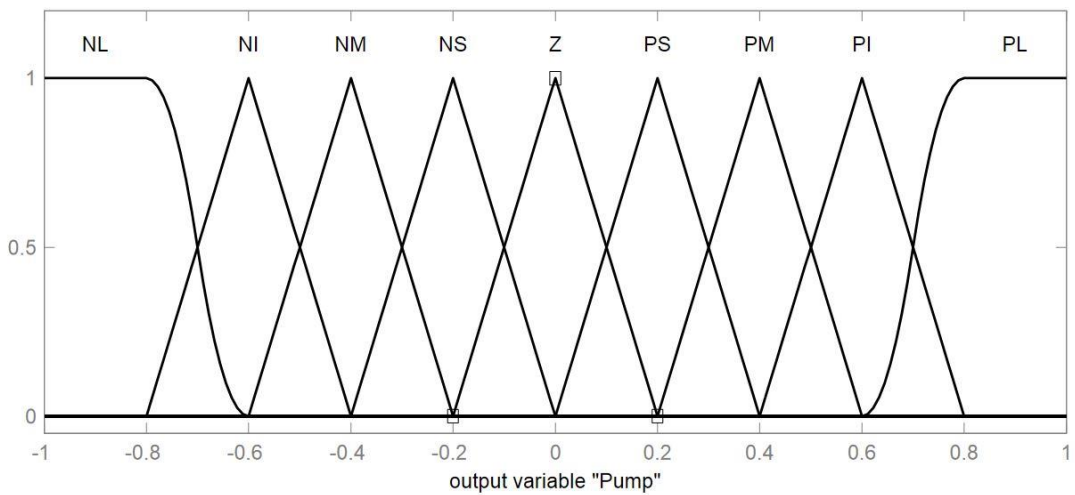


Figure 4.34. Output variable of FLC, motor applied voltage membership function for flow rate control loop.

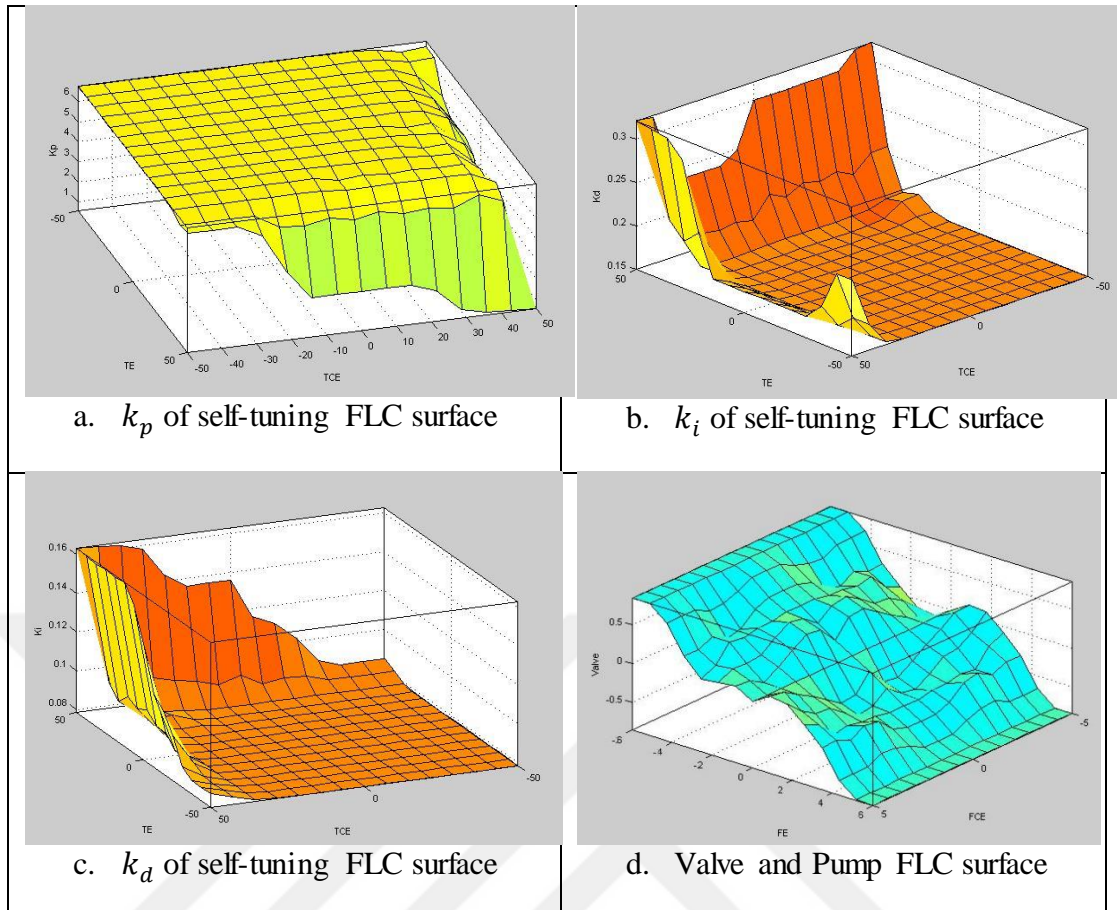


Figure 4.35. The output variable surfaces of both FLC controllers according to error and change of error for each control loop.

### 4.3.2. Controllers Performances through Control Inputs

In this section the behavior of MV controller for the closed loop system through each control input is observed. The simulation tests are done in stages for each subsequent subsection and the results are shown. From the results the closed loop system performances such as system time response, settling time and overshoot fluctuations escorting with reference point tracking are perceived.

#### 4.3.2.1. Statically Decoupled Linearized System Performances

The performance of the MV closed loop system is investigated through simulation tests, as the computer simulated model is shown in Figure 4.36.

The system is subjected to step change input through each the reference points and the behavior of the controlled variables for each single step are shown in Figures (4.37, 4.38). Also the system performance is tested through fluctuations around set point as shown in Figures (4.39, 4.40).

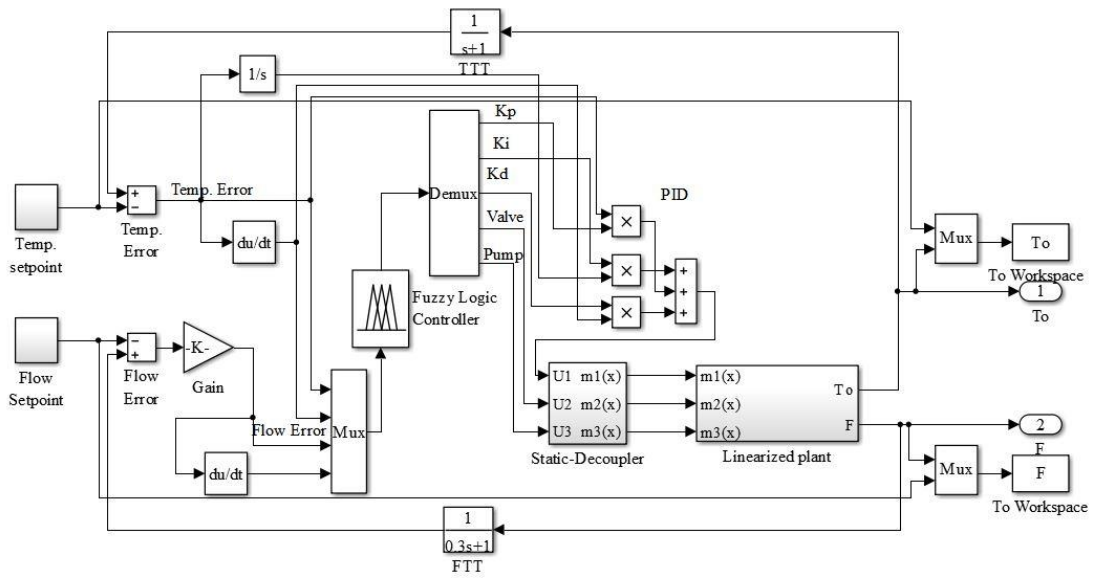
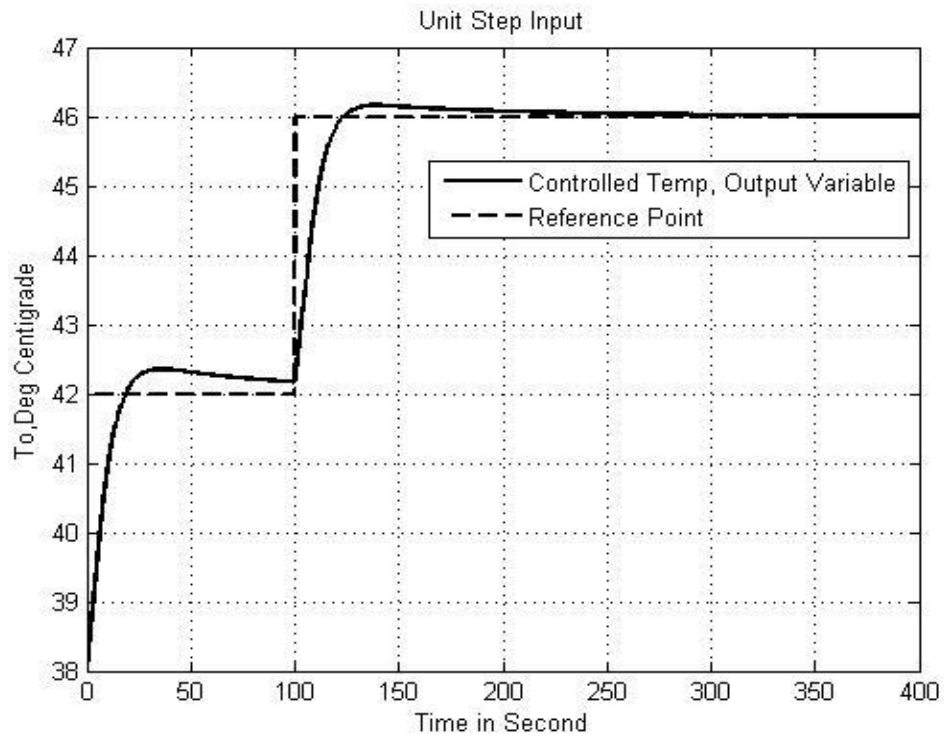
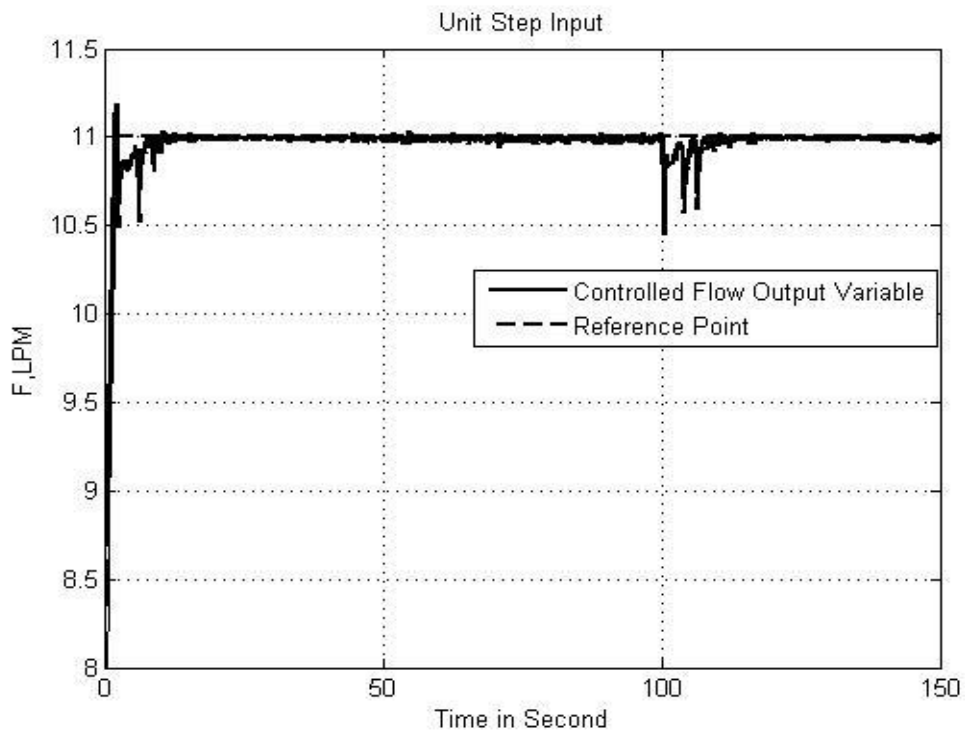


Figure 4.36. Statically decoupled linearized closed loop controlled MV system.

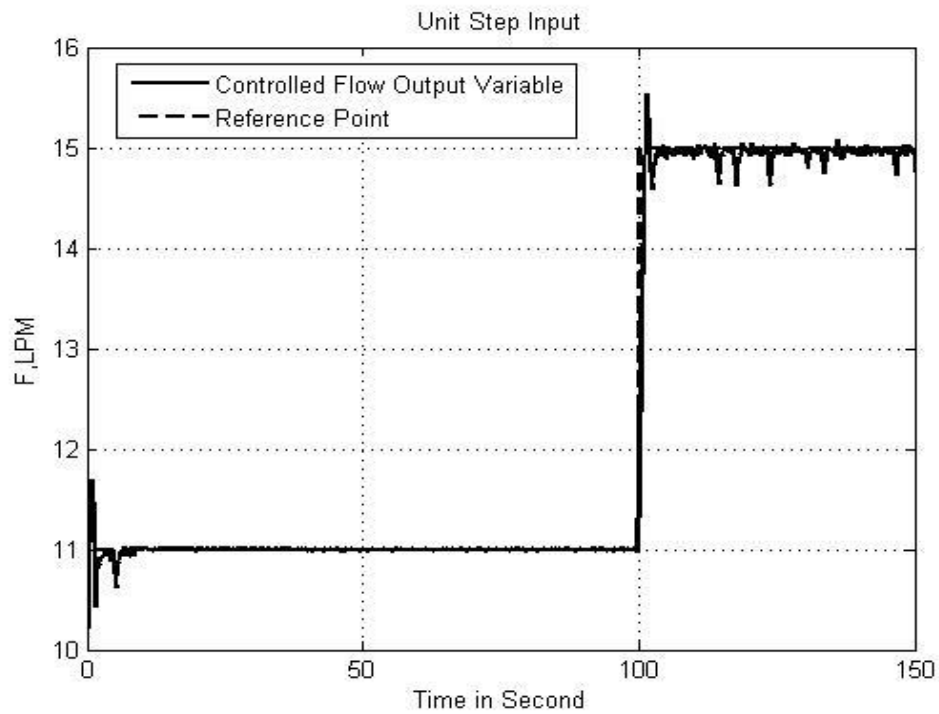


a. The temperature controlled variable behavior

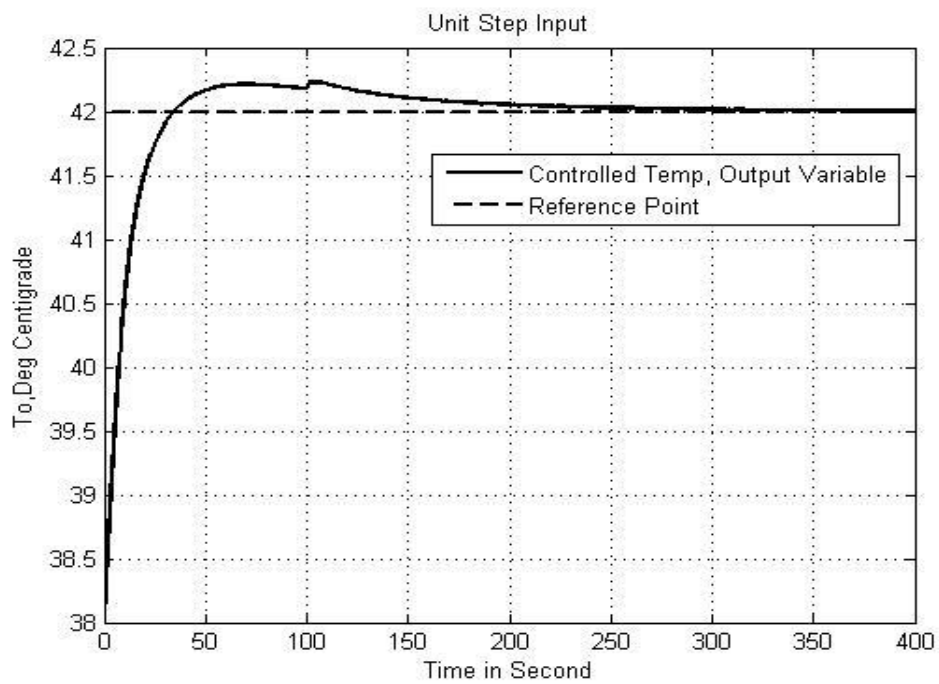


b. The flow rate controlled variable behavior

Figure 4.37. Response of statically decoupled linearized system to a step change to the temperature set point.

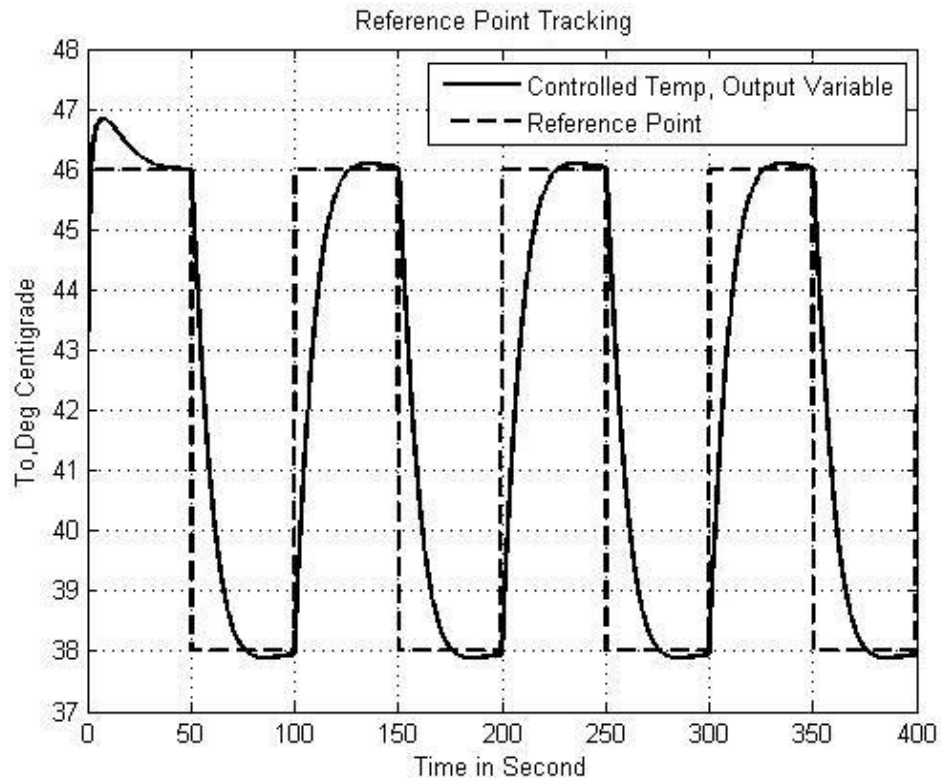


a. The flow rate controlled variable behavior

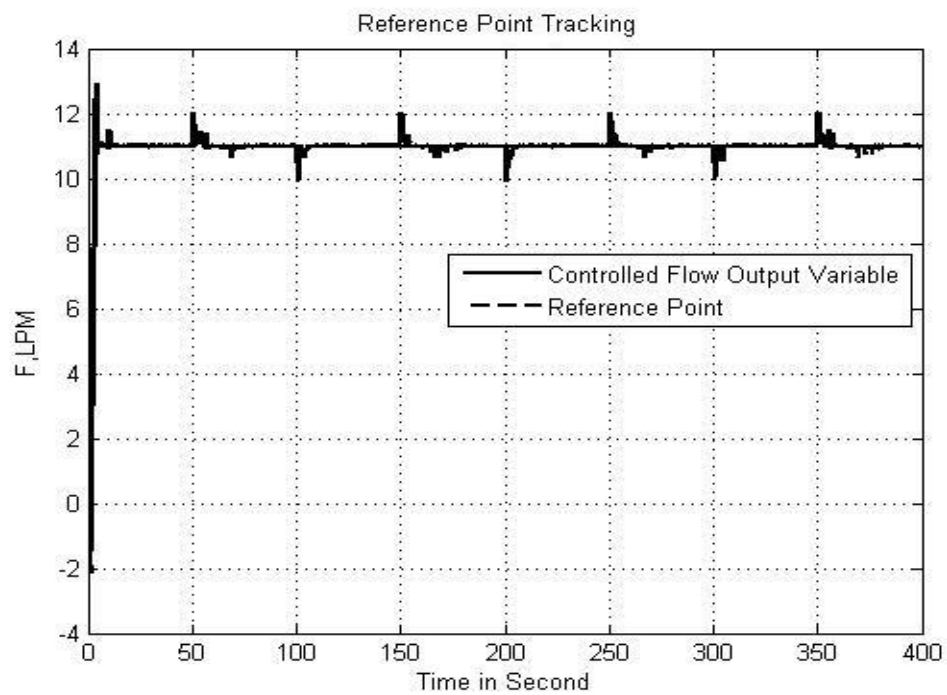


b. The temperature controlled variable behavior

Figure 4.38. Response of statically decoupled linearized system to a step change to the flow rate set point.

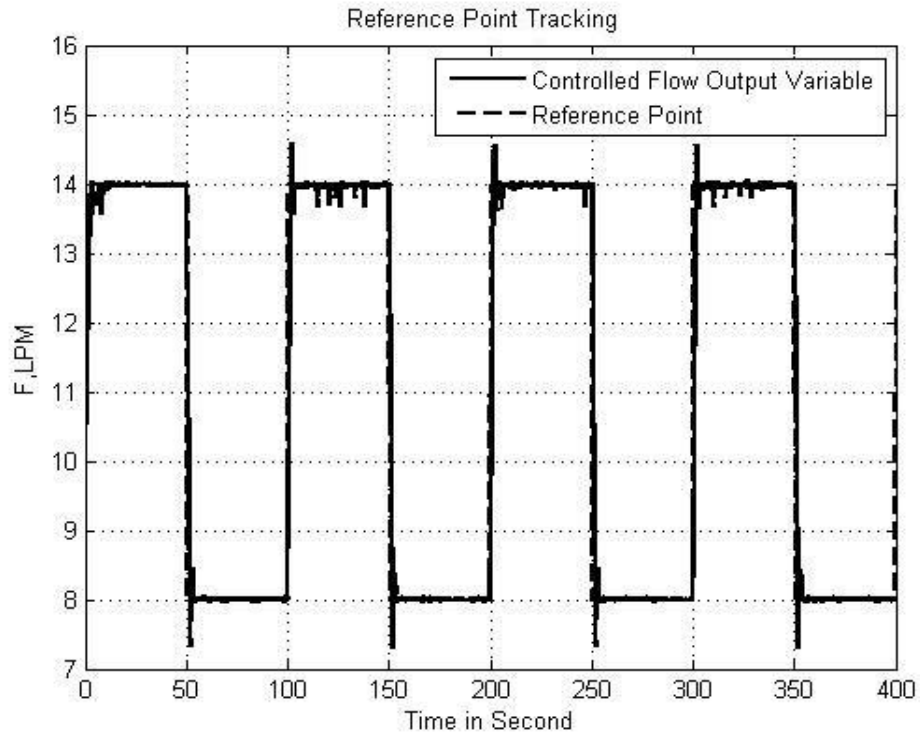


a. The temperature controlled variable behavior

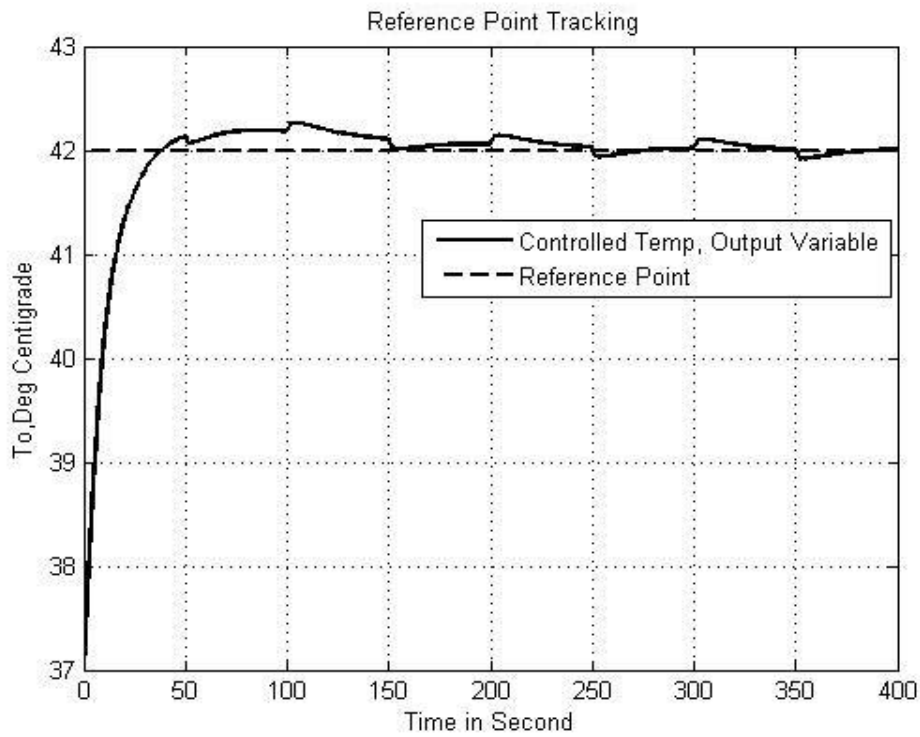


b. The flow rate controlled variable behavior

Figure 4.39. Response of statically decoupled linearized system injected with a square wave input to the temperature set point.



a. The flow rate controlled variable behavior



b. The temperature controlled variable behavior

Figure 4.40. Response of statically decoupled linearized system injected with a square wave input to the temperature set point.

### 4.3.2.2. Statically Decoupled Nonlinear System Performances

As in the previous section the system is tested this time using nonlinear system model as shown in Figure 4.41 and the results are shown in Figures (4.42 - 4.45).

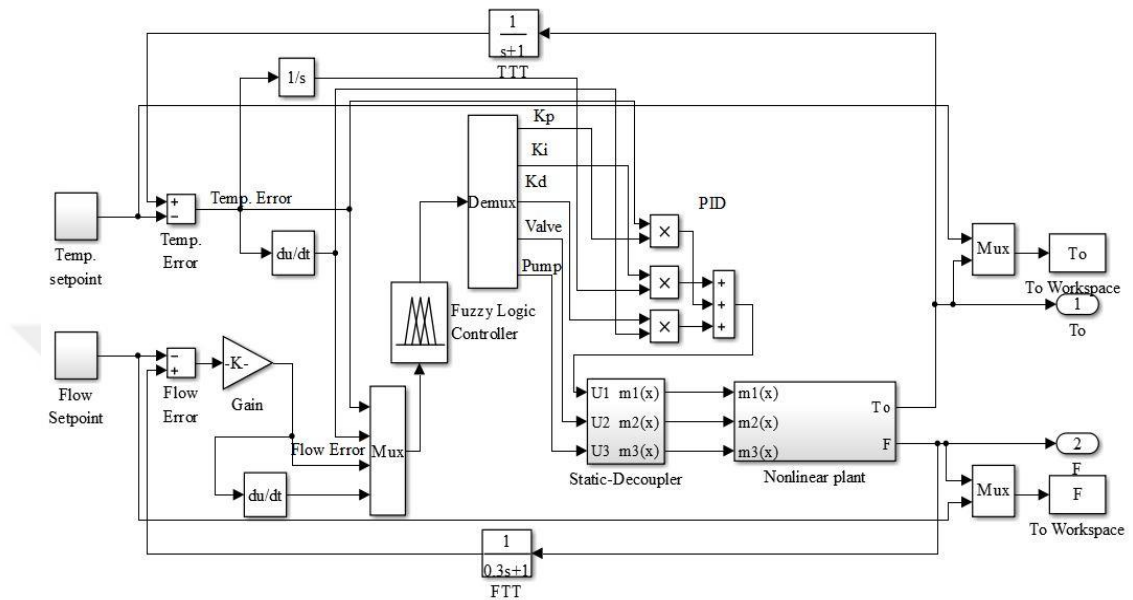
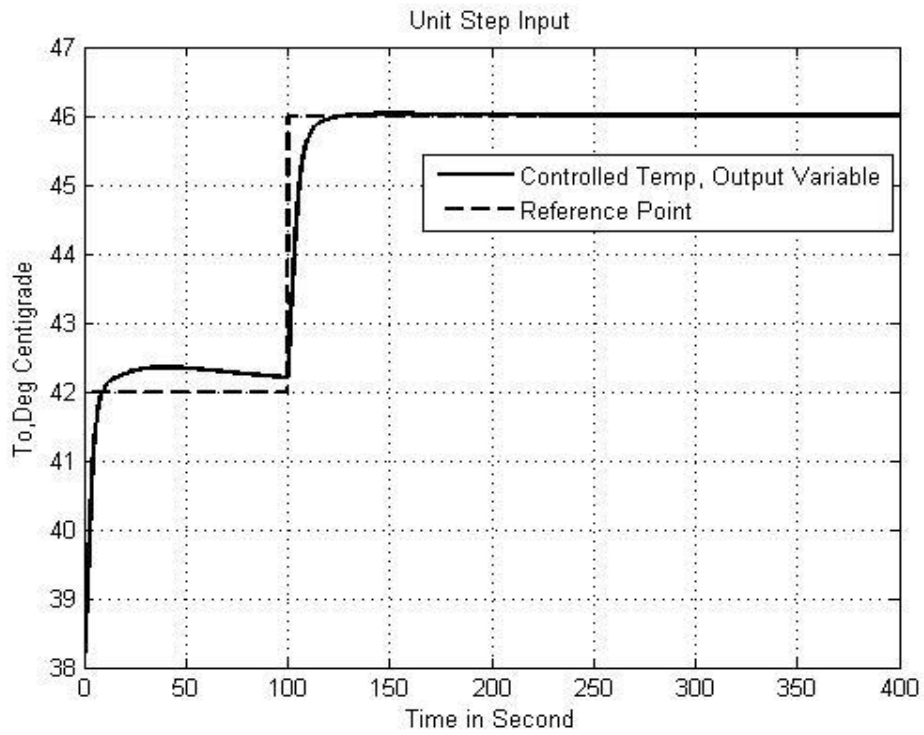
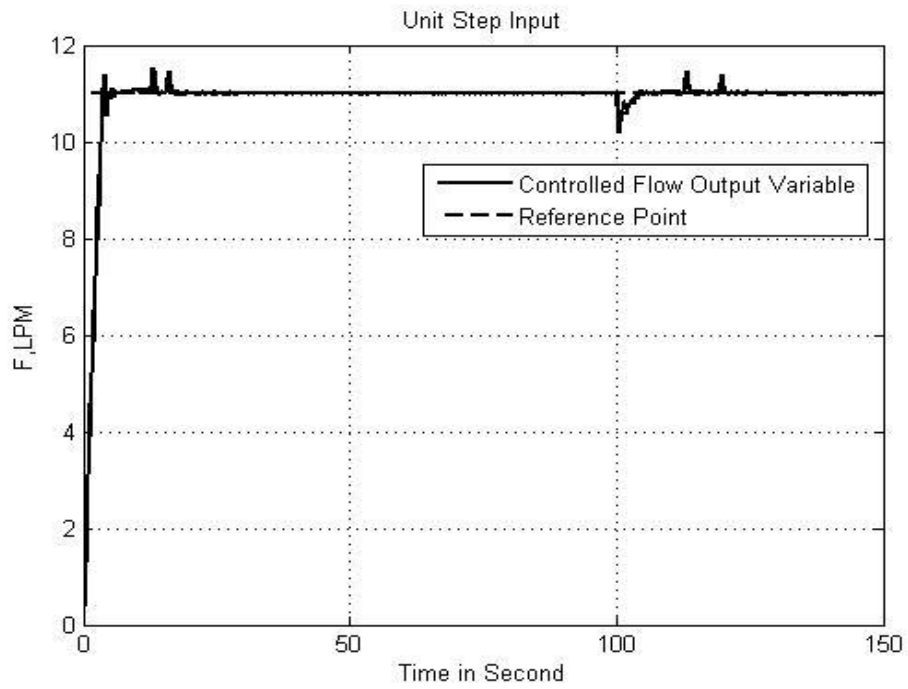


Figure 4.41. Statically decoupled nonlinear closed loop controlled MV system.



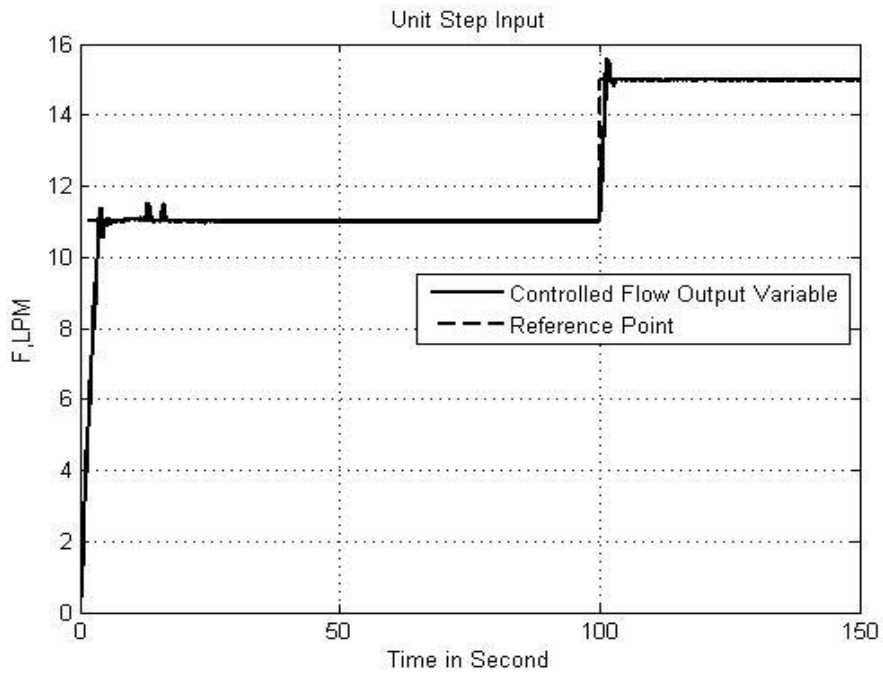


a. The temperature controlled variable behavior

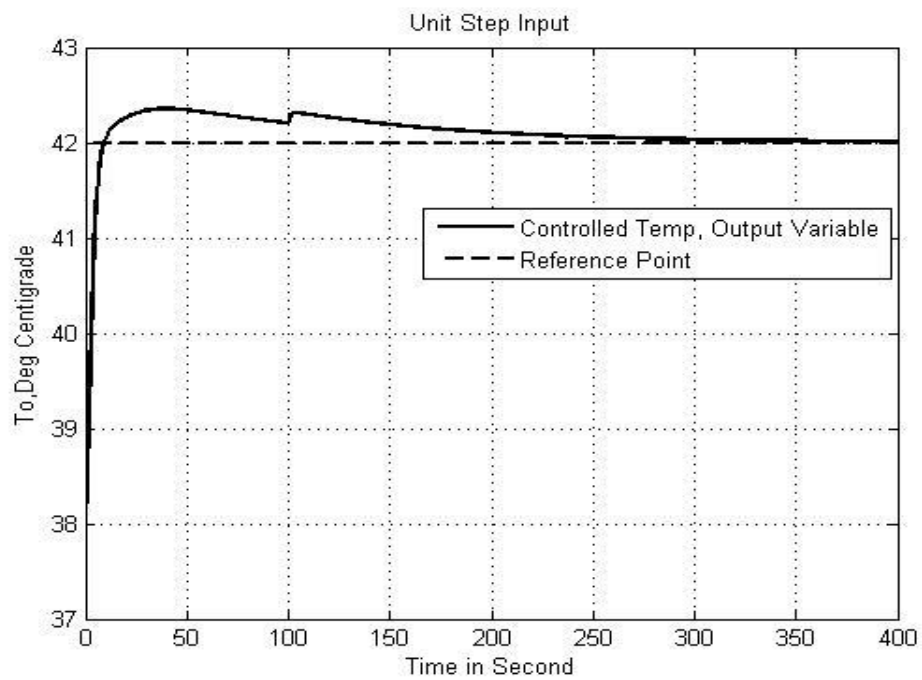


b. The flow rate controlled variable behavior

Figure 4.42. Response of statically decoupled nonlinear system to a step change to the temperature set point.

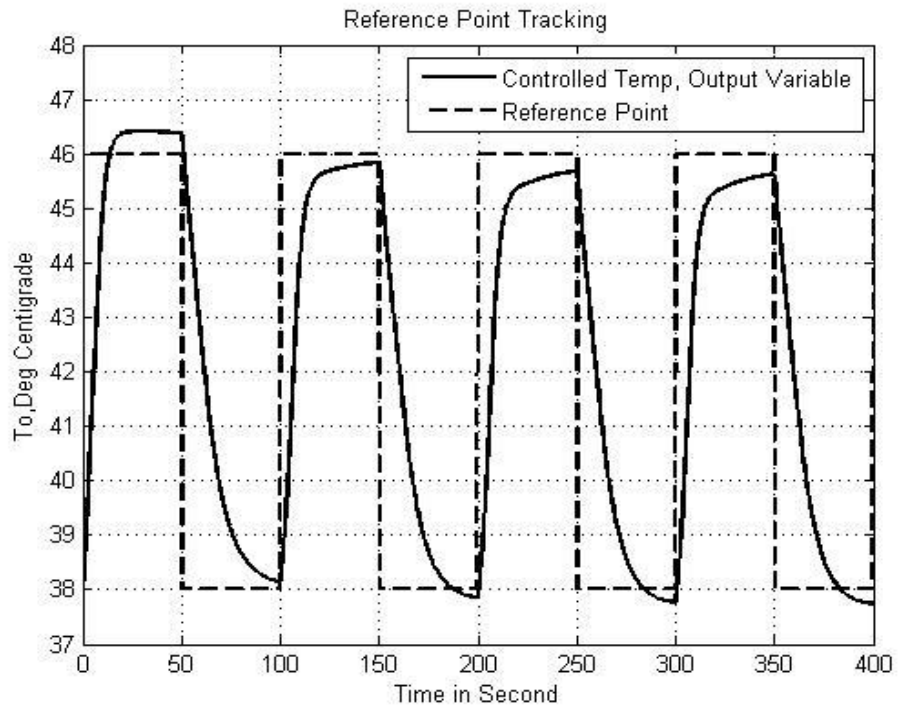


a. The flow rate controlled variable behavior

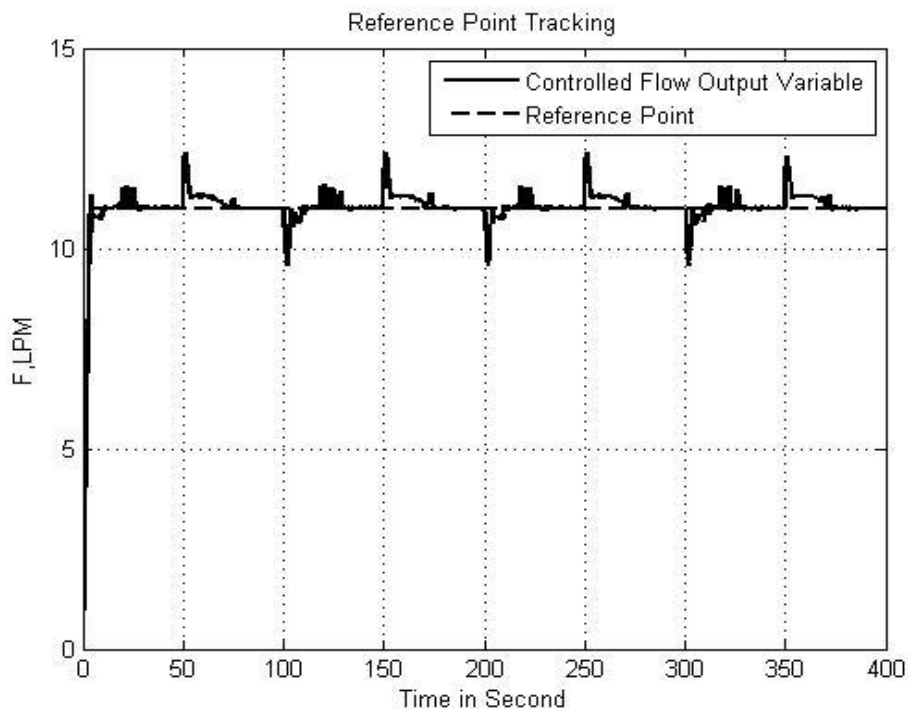


b. The temperature controlled variable behavior

Figure 4.43. Response of statically decoupled nonlinear system to a step change to the flow rate set point.

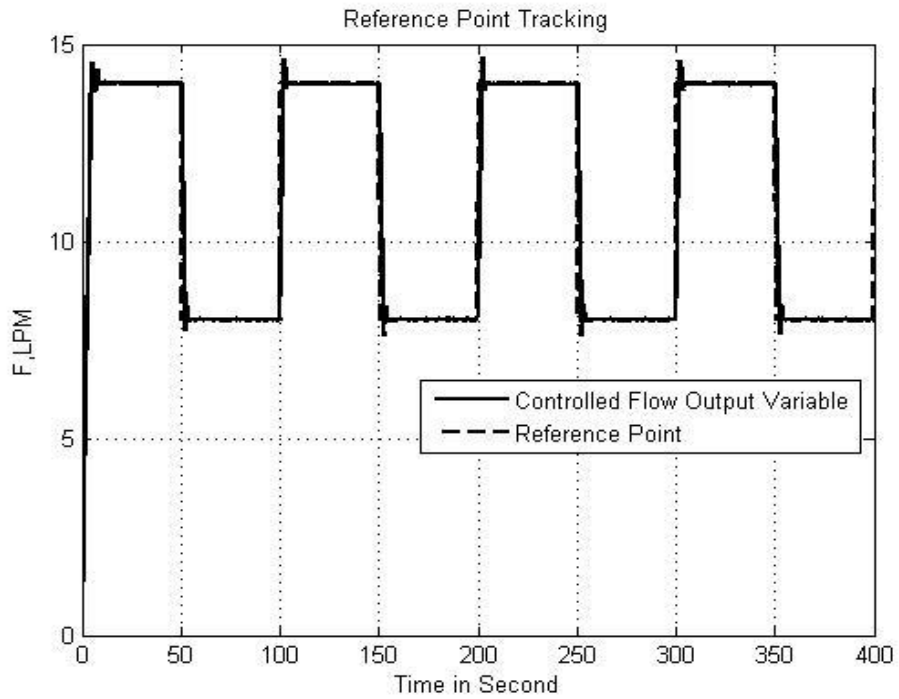


a. The temperature controlled variable behavior

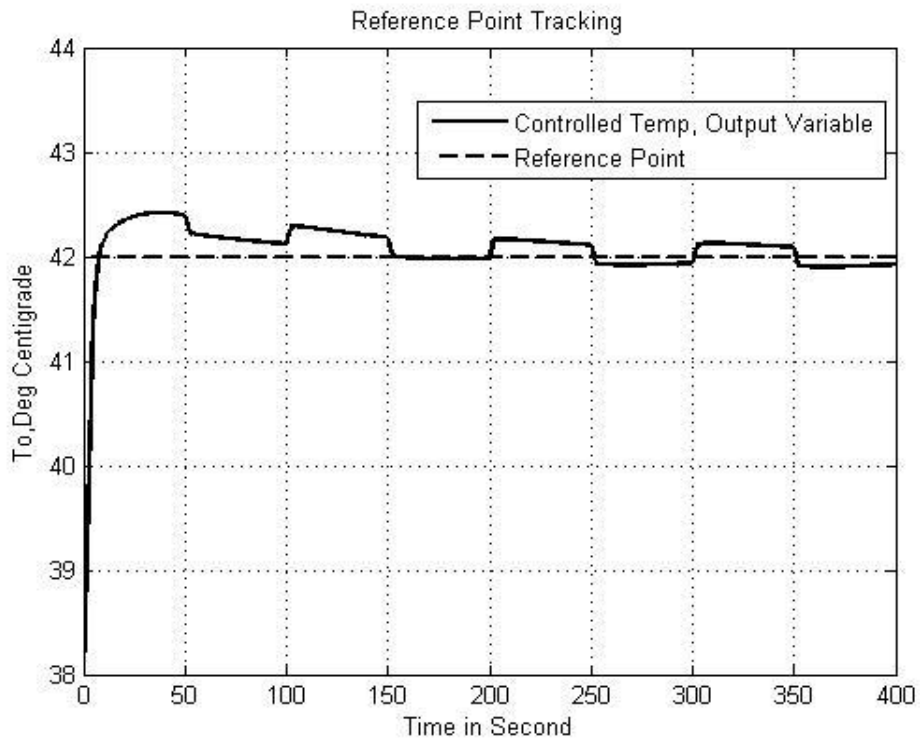


b. The flow rate controlled variable behavior

Figure 4.44. Response of statically decoupled nonlinear system injected with a square wave input to the temperature set point.



a. The flow rate controlled variable behavior



b. The temperature controlled variable behavior

Figure 4.45. Response of statically decoupled nonlinear system injected with a square wave input to the temperature set point.

### 4.3.2.3. Dynamically Decoupled Linearized System Performances

In this section the simulation tests are applied to the dynamically decoupled linearized system, by the same mechanism as two previous sections as shown in Figure 4.46. The results are shown in Figures (4.47 - 4.50).

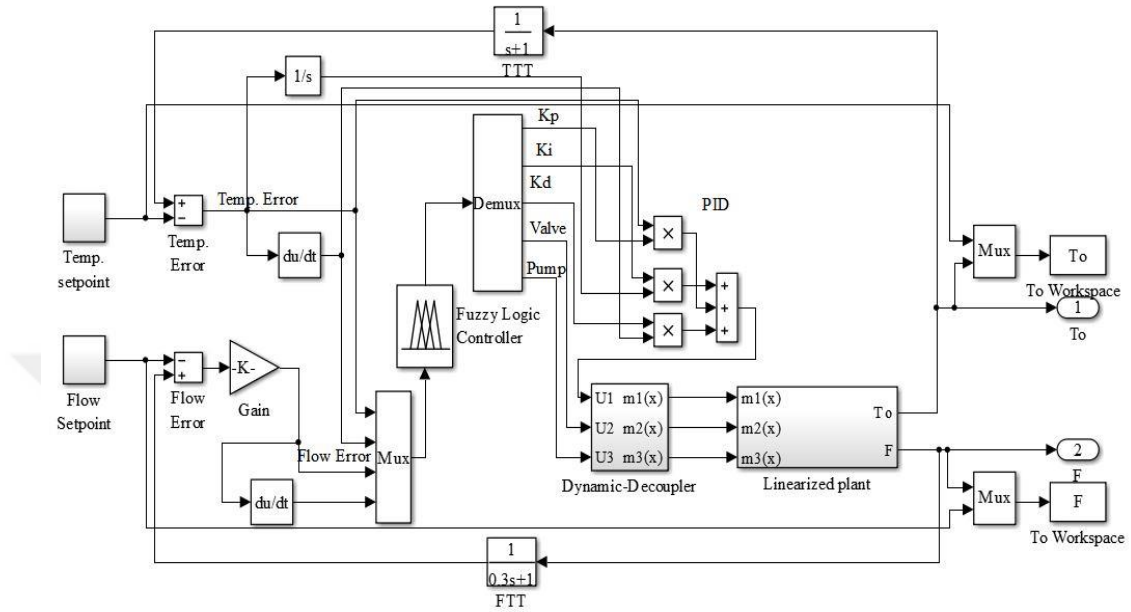
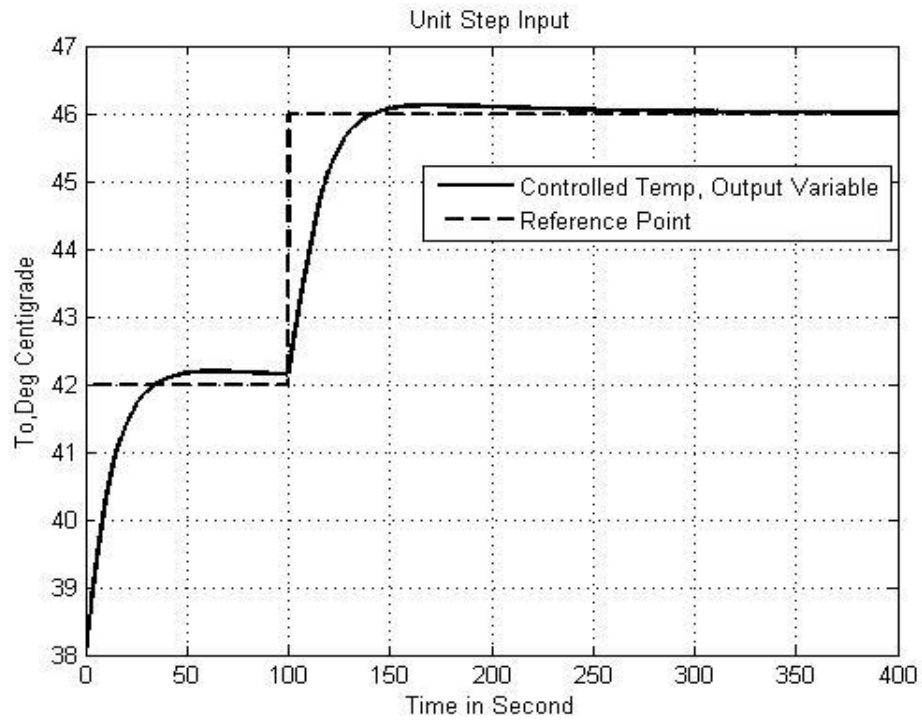
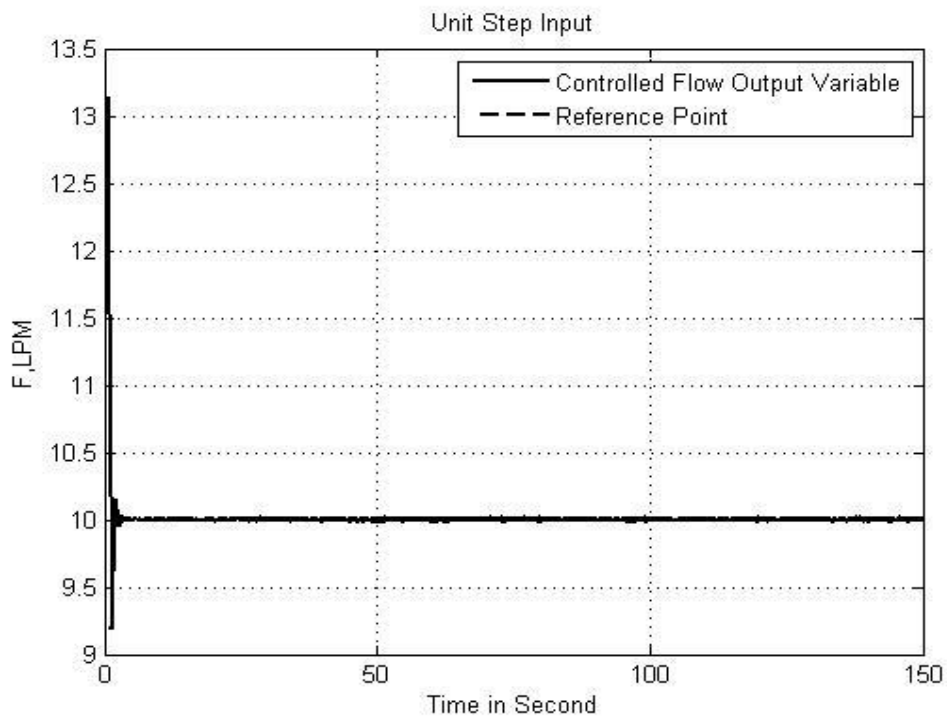


Figure 4.46. Dynamically decoupled linearized closed loop controlled MV system.

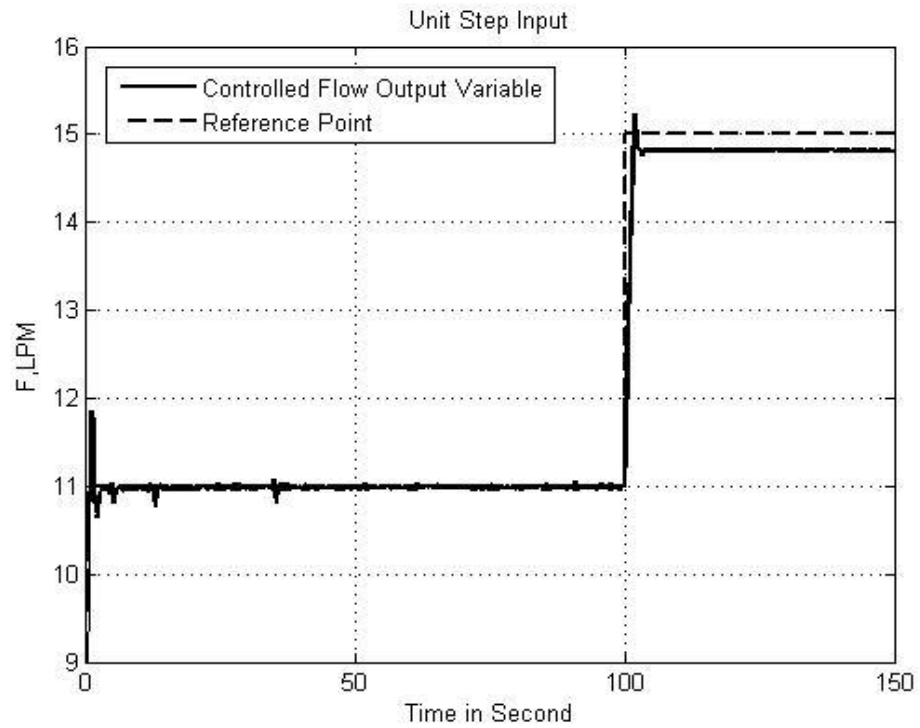


a. The temperature controlled variable behavior

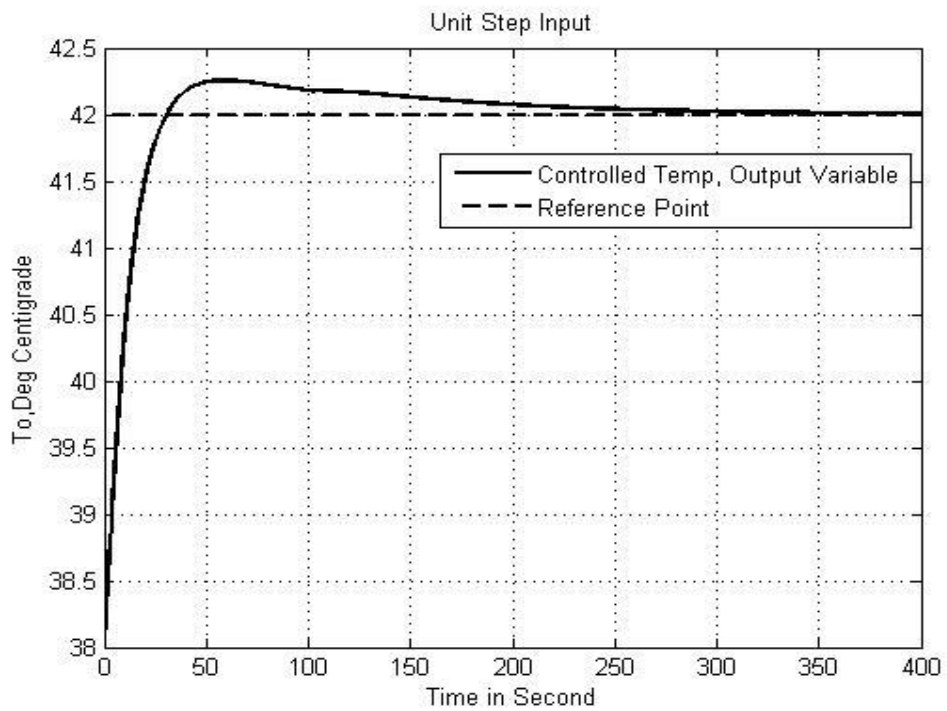


b. The flow rate controlled variable behavior

Figure 4.47. Response of dynamically decoupled linearized system to a step change to the temperature set point.

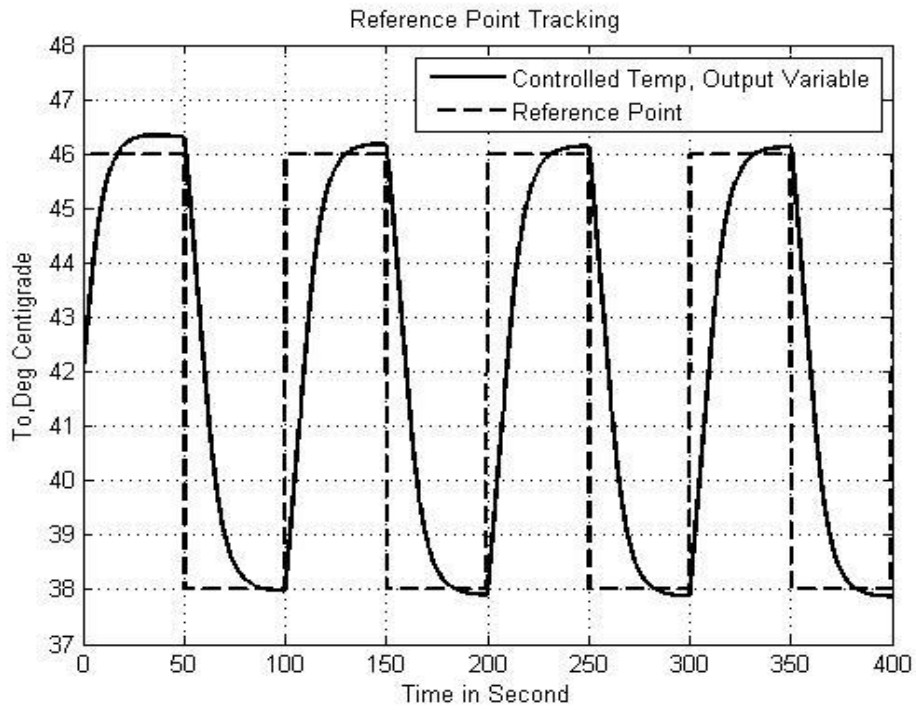


a. The flow rate controlled variable behavior

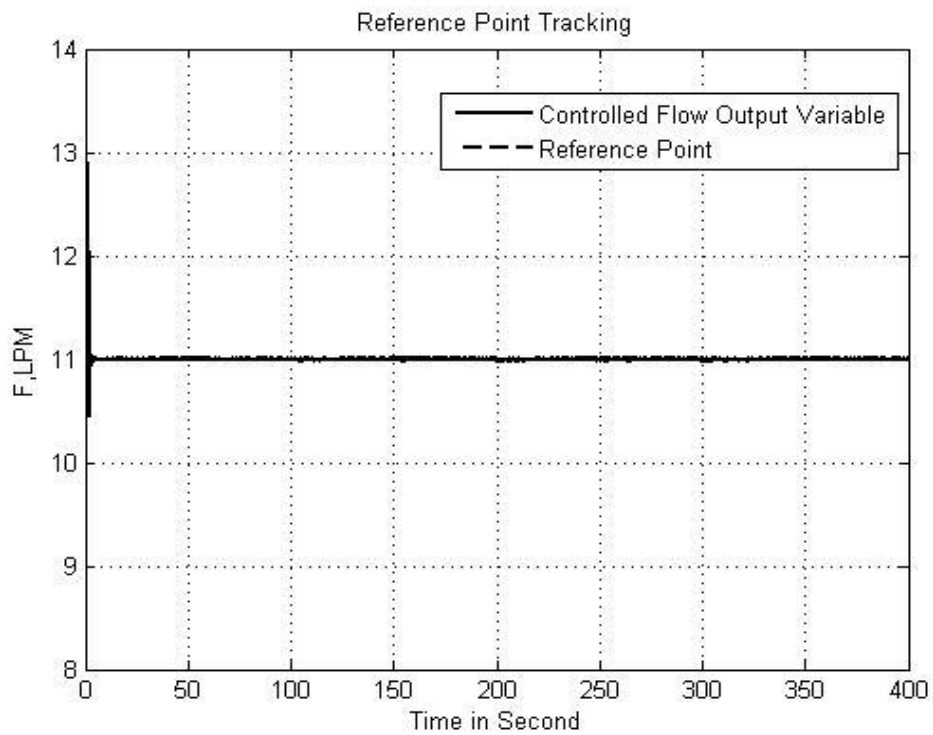


b. The temperature controlled variable behavior

Figure 4.48. Response of dynamically decoupled linearized system to a step change to the flow rate set point.



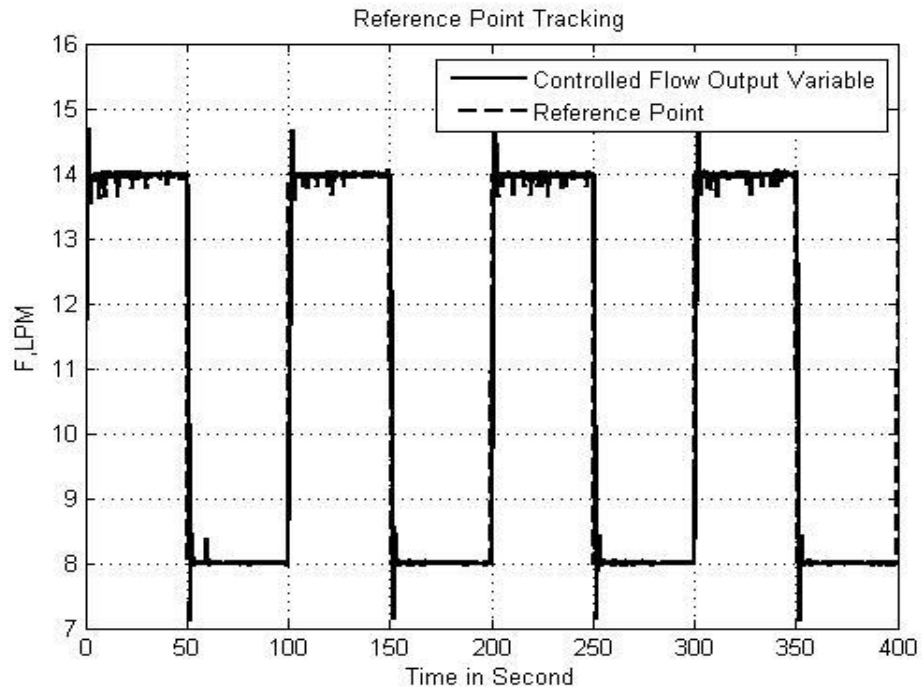
a. The temperature controlled variable behavior



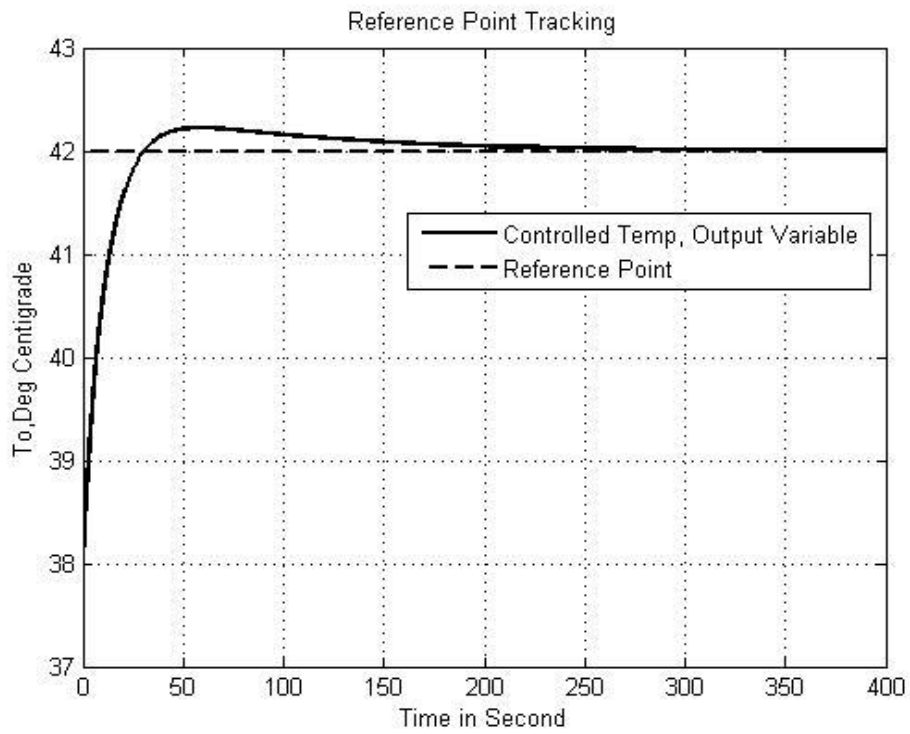
b. The flow rate controlled variable behavior

Figure 4.49. Response of dynamically decoupled linearized system injected with a square wave input to the temperature set point.





a. The flow rate controlled variable behavior



b. The temperature controlled variable behavior

Figure 4.50. Response of dynamically decoupled linearized system injected with a square wave input to the temperature set point.

#### 4.3.2.4. Dynamically Decoupled Nonlinear System Performances

The last simulation tests considering through control inputs are applied in this section, on the dynamically decoupled nonlinear system of which computer simulated model shown in Figure 4.51. The simulation results are shown in Figures (4.52 - 4.55).

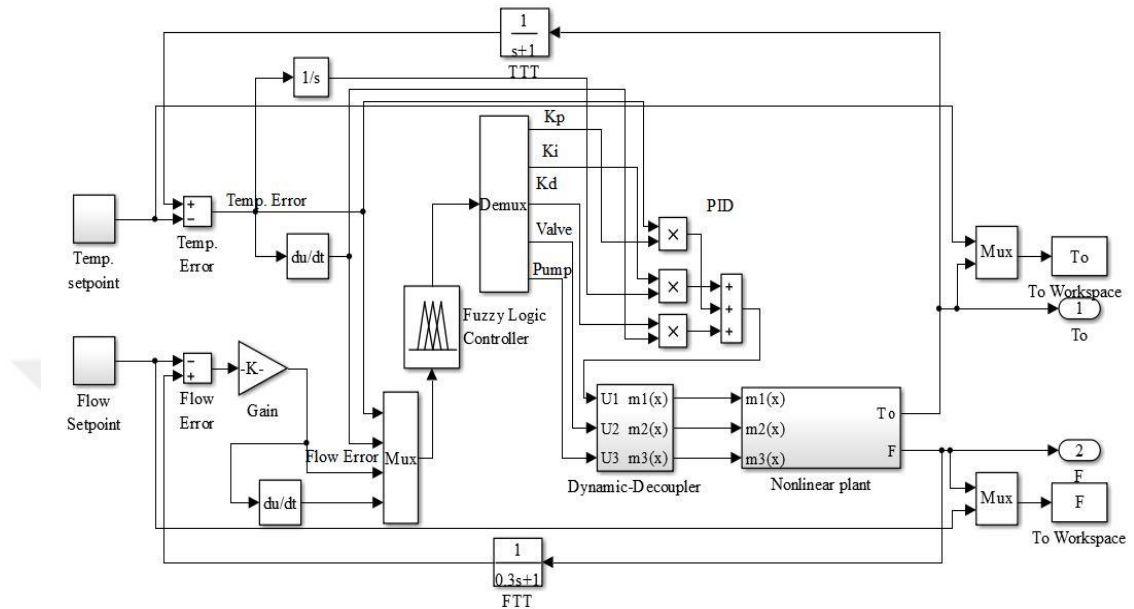
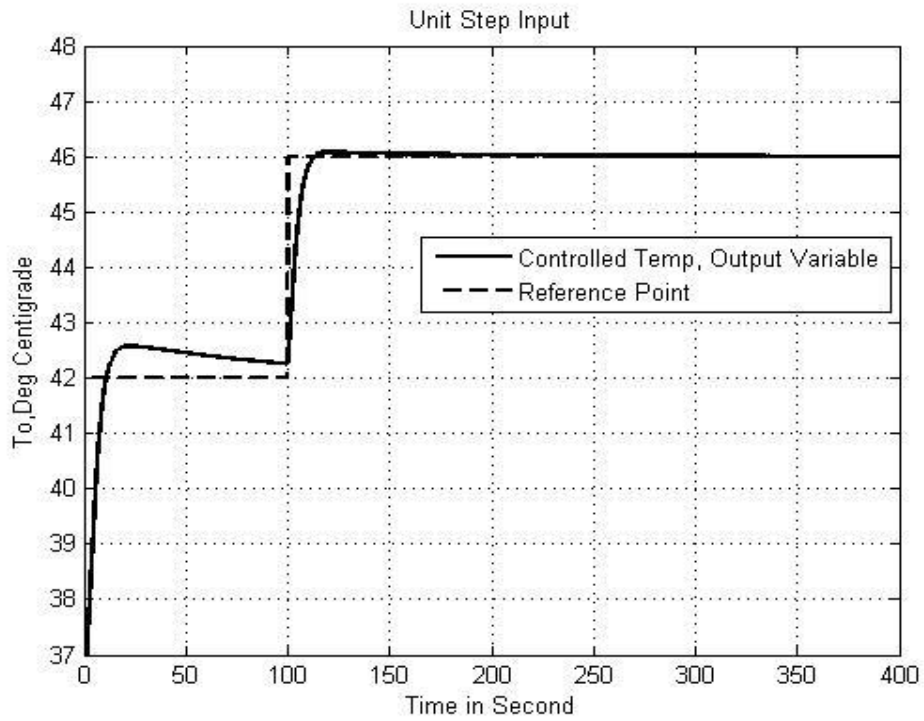
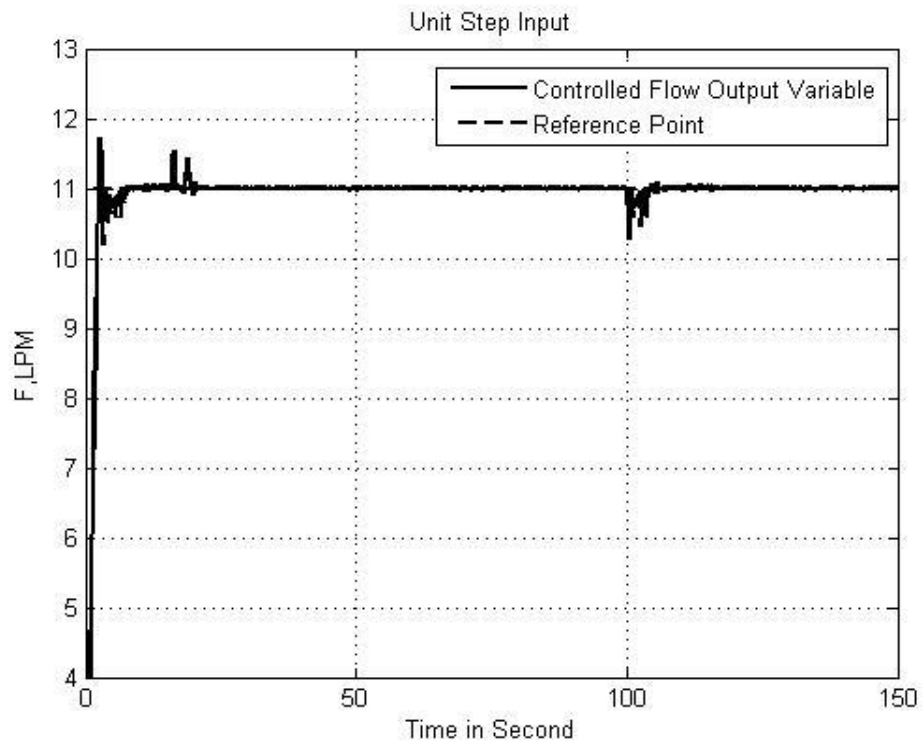


Figure 4.51. Dynamically decoupled nonlinear closed loop controlled MV system.

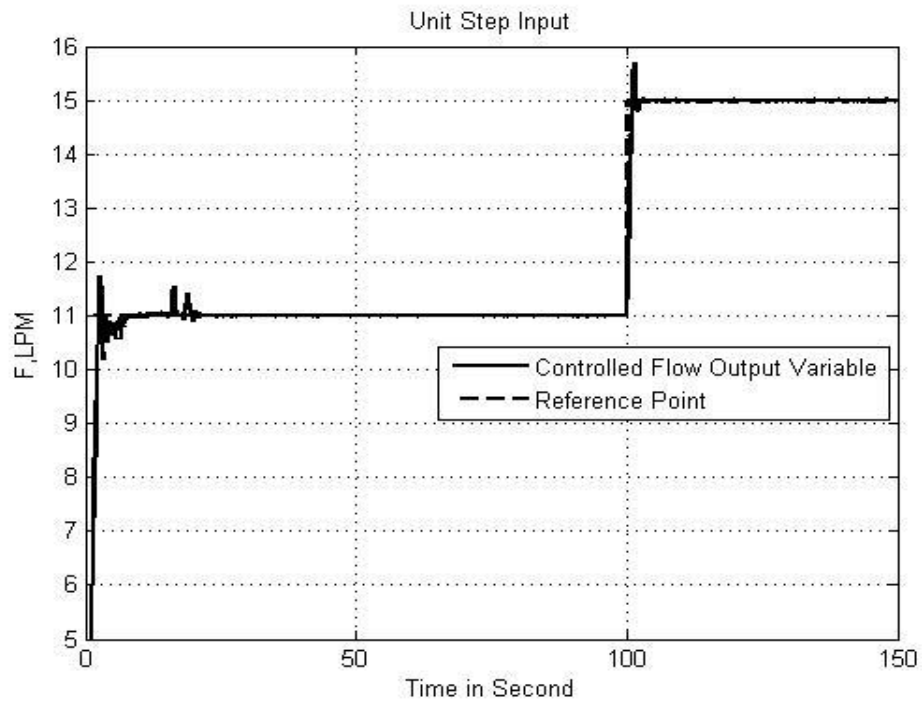


a. The temperature controlled variable behavior

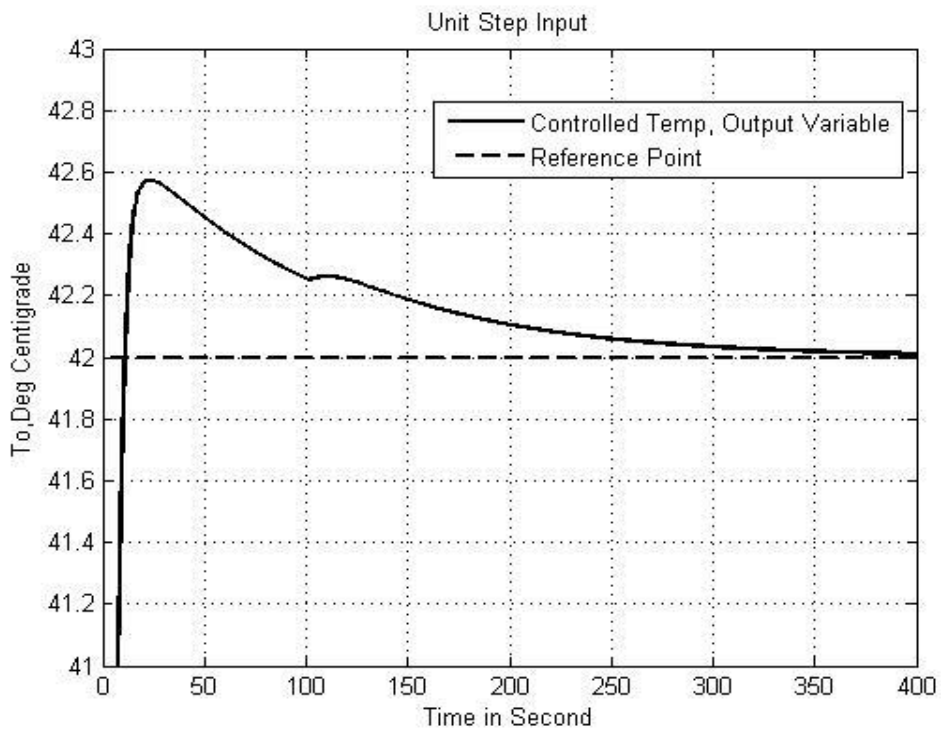


b. The flow rate controlled variable behavior

Figure 4.52. Response of dynamically decoupled nonlinear system to a step change to the temperature set point.

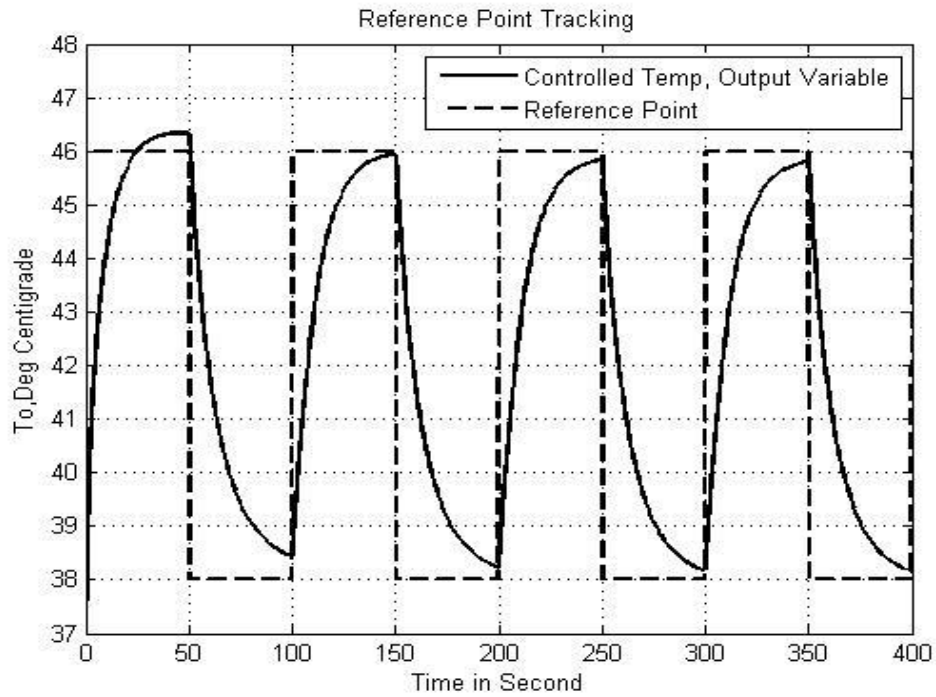


a. The flow rate controlled variable behavior

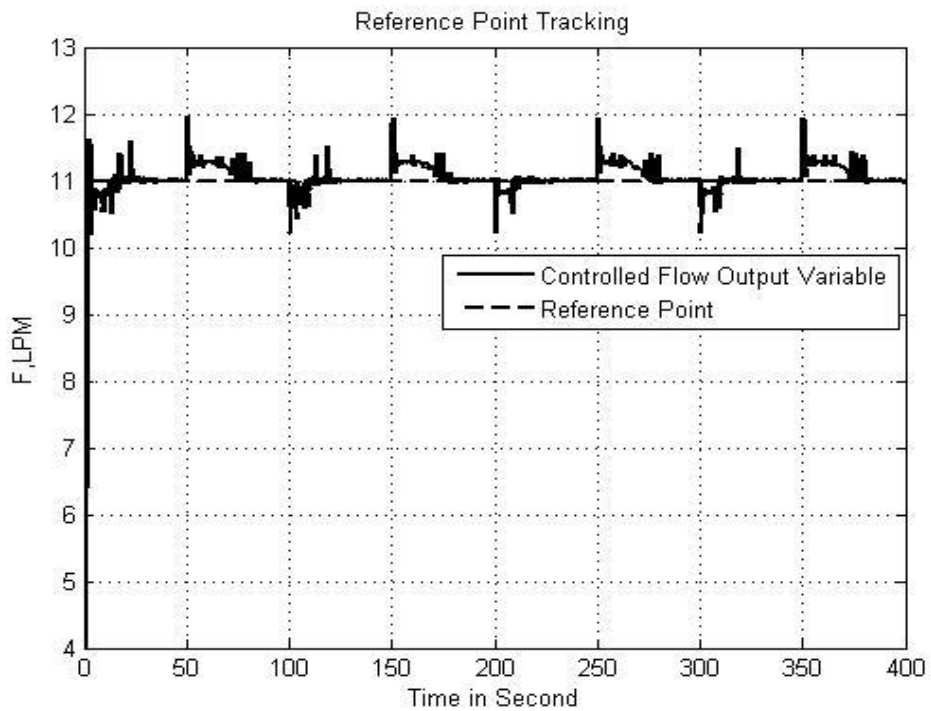


b. The temperature controlled variable behavior

Figure 4.53. Response of dynamically decoupled nonlinear system to a step change to the flow rate set point.

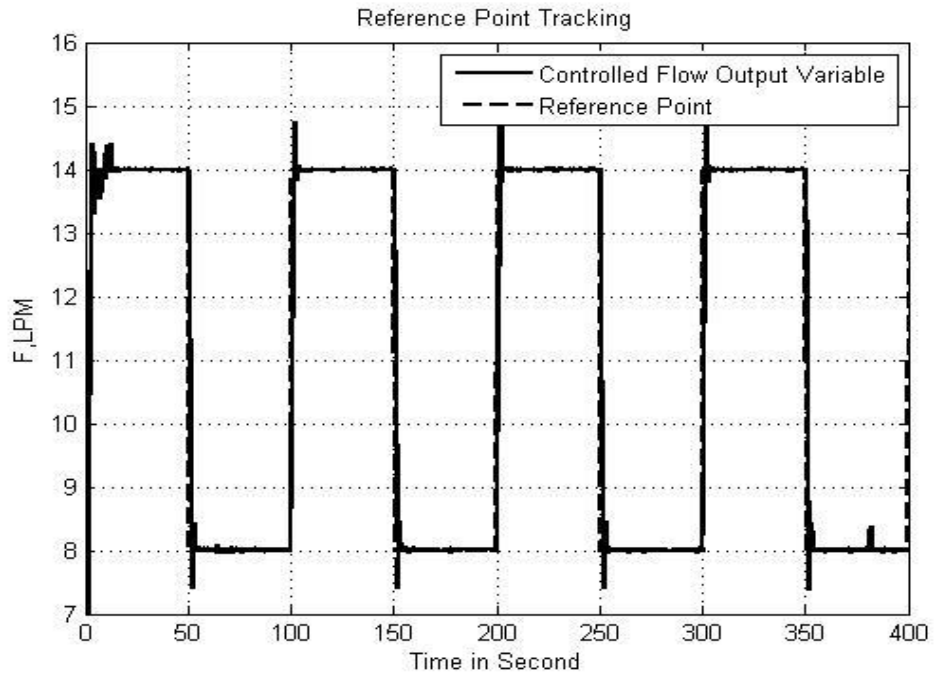


a. The temperature controlled variable behavior

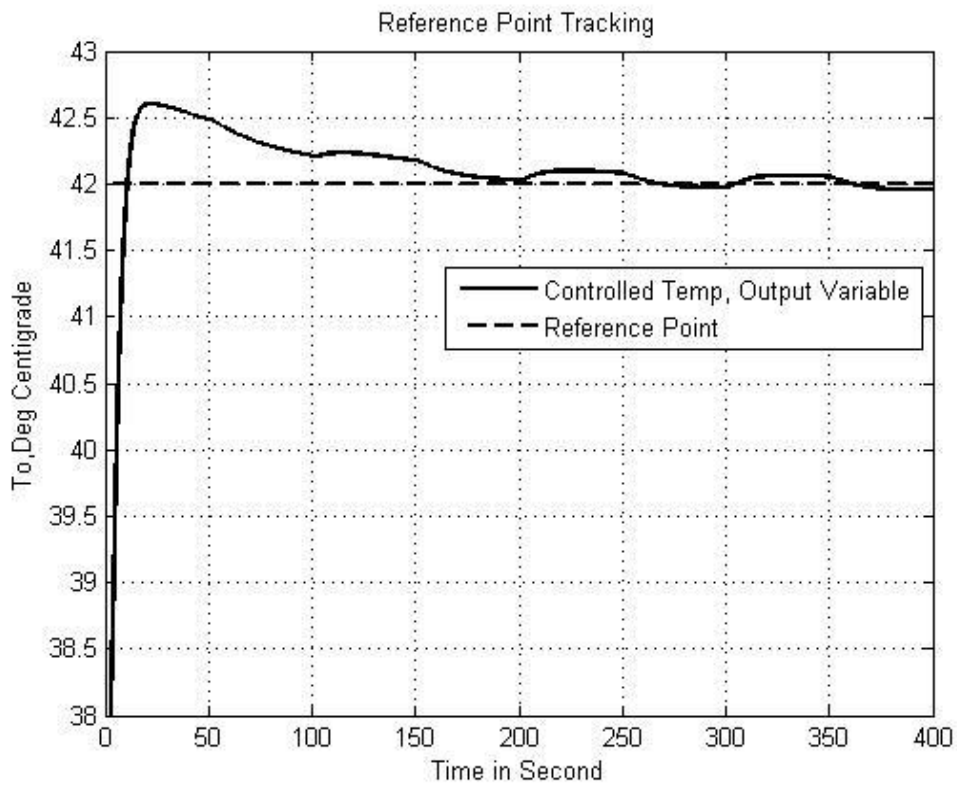


b. The flow rate controlled variable behavior

Figure 4.54. Response of dynamically decoupled nonlinear system injected with a square wave input to the temperature set point.



a. The flow rate controlled variable behavior



b. The temperature controlled variable behavior

Figure 4.55. Response of dynamically decoupled nonlinear system injected with a square wave input to the temperature set point.

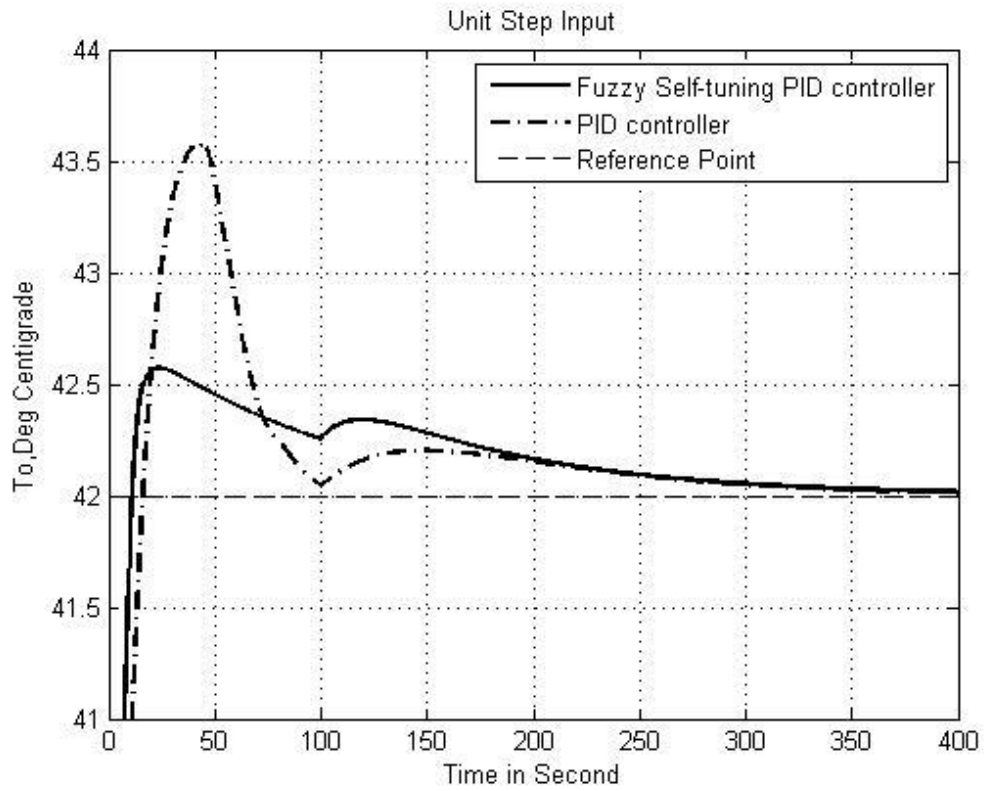
### **4.3.3. Controllers Performances through Disturbance Rejection**

As described in previous chapters, the major disturbances that may occur in this MV system are change of temperatures and pressures of each intake flow.

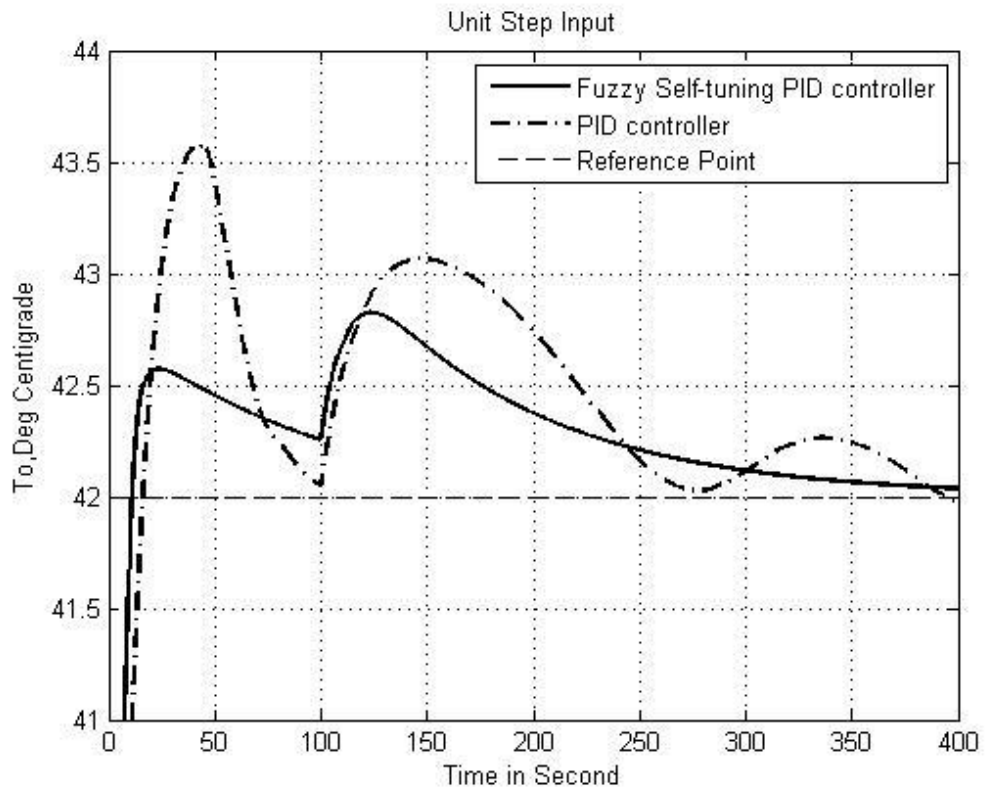
In this section the MV system is disturbed with three kinds of signals, which are step change, sine wave and random signal. These disturbance subjections are applied to the dynamically decoupled nonlinear system.

The magnitude of change or fluctuating of temperature and pressure are 8 centigrade degrees and 55 kPa, respectively. The MV output behavior results in accordance with each disturbing signal are simulated. The Figures (4.56 - 4.64) show the results.





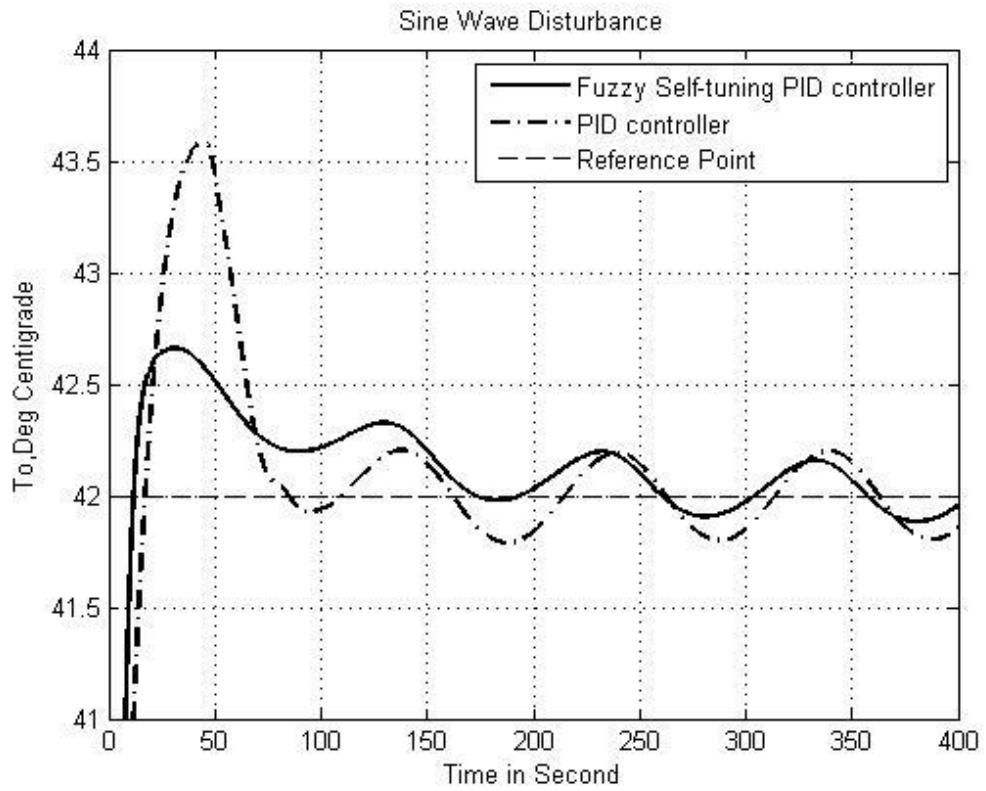
a. The temperature  $T_1$ , disturbed with a step change



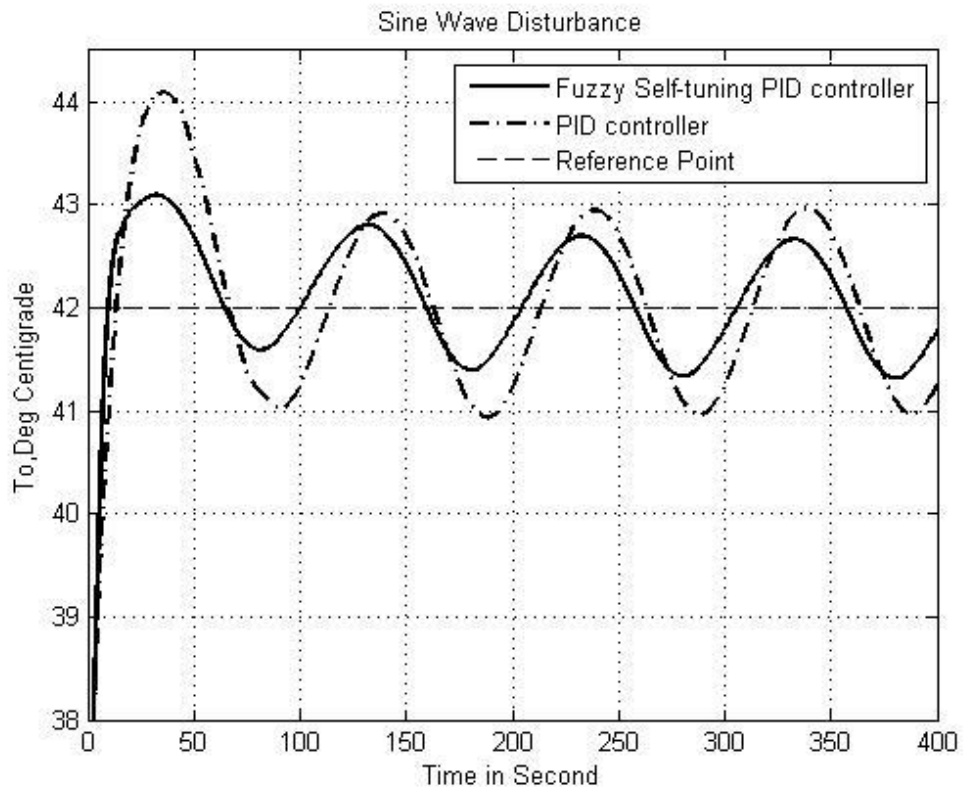
b. The temperature  $T_2$ , disturbed with a step change

Figure 4.56. System controlled temperature variable behavior through each intake flow temperature disturbed with a step change.



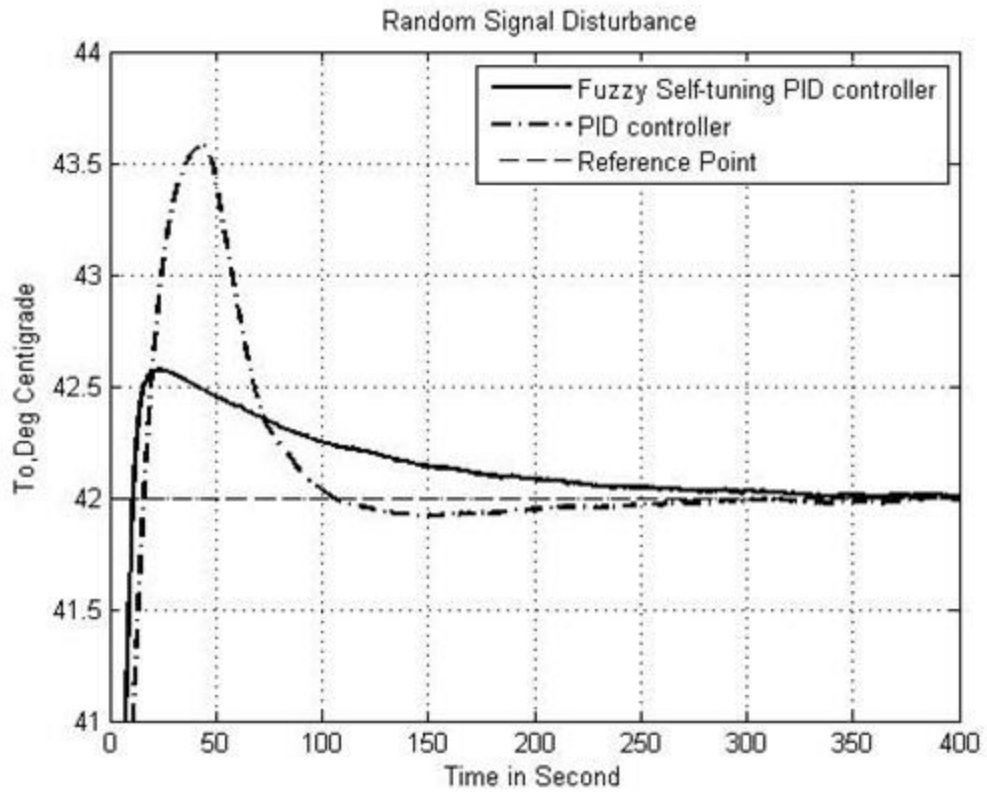


a. The temperature  $T_1$  fluctuated, disturbed a with a sine wave

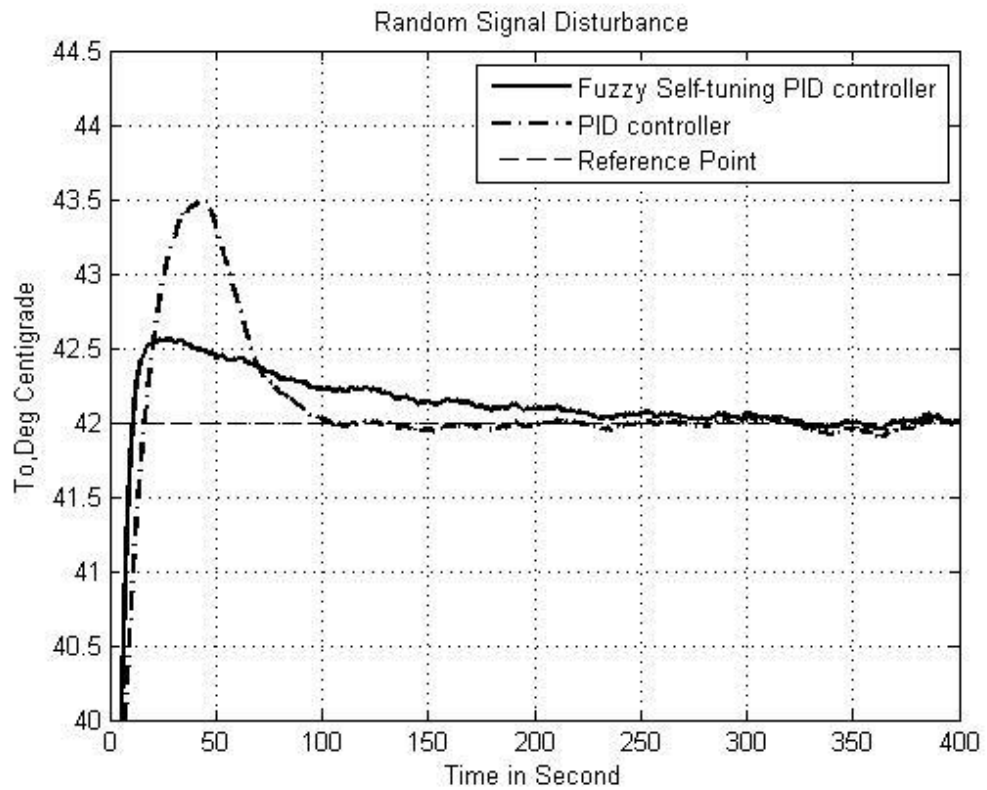


b. The temperature  $T_2$  fluctuated, disturbed with a sine wave

Figure 4.57. System controlled temperature variable behavior through each intake flow temperature disturbed with a sine wave.

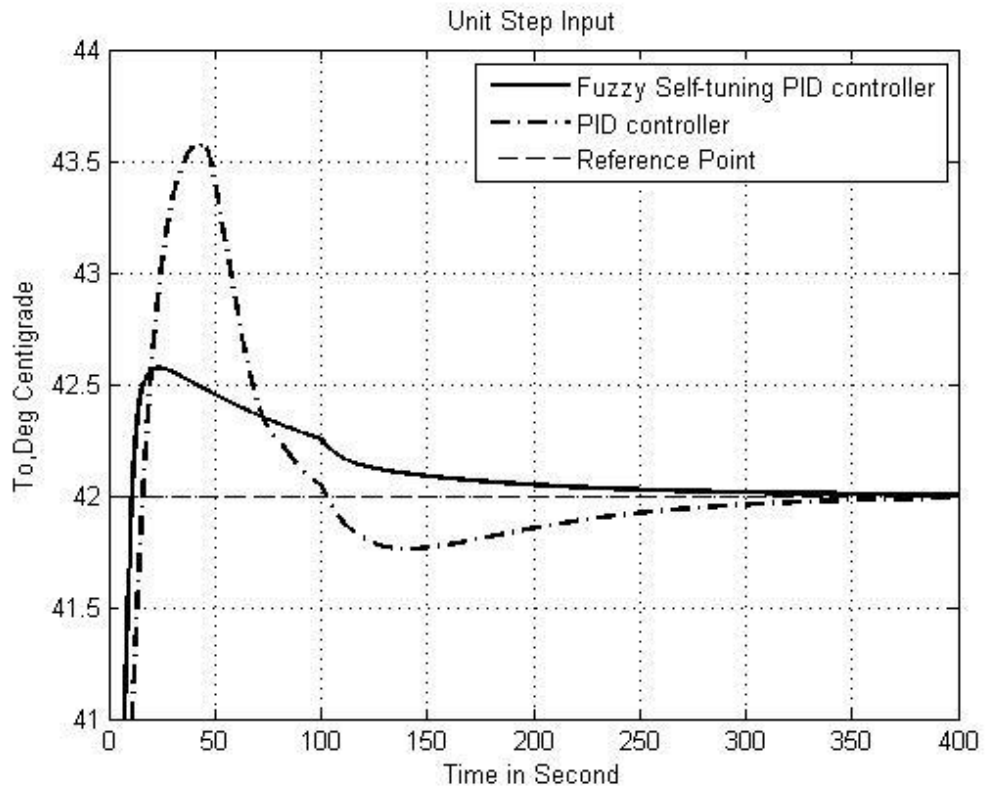


a. The temperature  $T_1$ , disturbed with a random signal

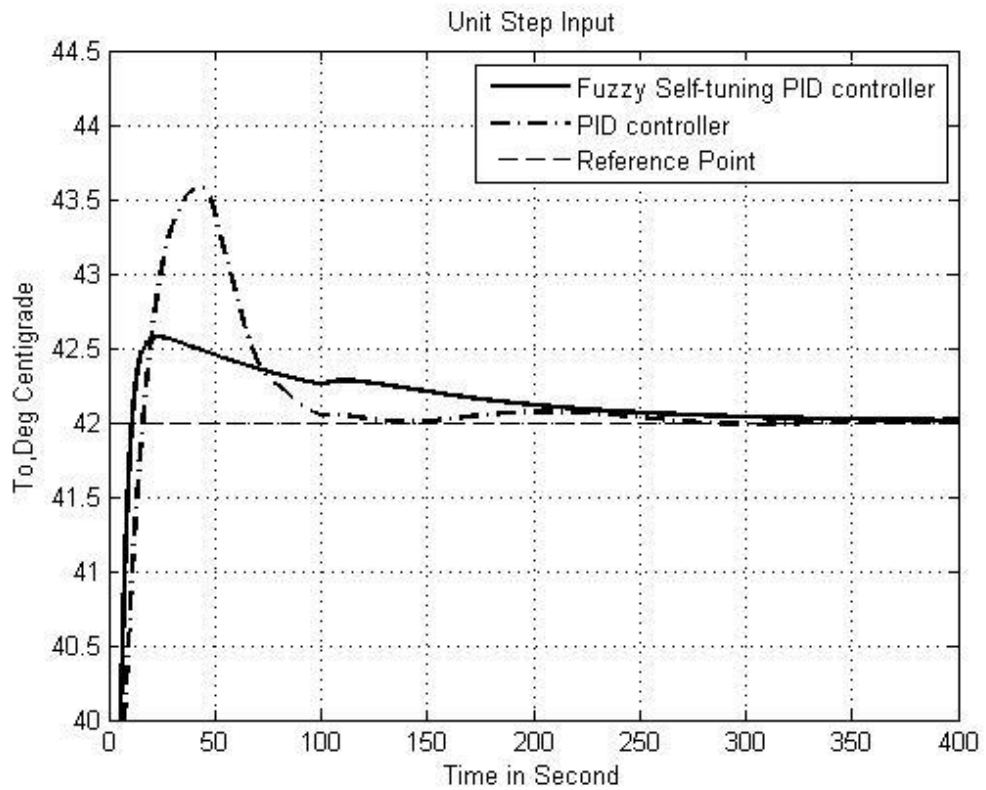


b. The temperature  $T_2$ , disturbed with a random signal

Figure 4.58. System controlled temperature variable behavior through each intake flow temperature disturbed with a random signal.

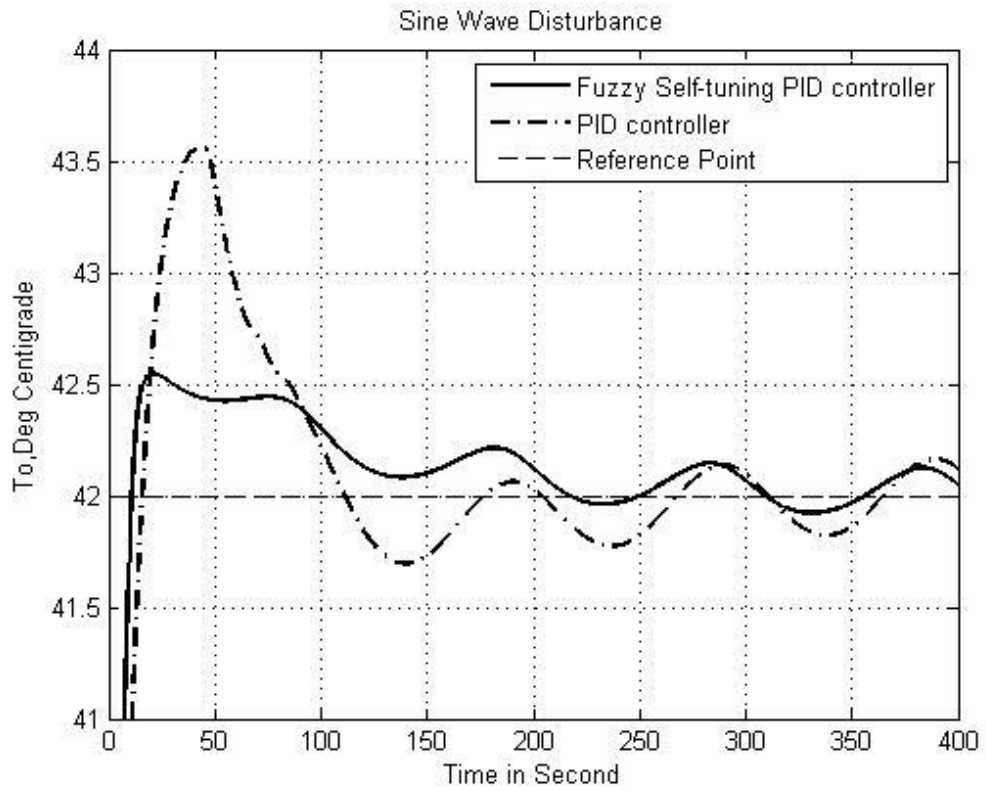


a. The pressure  $P_1$ , disturbed with a step change

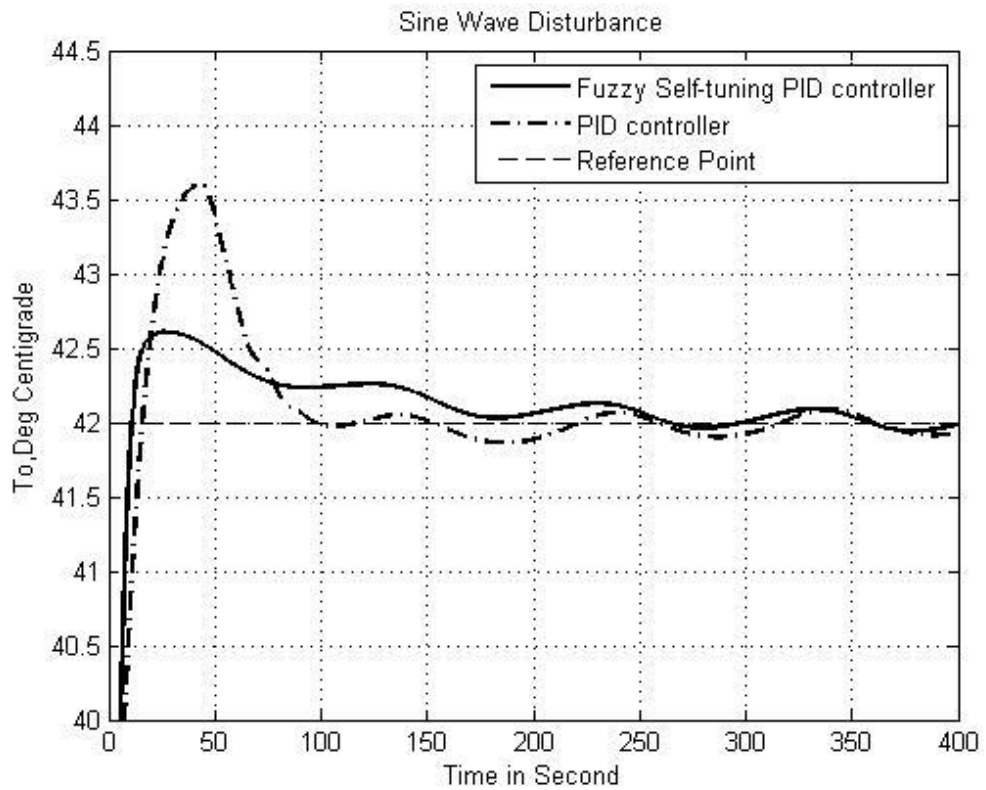


b. The pressure  $P_2$ , disturbed with a step change

Figure 4.59. System controlled temperature variable behavior through each intake flow pressure disturbed with a step change.

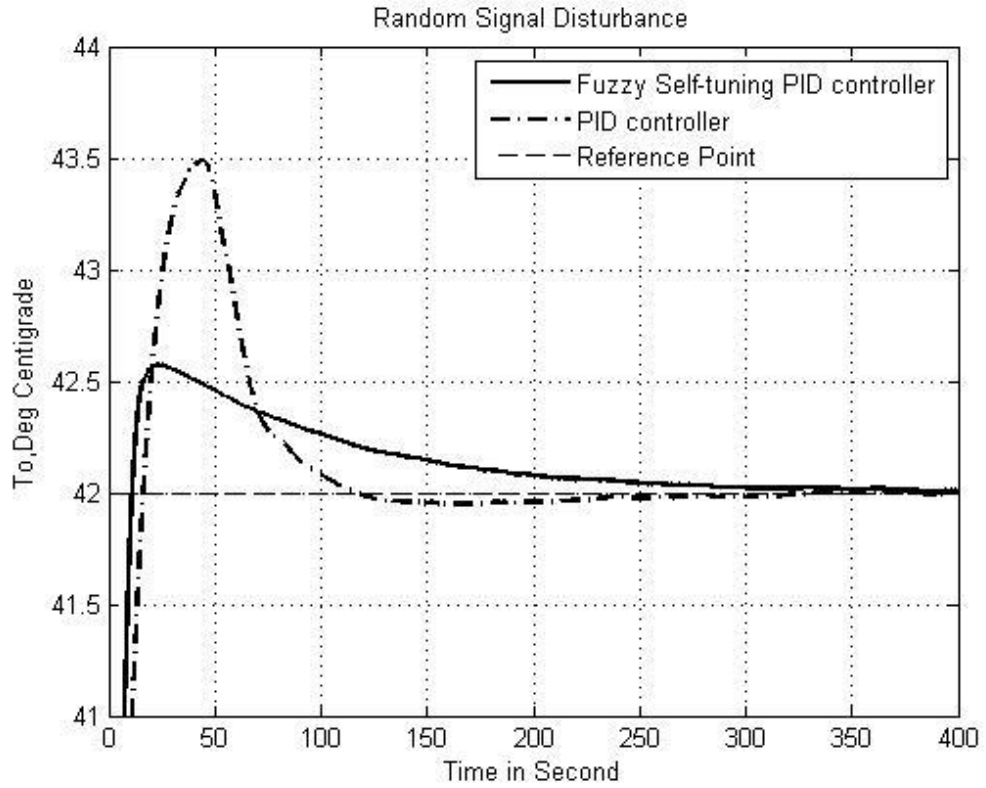


a. The pressure  $P_1$  fluctuated, disturbed with a sine wave

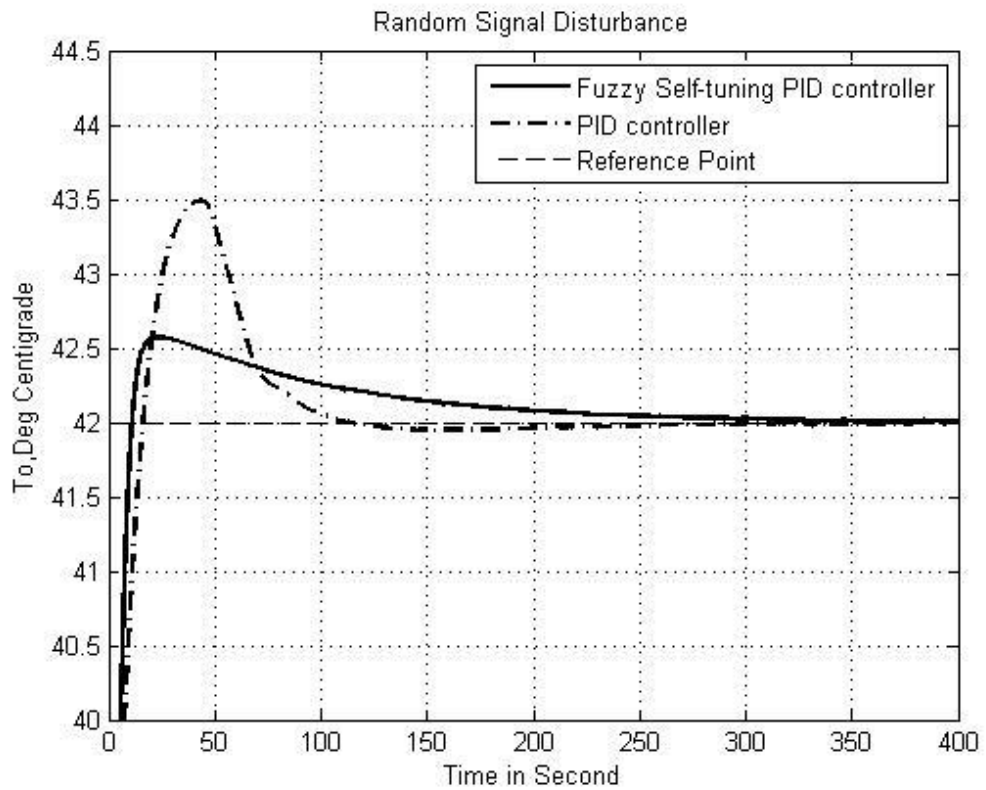


b. The pressure  $P_2$  fluctuated, disturbed with a sine wave

Figure 4.60. System controlled temperature variable behavior through each intake flow pressure disturbed with a sine wave.

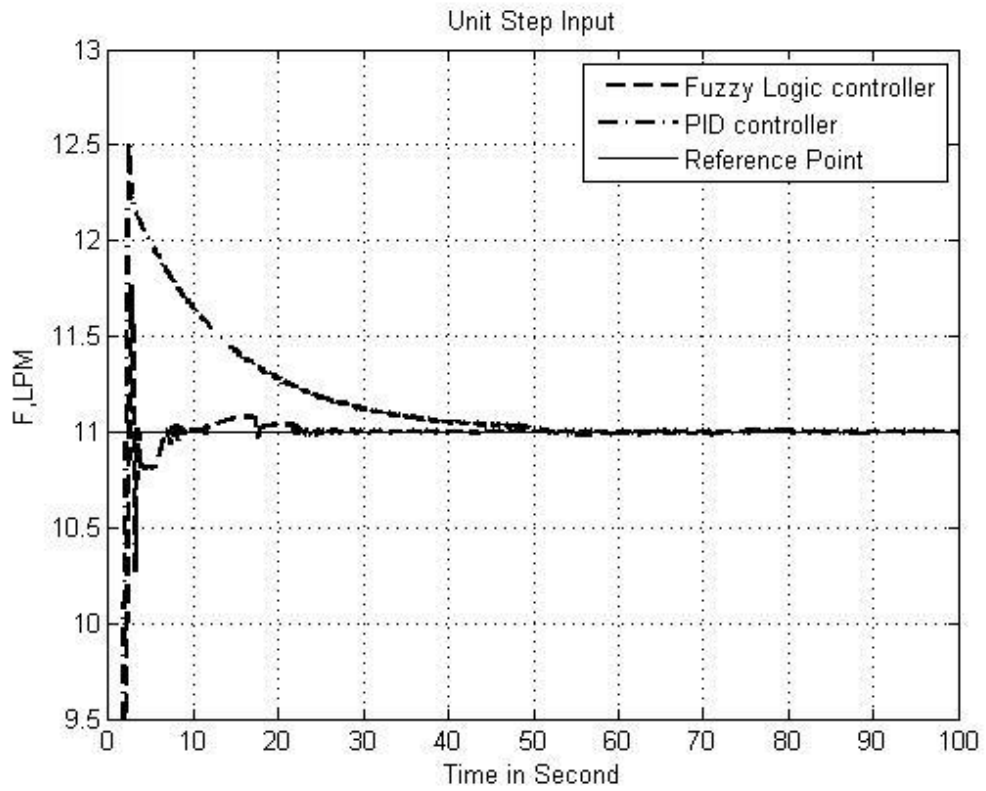


a. The pressure  $P_1$ , disturbed with a random signal

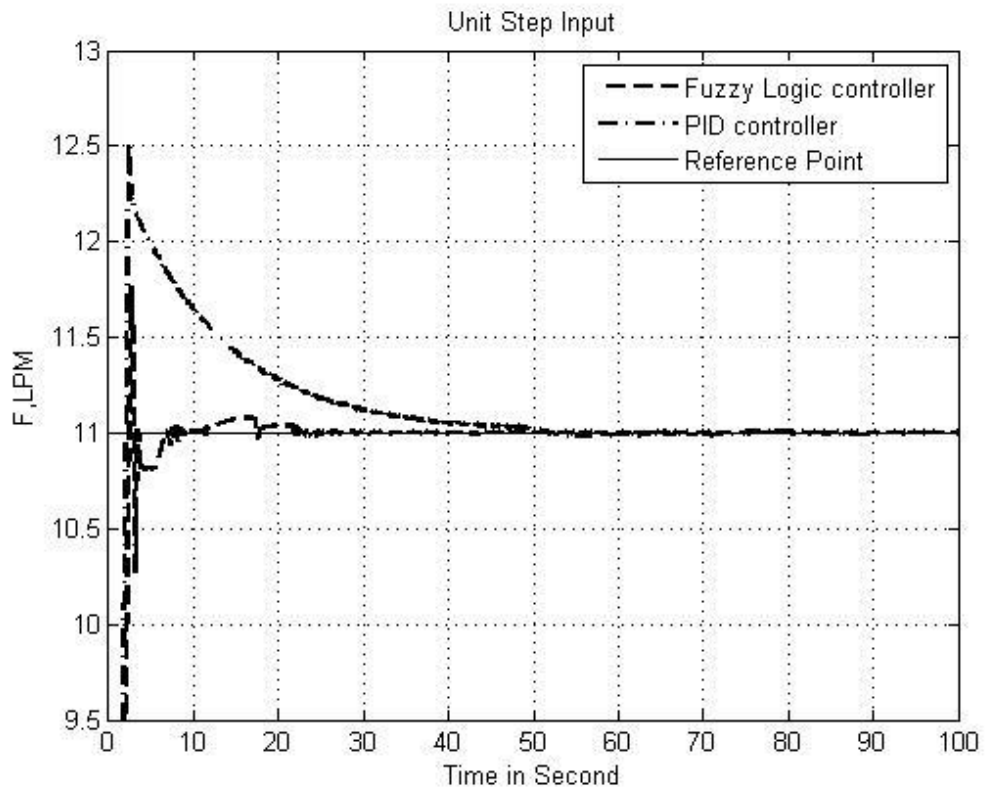


b. The pressure  $P_2$ , disturbed with a random signal

Figure 4.61. System controlled temperature variable behavior through each intake flow pressure disturbed with a random signal.

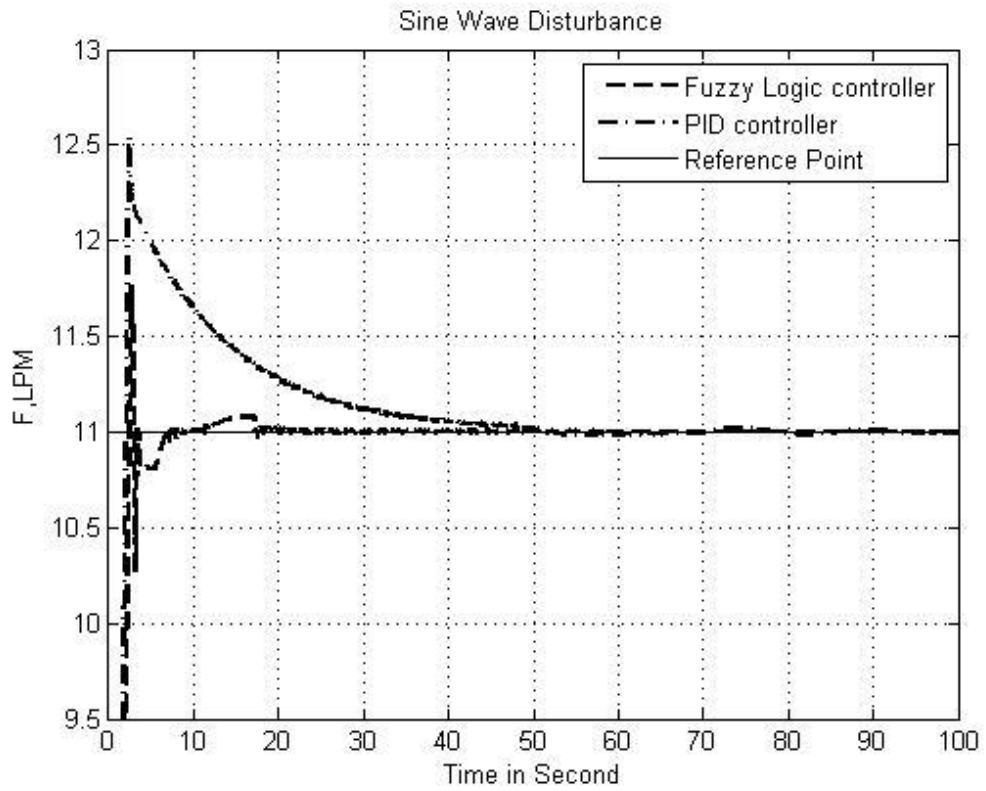


a. The pressure  $P_1$ , disturbed with a step change

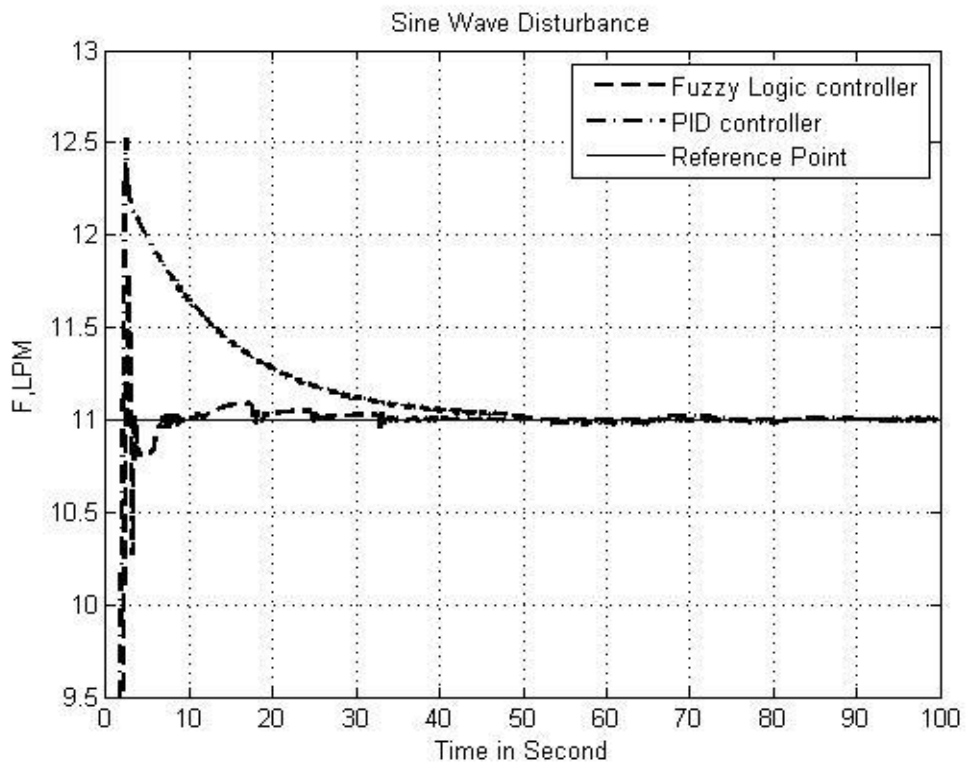


b. The pressure  $P_2$ , disturbed with a step change

Figure 4.62. System controlled flow rate variable behavior through each intake flow pressure disturbed with a step change.

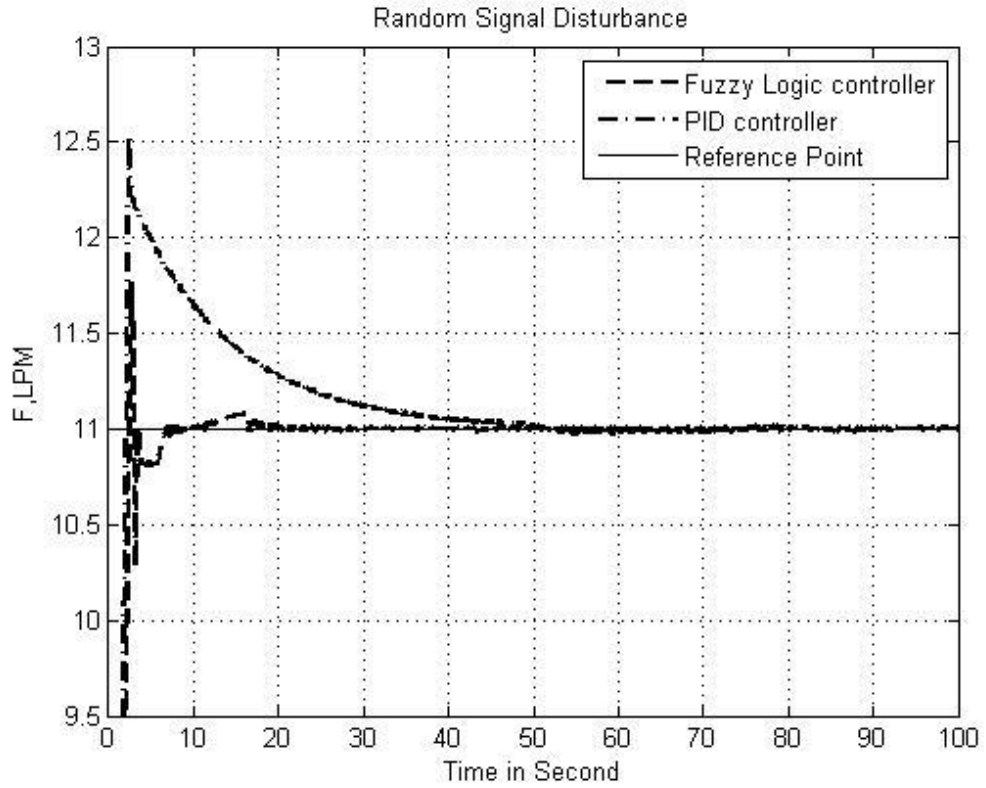


a. The pressure  $P_1$ , disturbed with a sine wave

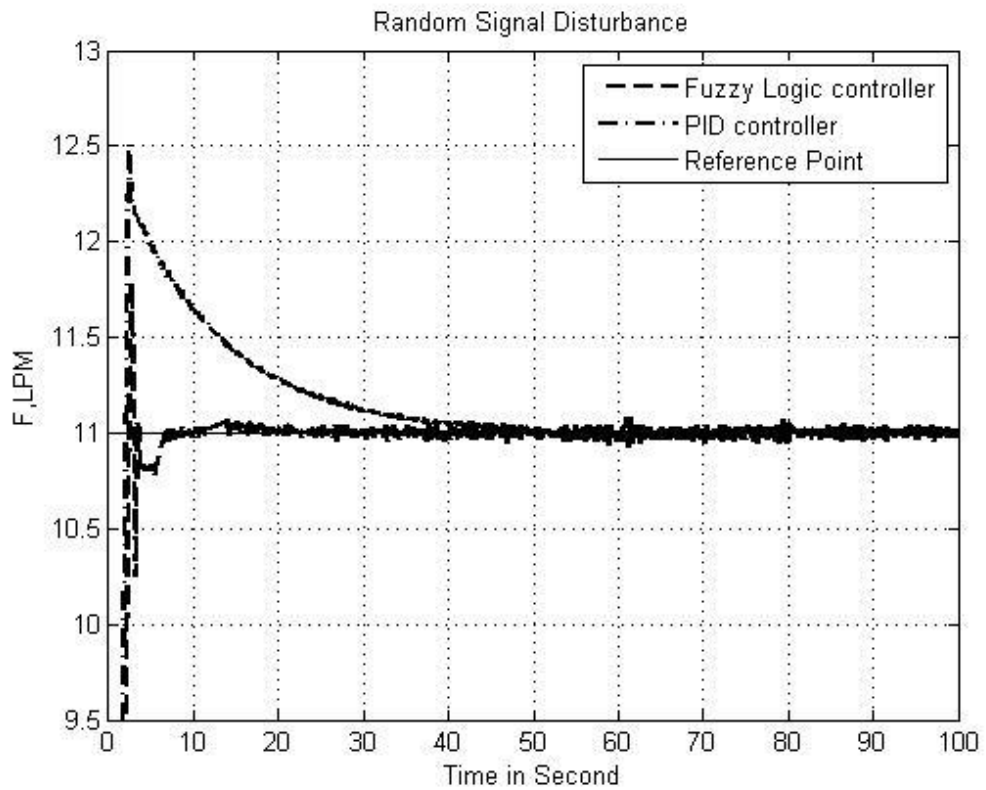


b. The pressure  $P_2$ , disturbed with a sine wave

Figure 4.63. System controlled flow rate variable behavior through each intake flow pressure disturbed with a sine wave.



a. The pressure  $P_1$ , disturbed with a random signal



b. The pressure  $P_2$ , disturbed with a random signal

Figure 4.64. System controlled flow rate variable behavior through each intake flow pressure disturbed with a random signal.



#### 4.3.4. Mean Square Error MSE

In this section one step further is applied, which is the mean square error (MSE) that is applied on each disturbance rejection test performed in previous section including step change, sine wave and random signal injected to the dedicated major disturbances. The purpose is to find the quicker response and robustness of the applied control methodologies in comparison to conventional controller.

In first step each intake temperature is injected with three disturbances as described above. The MSE numerically is found for each step as illustrated in Table 4.1, where the results are taken from reference Figures (4.56 to 4.64).

Table 4.1. Numerical MSE for temperature output variable of purposed Fuzzy Self-tuning PID controller against conventional PID controller to mentioned disturbance subjections.

	Fuzzy Self-tuning PID Controller	Conventional PID Controller
Step Change Disturbance to $T_1$	0.1529	0.7644
Sine Wave Disturbance to $T_1$	0.061	1.1051
Random Signal Disturbance to $T_1$	0.1368	0.8229
Step Change Disturbance to $T_2$	0.1529	0.7644
Sine Wave Disturbance to $T_2$	0.0314	0.6967
Random Signal Disturbance to $T_2$	0.1321	0.8356

Also the same disturbances are applied to the inlet pressures and the performances of the controllers individually for temperature and flow rate control are given in Tables (4.2, 4.3)

Table 4.2. Numerical MSE for temperature output variable of purposed Fuzzy Self-tuning PID controller against conventional PID controller to mentioned disturbance subjections.

	Fuzzy Self-tuning PID Controller	Conventional PID Controller
Step Change Disturbance to $P_1$	0.1529	0.7644
Sine Wave Disturbance to $P_1$	0.1884	0.6395
Random Signal Disturbance to $P_1$	0.1552	0.7434
Step Change Disturbance to $P_2$	0.1529	0.7644
Sine Wave Disturbance to $P_2$	0.1784	0.6576
Random Signal Disturbance to $P_2$	0.1154	0.9305

Table 4.3. Numerical MSE for flow rate output variable of purposed Fuzzy Logic controller against conventional PID controller to mentioned disturbance subjections.

	Fuzzy Logic Controller	Conventional PID Controller
Step Change Disturbance to $P_1$	0.0043	0.5130
Sine Wave Disturbance to $P_1$	0.0053	0.5158
Random Signal Disturbance to $P_1$	0.0037	0.5088
Step Change Disturbance to $P_2$	0.0043	0.5130
Sine Wave Disturbance to $P_2$	0.0052	0.5089
Random Signal Disturbance to $P_2$	0.003	0.5422

#### 4.4. Discussion

The linearized MV system in state space form is depicted in Figure 4.1 which is given in Equations (2.37, 2.38) and tested via computer simulations with comparing to the non-linear system as depicted in Figure 4.2 which stands for the nonlinear developed differential system Equations (2.31, 2.34). Simulation tests are conducted by applying step changes to all inputs successively and observing the responses at the outputs. Results are given through Figures (4.4 – 4.9). These figures show that the linearized system nearly gives the same response as the non-linear system as expected. The function of linearization is to linearize the complicated nonlinear system around some steady state values and giving it through state space or Laplace form in order to ease and simplify the control system design. Precisely in our work which is the interacted MV system, linearization is facilitated in decoupling.

Decoupler design is depicted in Figure 3.32 and given by the formulae in (3.4 – 3.6), which consist of two parts of static and dynamic as depicted in Figures (4.10, 4.11) and tested via computer simulations. Simulation tests are conducted by applying step inputs to all inputs successively and observing the responses at the outputs with and without static and dynamic decoupling on the linearized and nonlinear system. Results of the linearized and nonlinear systems are given in Figures (4.13 – 4.18) and Figures (4.20 – 4.25) respectively, where Figures (4.13 – 4.15) and Figures (4.20 – 4.22) present the response of the temperature process to a step change in manipulated variable inputs of  $U_1$ ,  $U_2$  and  $U_3$ , for both linearized and non-linear systems respectively. Similarly, Figures (4.16 – 4.18) and Figures (4.22 – 4.25) depict the response of the flow process to the same input changes. The function of the decoupler is to eliminate the effect of a cross transfer function as mentioned in the previous section. This means a reduction in the effect of  $U_1$  on  $F$  and that of  $U_2$  and  $U_3$  on  $T_o$ .

Figures (4.14, 4.15) and Figures (4.21, 4.22) show clearly the performance of the decoupler in reducing the interaction of  $U_2$  and  $U_3$  with  $T_o$ , and again for both systems Figure (4.16, 4.23) prove that designed decouplers eliminates the interaction of  $U_1$  with  $F$ . These figures mentioned above show a significant discrepancy between responses with and without decoupling states for both linearized and nonlinear systems, which is not observed in Figures (4.13, 4.17 and 4.18) and Figures (4.20, 4.24 and 4.25) as expected.

Also for desired performances of the controllers of the closed loop, system simulation tests are conducted by applying step and square wave inputs to all inputs successively and observing the responses at the outputs with static and dynamic decoupling on the linearized and nonlinear system as in Section (4.3.2). Results of the both MV controllers for the statically decoupled linearized system (Section 4.3.2.1), dynamically decoupled linearized system (Section 4.3.2.2), statically decoupled nonlinear system (Section 4.3.2.3) and finally dynamically decoupled nonlinear system (Section 4.3.2.4) are shown in Figures ((4.37 – 4.40), (4.42 – 4.45), (4.47 – 4.50) and (4.52 – 4.55)) respectively. Under these results an adequate investigation could be done, where Figures (4.37a, 4.42a, 4.47a and 4.52a) and Figures (4.39a, 4.44a, 4.49a and 4.54a) present the response of the temperature process to a step and square wave change in temperature set point respectively for all sections. Also Figures (4.38b, 4.43b, 4.48b and 4.53b) and Figures (4.40b, 4.45b, 4.50b and 4.55b) present the response of the temperature process to a step and square wave change in flow rate set point respectively for all sections. These figures mentioned above show and emphasize that a quick and smooth performance for the temperature control process through fuzzy logic self-tuning PID control is achieved applying to both linearized and nonlinear systems. Figures (4.38a, 4.43a, 4.48a and 4.53a) and Figures (4.40a, 4.45a, 4.50a and 4.55a) present the response of the flow rate process to a step and square wave change in flow set point respectively for all sections. Also Figures (4.37b, 4.42b, 4.47b and 4.52b) and Figures (4.39b, 4.44b, 4.49b and 4.54b) present the response of the flow rate process to a step and square wave change in temperature set point respectively for all sections. These figures mentioned above show that a good response without overshooting for the flow rate process within some fluctuating error near set point value before the controlled variable settle down through FLC with a proportional gain is achieved applying to both linearized and nonlinear systems. Also the result of

second loop decoupler are illustrated more, which make small dip and smooth fluctuation around set point value for the step change and square wave respectively through all tests.

At last the high performance and robustness of the system through designed controller's ability to reject the disturbances are investigated. In this thesis we focused on four of the major disturbances ( $T_1$ ,  $T_2$ ,  $P_1$  and  $P_2$ ). Each of them are disturbed by a step change, sine wave and random signal. Beside the current implemented controllers, also the results are compared with the conventional PID controller results.

The temperature controlled variable behavior for each disturbance are shown in Figures (4.56 – 4.61) escorting MSE of controllers as given in Tables (4.1, 4.2). From the figures and tables we can observe that proposed and designed controllers give quicker response with smaller peak values also sooner reaching the steady state value. The MSE values emphasize these results.

The flow rate controlled variable behavior for each disturbance is shown in Figures (4.62 – 4.64) escorting MSE of controllers as given in Tables 4.3. From the figures and tables we can observe that the PID controller give a high overshoot resulted from zero initial value. But during steady state it gives the same response. Importance of proposed and designed controller is that it nearly gives same response for different magnitudes of disturbances. Also sooner reaching the steady state value, the MSE values emphasize the results.

## CHAPTER V

### CONCLUSIONS

#### 5.1. Concluding Remarks

The objective of this work is to develop the mathematical model of the specific CST and design appropriate controllers for the desired controlled variables. The state variables of the system are the tank temperature and the pump speed while the system consists of a storage tank flowing in by two intakes through two controlled valves and sucked out through a variable speed DC motor pump. The controlled variables are tank temperature and outflow rate. As long as the system has interactions between its control loops, a decoupler is designed through the classic model block diagram after the system is linearized for this purpose. Two partly controllers are designed for the desired control purposes in the system: the Fuzzy logic self-tuning PID control for controlling the temperature and the proportional gain with fuzzy logic controller to overcome the flow rate control purpose. All stage results including linearization, decoupling and controllers which are designed, are tested in computer simulations. Beside the conventional PID controller, comparison with mentioned controllers are performed in disturbance rejection performance and robustness.

Linearizing behavior results are observed in simulated system and compared with the nonlinear real system through each control input subjected to a step change. It is observed that the linearized system behaves very close to the nonlinear system. Then according to the mechanism for the control purpose the decoupler performances are simulated. The static and dynamic decoupler performances on both linearized and nonlinear systems are tested. It is observed that both decouplers nearly cancel out the interactions in linearized system and big reduction is achieved in nonlinear system. At last the designed controller performance for all above cases are simulated through various tests including input step change and square wave escorting with various injections to the major disturbances. It is observed that the system has good response to reference set point tracking with desired accepted time response with a small error and also has robust characteristic to reject the disturbances.

As a result, the designed controllers for the system move the system controlled variables to track their reference set points with a desired quick response and able to reject the major disturbances. Simulation results show that temperature control objective has sluggish response if compared with flow rate control objective, according to the physic property of stored energy in the tank. Also they show that the flow rate response has the tiny fluctuation before getting the steady state, also due to the pump speed variations which has great effect on the flow rate. In disturbance rejection model, PID controller performances for both controlled variables are observed and MSE values for each case are shown. It is seen that PID control is not convenient as the designed controllers to use in disturbance rejection especially in different magnitudes of disturbed signals.

## **5.2. Future Work and Recommendations**

In future research work, the aim is implementing the proposed system to a real system in order to practice the designed control methods. The methods may be implemented through a microcontroller or PLC environment. Also the fuzzy rules may be improved to get a more precise results. The simulations and real system results may be compared in order to show the properness of the developed mathematical model of the system and the control design performance in a physical environment.

## REFERENCES

- [1] Tokuda, M., Yamamoto, T., & Monden, Y. (2002). A design of multiloop PID controllers with neural-net based decoupler. In *Intelligent Control, 2002. Proceedings of the 2002 IEEE International Symposium on* (pp. 448-453). IEEE.
- [2] Numsomran, A., Wongkhum, T., Suksri, T., Nilas, P., & Chaoraingern, J. (2007). Design of decoupled controller for TITO system using characteristic ratio assignment. In *Control, Automation and Systems, 2007. ICCAS'07. International Conference on* (pp. 957-962). IEEE.
- [3] Qinling, Z., & Zhiqiang, G. (2015). On decoupling control of uncertain and multivariable systems with time delays. In *Society of Instrument and Control Engineers of Japan (SICE), 2015 54th Annual Conference of the* (pp. 718-723). IEEE.
- [4] Khare, Y. B., & Singh, Y. (2010). PID control of heat exchanger system. *International Journal of Computer Applications*, 8(6), 22-27.
- [5] Juang, C. F., & Chen, J. S. (2006). Water bath temperature control by a recurrent fuzzy controller and its FPGA implementation. *IEEE Transactions on Industrial Electronics*, 53(3), 941-949.
- [6] Mary, M. P., & Marimuthu NS Albert Singh. N. (2007). Design of Intelligent Self-Tuning Temperature Controller for Water Bath Process. *International Journal of Imaging Science and Engineering (IJISE)*, ISSN, 9955.
- [7] Chen, C. H., & Lin, C. T. (2007). A functional-link-based fuzzy neural network for temperature control. In *2007 IEEE Symposium on Foundations of Computational Intelligence, Vols 1 and 2* (pp. 53-58).
- [8] Tavoosi, J., Alaei, M., & Jahani, B. (2011). Temperature Control of Water Bath by using Neuro-Fuzzy Controller. In *5th Symposium on Advance in Science & Technology. May12-17*.
- [9] P. Sujatha, P., Therese., & Kesavan, N.(2010). Fuzzy self tuning of PID controller for multivariable process. *Journal of Computing, Vol.2, issue 8, pp. 2151-961*.
- [10] Mangar, L. O., & Rathee, V. (2009). A comparative study between fuzzy logic control and adaptive Neuro-Fuzzy control for water bath system. In *2009 Second International Conference on Emerging Trends in Engineering & Technology* (pp. 962-965). IEEE.

- [11] Treesatayapun, C., Uatrongjit, S., & Kantapanit, K. (2002). Fuzzy graphic rule network and its application on water bath temperature control system. In *Proceedings of the 2002 American Control Conference (IEEE Cat. No. CH37301)* (Vol. 1, pp. 476-480). IEEE.
- [12] Jahmeerbacus, M. I. (2015). Flow rate regulation of a variable speed driven pumping system using fuzzy logic. In *Electric Power and Energy Conversion Systems (EPECS), 2015 4th International Conference on*(pp. 1-6). IEEE.
- [13] Khan, M. W., Choudhry, M. A., & Zeeshan, M. (2013). Multivariable adaptive Fuzzy logic controller design based on genetic algorithm applied to HVAC systems. In *Computer, Control & Communication (IC4), 2013 3rd International Conference on* (pp. 1-6). IEEE.
- [14] Xu, X., & Yu, W. (2005). Application of neuron-based adaptive control system to the operation of marine water pumps. In *Canadian Conference on Electrical and Computer Engineering, 2005.* (pp. 1355-1358). IEEE.
- [15] Vojtesek, J., & Dostal, P. (2015). Adaptive control of water level in real model of water tank. In *Process Control (PC), 2015 20th International Conference on* (pp. 308-313). IEEE.
- [16] Smith, C. A., & Corripio, A. B. (1985). Principles and practice of automatic process control (Vol. 2). New York: Wiley.
- [17] PRABHU MURUGAN, B. S. (1995). Flow and temperature control using advanced strategies (Doctoral dissertation, Texas Tech University).
- [18] Janevska, G. (2013). Mathematical Modeling of Pump System. In *Proceedings in EIIC-The 2nd Electronic International Interdisciplinary Conference* (No. 1).
- [19] Grugel, M. E. (1998). Modeling the viscous torque acting on a rotating object. Physics Department, The College of Wooster, Wooster, Ohio.
- [20] *engineeringtoolbox*. (n.d.). Retrieved May 20, 2016, from [http://www.engineeringtoolbox.com/centrifugal-pumps-d\\_54.html](http://www.engineeringtoolbox.com/centrifugal-pumps-d_54.html)
- [21] Jide, J. P, Oladele, J. O., & Charity, S. O. (2015). Modelling and Simulation of Armature-Controlled Direct Current. *SSRG International Journal of Electrical and Electronics Engineering (SSRG-IJEEE), volume 2 Issue*.
- [22] Bernard, A. (2013). Speed control of separately excited DC motor using artificial intelligent approach (Doctoral dissertation, Universiti Tun Hussein Onn Malaysia).
- [23] Erin Knight, M. R. (n.d.). *Wikipedia*. Retrieved October 31, 2015, from <http://controls.engin.umich.edu/wiki/index.php/ValveModeling>
- [24] Bequette, B. W. (1998). Process Dynamics\_ Modeling, Analysis and Simulation. Prentice Hall.
- [25] Shoukry, G. F. (2008). State-space realization for nonlinear systems. Georgia Institute of Technology.



- [26] Dorf, R. C., & Svoboda, J. A. (2010). Introduction to electric circuits. John Wiley & Sons.
- [27] Cochin, I. (1997). Analysis and design of dynamic systems. Addison- Wesley.
- [28] Albertos, P., & Antonio, S. (2006). Multivariable control systems: an engineering approach. Springer Science & Business Media.
- [29] Seborg, D. E., Mellichamp, D. A., Edgar, T. F., & Doyle III, F. J. (2010). Process dynamics and control. John Wiley & Sons.
- [30] Bařka, S., & Dworak, P. (2007). On decoupling of LTI MIMO systems with guaranteed stability. *Pomiry, Automatyka, Kontrola*, 53, 46-51.
- [31] Goodwin, G. C., Graebe, S. F., & Salgado, M. E. (2001). Control system design (Vol. 240). New Jersey: Prentice Hall.
- [32] Li, T., Su, Y., & Zhong, B. (2007). Remodeling for fuzzy PID controller based on neural networks. In *Fuzzy Information and Engineering* (pp. 714-725). Springer Berlin Heidelberg.
- [33] Yang, Y., & Bian, H. (2012). Design and Realization of Fuzzy Self-tuning PID Water Temperature Controller Based on PLC. In *Intelligent Human-Machine Systems and Cybernetics (IHMSC), 2012 4th International Conference on* (Vol. 2, pp. 3-6). IEEE.
- [34] Wei, J. (2010). Research on the temperature control system based on fuzzy self-tuning PID. In *Computer Design and Applications (ICCD), 2010 International Conference on* (Vol. 3, pp. V3-13). IEEE.
- [35] Mohan, B. M., & Sinha, A. (2006). The simplest fuzzy PID controllers: mathematical models and stability analysis. *Soft computing*, 10(10), 961-975.
- [36] Pathmanathan, E., & Ibrahim, R. (2010). Development and implementation of fuzzy logic controller for flow control application. In *Intelligent and Advanced Systems (ICIAS), 2010 International Conference on* (pp. 1-6). IEEE.
- [37] Hai-chu, C., Hui, Y., Hua, Z., & Rui-hua, Z. (2010). Study of proportion and fuzzy control method upon precision micro-flow valve. In *Future Computer and Communication (ICFCC), 2010 2nd International Conference on* (Vol. 3, pp. V3-581). IEEE.
- [38] Zhi-huai, X. I. A. O., & Yu, C. (2010). Adaptive Fuzzy PID controller's application in constant pressure water supply system. In *The 2nd International Conference on Information Science and Engineering* (pp. 6430-6433). IEEE.
- [39] Lopez, C. (2014). MATLAB Control Systems Engineering. Apress.
- [40] Octavia, N., Maung, M. M., & Tun, H. M. (2014). Performance Evaluation of Fuzzy Logic Controller in Water Bath Temperature Control System. *International Journal of Science, Engineering and Technology Research*, 3(6), 1623-1629.



## APPENDICES

### A.1. DC Motor Specifications

100ZYT Series Electric DC Motor are widely used for wires, cables, light industry, spinning, papermaking, chemical industry, printing and dyeing, metallurgy, rubber, wiredrawing, extrusion machinery, medical equipment, food processing, printing and packaging and other industries, and can achieve step-less speed regulation by constant torque by being equipped with the speed regulator.

In current thesis, under this motor characteristic specifications the electrical element and variables are found and calculated. According to the Dc motor schematic diagram and formulas.



Figure A.1. 100ZYT Series Electric DC Motor 100ZYT36-200-1700.

Table A.1. 100ZYT Series Electric DC Motor Specification.

型号 Model	额定电压 Rated voltage (v)	空载转速 No-load speed (R/min)	额定电流 Rated current (A)	额定功率 Rated power (w)	额定转速 Rated speed (r/min)	额定转矩 rated torque (mN.m)
100ZYT24-100-1900	24	2300	5.63	100	1900	0.51
100ZYT36-200-1700	36	1950	7.4	200	1700	1.13
100ZYT36-300-1700	36	1950	11.2	300	1700	1.69
100ZYT36-400-2500	36	2800	14.8	400	2500	1.53
100ZYT12-400-1500	12	1800	44.5	400	1500	2.55
100ZYT24-500-1800	24	2200	28.2	500	1800	2.65

## A.2. Pump Impeller Specifications

SHURFLO REVOLUTION™ 4008 SERIES PUMP is considered. The flow change against the height is illustrated, also in order to achieve kw constant different values of speed considered.



Figure A.2. SHURFLO REVOLUTION™ 4008 SERIES PUMP.

Table A.2. SHURFLO pump manufacture characteristic.  
PERFORMANCE @ 12V DC

PRESSURE		FLOW		CURRENT
BAR	PSI	GPM	LPM	AMPS
0.0	0	3.0	12.1	2.2
0.7	10	2.2	8.3	3.3
1.4	20	1.8	6.8	4.3
2.1	30	1.5	5.6	5.1
2.8	40	1.2	4.5	6.0
3.4	50	0.5	1.8	6.8

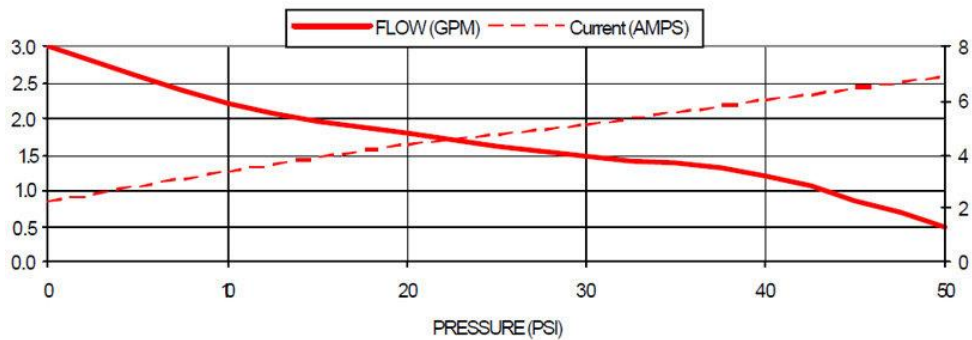


Figure A.3. SHURFLO pump manufacture characteristic curve.

### A.3. Estimated J Pump Moment of Inertia

The moment inertia of a pump impeller may be estimated using the method relationship proposed by Wylie et al. as shown below.

$$J = 1.5 * 10^7 * \left(\frac{P_w}{W^3}\right)^{0.9556} \quad (\text{A.1})$$

Here the shaft power  $P_w$  of the pump may be calculated as shown below

$$P_w = \frac{\rho * f(t) * h * g}{\eta * 3.6 * 10^6} \quad (\text{A.2})$$

In addition to the inertia of the pump impeller, inertia of the motor may not be available from the vendor and therefore requires estimation.